

THE EVALUATION OF A SYNTHETIC MATERIAL
FOR USE AS A WAVE PROTECTION AGENT ON IRRIGATION DAMS

Richard W. Stephenson
Larry D. McCallister
Dennis L. Dutton

MISSOURI WATER RESOURCES RESEARCH CENTER

University of Missouri

PROJECT NUMBER - B-122-MO

Agreement Number 14-34-0001-8098

Dates 10/77 - 10/79

COMPLETION REPORT

1 March, 1980

The work upon which this publication is based was supported (or supported in part) by funds provided by the United States Department of the Interior, Office of Water Resources Research, as authorized under the Water Resources Research Act of 1964.

ABSTRACT

This report presents the results of a field and laboratory testing program to evaluate the performance of a slope protection method utilizing a new synthetic fabric material in the form of soil filled bags.

The field study was performed to evaluate the feasibility of filling and placing the bags on an operational irrigation dam using equipment and resources available to a typical farmer. Test sections on the dam were monitored to determine the amount of wave erosion of both unprotected and protected slopes of the dam. Tensile strength tests were performed on samples of the fabric. The results of the strength tests indicate the durability of the system. Laboratory immersion tests were conducted on two soil materials used to fill the bags. The results of the immersion tests were then compared to the field performance of each material in the bags.

The results of this investigation indicate that the system is readily installed on irrigation dams and offers excellent slope protection. The factors which influence the practicality of the system include the cost of alternate slope protection methods, the position of the irrigation dam in relation to local winds and the availability of fill material for the bags. A medium-scale laboratory model study was performed on a new synthetic fabric designed to be used in the form of soil-filled "sand pillows" in order to determine the relationship that affect the stability of the pillows and to determine basic design criteria for the protection system.

The model testing of the sand pillow system was performed to evaluate the parameters that affect the stability of the pillows when placed on an embankment slope. The results of the model investigation were

consolidated and analyzed to develop design criteria for the individual pillows.

The results of the model study investigation indicate that the stability of sand pillows is primarily a function of wave height, wave period, embankment slope angle, and individual sand pillow weight. A possible design equation was developed for a silty clay soil such that the wave height calculated for a given reservoir could be utilized to determine the weight of the individual sand pillow necessary to economically and effectively protect the embankment.

The results of the laboratory and field evaluation investigation indicate that the sand pillow method offers excellent slope protection. However, since some soils appear to be readily lost through fabric when subjected to repeated wave action, some limiting minimum particle size specification is required in order to prevent unnecessary maintenance of the system.

ACKNOWLEDGEMENTS

Research of this magnitude requires the assistance of many different organizations and people. The authors would like to take this opportunity to show their appreciation to the following:

Mr. Jake Freyer for allowing the use of his irrigation dam for this study. His assistance in preparing for and installing the slope protection system was invaluable.

The U.S. Department of Agriculture, Soil Conservation Service personnel of Audrain County, particularly Mr. Terry Hill and Mr. Dennis Shirk, were most helpful in selecting the project site.

Mr. Vee Varish and the Future Farmers of America Chapter of Scotts Corner High School provided the assistance necessary to fill and place the slope protection system.

The funding necessary for this investigation was provided by the United States Department of the Interior, Office of Water Resources and Technology.

The Monsanto Textile Company provided the acrilan bags used on the field and laboratory study.

George E. Smith and Joanne Gregory of the Water Resources Research Center in Columbia, Missouri provided invaluable administrative assistance.

Mr. Ken Hass of UMR and Dr. Samuel P. Clemence formerly of UMR now of Syracuse University provided their expert guidance in the conception and development of the project.

TABLE OF CONTENTS

	Page
ABSTRACT.....	ii
ACKNOWLEDGMENTS.....	iv
TABLE OF CONTENTS.....	v
LIST OF ILLUSTRATIONS.....	viii
LIST OF TABLES.....	xii
I. INTRODUCTION.....	1
A. DEFINITION OF THE PROBLEM.....	1
B. SCOPE OF THE REPORT.....	5
1. Field Study.....	5
2. Model Study.....	6
II. ENGINEERING USE OF FABRICS.....	6
III. FABRIC TESTING PROGRAM.....	11
A. RESISTANCE TO DETERIORATION.....	11
1. Testing Method.....	11
2. Results.....	12
B. SOIL RETENTION CHARACTERISTICS OF THE FABRIC.....	16
1. Immersion Tests.....	16
a. Apparatus.....	16
b. Testing Material.....	16
c. Procedure.....	19
2. Grain Size Distribution Analysis.....	21
3. Soil Loss Results.....	23
4. Grain-Size Distribution Results.....	32
IV. FIELD TESTING OF SAND PILLOWS FOR EROSION CONTROL.....	35
A. INTRODUCTION.....	35
B. FIELD EVALUATION OF THE SLOPE PROTECTION METHOD.....	36

Table of Contents, continued

	Page
1. Introduction.....	36
2. Installation of the Slope Protection System.....	37
3. In-Situ Monitoring of the Slope Protection System...	47
4. Results.....	47
a. Field Performance of the Slope Protection System	47
i. Feasibility of Installation on Farm	
Irrigation Dam.....	49
ii. Erosion Resistance of the Slope Protection	
System.....	52
V. MODEL STUDY INVESTIGATIONS OF SAND PILLOWS FOR SLOPE	
PROTECTION.....	57
A. GENERAL MODEL THEORY.....	58
B. MODEL STUDIES.....	59
C. TESTING EQUIPMENT AND PROCEDURES.....	67
1. Introduction.....	67
2. Model Testing Program.....	67
a. Wave Tank and Wave Generator Description....	67
b. Wave Tank Calibration.....	67
c. Survey Equipment.....	76
d. Testing Material.....	77
e. Testing Procedure.....	79
D. RESULTS OF MODEL TESTING PROGRAM.....	82
1. Wave Damage.....	82
2. Scaling Effects.....	98
3. Wave Period Effect.....	104

Table of Contents, continued

	Page
4. Embankment Slope Angle Effects.....	107
5. Wave Runup Effects.....	111
6. Other Considerations.....	111
7. Data Scatter.....	113
8. Stability Prediction and Design Equation.....	114
VI. CONCLUSIONS AND APPLICATIONS.....	119
A. FIELD TESTING PROGRAM.....	119
B. MODEL TESTING PROGRAM.....	121
VII. RECOMMENDATIONS.....	123
BIBLIOGRAPHY.....	127
APPENDIX A: THEORETICAL DEVELOPMENT OF THE STABILITY NUMBER, N.....	135
APPENDIX B: DAMAGE CURVES.....	140
APPENDIX C: CROSS SECTION OF THE UNPROTECTED SLOPE OF THE EMBANKMENT	148
APPENDIX D: NOTATIONS.....	160

LIST OF ILLUSTRATIONS

Figure	Page
1. Progressive Wave Damage to an Irrigation Dam.....	3
2. Salvaged Brick Used for Slope Protection.....	3
3. Asphalt and Concrete Slabs Used for Slope Protection.....	4
4. Typical Dura-bag and Perma-bag Structures.....	9
5. Front and Side View of Dunking Apparatus.....	17
6. Test Soil Bags.....	18
7. Grain Size Distribution Curves of Tested Soils.....	20
8. Samples Ready for Testing.....	22
9. Typical View of Completed Immersion Test.....	24
10. Average Percent of Soil Lost for Mexico Clay Sample.....	27
11. Combined Average Percent of Soil Lost for Mexico Clay Sample....	28
12. Average Percent Soil Loss as a Function of Vibration for Quincy Loess.....	29
13. Comparison of Grain Size Analyses for Mexico Clay.....	33
14. Comparison of Grain Size Analyses for Quincy Loess.....	34
15. East-West Portion of the Project Site--November, 1970.....	38
16. North-South Portion of the Project Site--November, 1970.....	38
17. Configuration of the Project Site.....	39
18. Fertilizer Cart and Tractor Used to Fill Bags.....	41
19. Bag Being Filled.....	42
20. Overview of Filling Operation.....	43
21. Sewing the Bag.....	44
22. Finishing the Seam.....	45
23. Positioning the Bags on the Dam.....	46
24. Positioning the Slope Protection System.....	46
25. Location of the Test Section of the Dam.....	48

List of Illustrations, continued

Figure	Page
26. View of Unprotected Slope versus Protected Slope.....	54
27. Undercutting of Vertical Cut Due to Wave Action.....	55
28. Slumping of Embankment Slope Due to Undercutting by Wave Action.	55
29. Damage Cross-Section.....	63
30. Effect of Wave Period on Zero-Damage Stability of Dumped Stone..	65
31. Effect of Embankment Slope on Zero-Damage Stability of Dumped Stone.....	66
32. Right Side of Wave Tank.....	68
33. Left Side of Wave Tank Showing Paddle and Motor.....	69
34. Reinforced Plexiglass Paddle.....	70
35. Motor and Pulley Assembly.....	70
36. Step Resistance Wave Rod, Power Supply, and Recorder.....	72
37. Wave Rod in Water with Approaching Waves.....	73
38. Wave Rod in Water with Wave Passing.....	74
39. Typical Chart Recording.....	78
40. Model Sand Pillows.....	78
41. Typical Sand Pillow Configuration on a Model Slope.....	81
42. Typical Model Failure, Slope: 1 on 4, Test No. 9.....	84
43. Typical Model Failure, Slope: 1 on 3, Test No. 1.....	84
44. Typical Model Failure, Slope: 1 on 5, Test No. 13.....	85
45. Start of Model Failure (Test No. 10).....	86
46. Progressive Failure of Model Slope, (Test No. 10).....	87
47. Complete Failure of Model Slope, (Test No. 10).....	88
48. Typical Damage Curve.....	89
49. Typical Wave Damage Development.....	91

List of Illustrations, continued

Figure	Page
50. Typical Damage (D_A) Profiles for Protected and Unprotected Slopes, (Slope: 1 on 2).....	94
51. Typical Damage (D_A) Profiles for Protected and Unprotected Slopes, (Slope: 1 on 3).....	95
52. Typical Damage (D_A) Profiles for Protected and Unprotected Slopes, (Slope: 1 on 4).....	96
53. Typical Damage (D_A) Profiles for Protected and Unprotected Slopes, (Slope: 1 on 5).....	97
54. Area Damage (D_A).....	99
55. Reynolds Number as a Function of Stability.....	101
56. Stability Correction for Scale Effect.....	103
57. Stability as a Function of Wave Period.....	106
58. Minimum Zero-Damage Stability as a Function of Embankment Slope.	108
59. Relative Runup as a Function of Wave Steepness and Embankment Slope.....	112
60. A Comparison of Hindcast Zero-Damage Wave Heights and Actual Zero-Damage Wave Heights for all Model Tests.....	116
61. Zero-Damage Stability Curves for Acrilan Sand Pillows.....	117
62. Damage Curve for Tests Nos. 1 and 2.....	141
63. Damage Curve for Tests Nos. 3 and 4.....	142
64. Damage Curve for Tests Nos. 6, 7, and 8.....	143
65. Damage Curve for Tests Nos. 9 and 10.....	144
66. Damage Curve for Tests Nos. 11 and 12.....	145
67. Damage Curve for Tests Nos. 13 and 14.....	146
68. Damage Curve for Tests Nos. 15 and 16.....	147

List of Illustrations, continued

Figure	Page
69. Cross Section at Profile D.....	149
70. Cross Section at Profile E.....	150
71. Cross Section at Profile F.....	151
72. Cross Section at Profile G.....	152
73. Cross Section at Profile H.....	153
74. Cross Section at Profile I.....	154
75. Cross Section at Profile J.....	155
76. Cross Section at Profile K.....	156
77. Cross Section at Profile L.....	157
78. Cross Section at Profile M.....	158
79. Cross Section at Profile N.....	159

LIST OF TABLES

Table	Page
I. Results of Tensile Tests on the Original Fabric.....	13
II. Results of Tensile Tests on the Fabric After Seven Months of Exposure.....	14
III. Results of Tensile Tests on the Fabric after One Year of Exposure.....	15
IV. Soil Lost Through Fabric For Mexico Clay.....	26
V. Effect of Vibration on Quincy Loess.....	30
VI. Model Test Results.....	93
VII. Model Test Results in Dimensionless Form.....	105
VIII. Minimum Zero-Damage Stability Numbers.....	109
IX. Comparison of Stability Equation.....	110
X. Model Runup Results.....	110
XI. Variables and Corresponding Dimension and Dimensionless Parameters.....	137

For small embankments, the cost may often exceed 50% of the total cost of the dam. In northern Missouri, dumped stone riprap must be transported from distant rock quarries at great expense. Local owners have used scrap material from a nearby brick factory (Figure 2) with good success, and some have managed to acquire concrete and asphalt slabs from nearby highway construction sites (Figure 3). However, these protection materials are not generally available in great quantity and can be expensive to acquire.

In 1963, the Monsanto Textile Company began exploring the possibility of using a new acrylic fabric to make sandbags for the military services. This new fabric, called Acrilan*, has many important advantages over conventional slope protection materials. Among these advantages are:

1. Durability--the material has outstanding biodegradation and ultraviolet light resistance giving it a much longer life-span than sandbags (or pillows) made of jute, cotton, nylon, etc.
2. Ease and economy of installation--the sand pillows can be filled with sand or soil from the construction site.
3. Ease of repair--if a sand pillow inadvertently becomes torn, it can easily be replaced with a new one.
4. Cost/benefit relationships.

The sand pillow slope protection system is presently being tested by the U.S. Corps of Engineers, New Orleans District, on the Red River at Morameal, Bossier Parish, near Shreveport, Louisiana. Because of favorable results that have been obtained from the Red River project, the use of sand pillows as means of slope protection for irrigation dams was proposed by the university of Missouri at Rolla and tested on an embankment in Audrain County, Near Mexico, Missouri.

* Registered Trademark of Monsanto

I. INTRODUCTION

A. DEFINITION OF THE PROBLEM

The development of agricultural irrigation in the Midwest has produced a number of irrigation reservoirs for the purpose of storing water for use during the dry seasons. The embankments used for impoundment of water are generally not designed by geotechnical engineers nor is there usually any engineering supervision of these embankments during construction. The embankments are often located in areas of rather flat topography with very little shelter from wind. Generally, the material used for construction is the material existing at the site and is often either silty clay or clayey silt or both.

The three facts, lack of quality control, flat topography, and fine-grained soil, combine to produce optimum conditions for wind generated wave erosion. The lack of quality control often results in poor compaction and moisture conditions of the embankment during construction. Flat, open topography leads to high wind velocities over the terrain. Silty soils are characteristically easily eroded by wave action and have an increased rate of erosion over other soils.

The problem of erosion has been a major concern of embankment owners for many years. Wave erosion causes constant damage to an expensive investment as depicted in Figure 1. Because of excessive wave damage to an irrigation dam near Mexico, Missouri, in the spring of 1977 that resulted in near failure of the embankment, the attention of embankment owners focused on an economically feasible way to protect their investments.

Various means of slope protection often used on large dams include dumped stone riprap, asphalt or soil-cement facing, concrete slabs and many forms of tribars and quadrapods. However, the cost of protecting these large dams frequently ranges from 10% to 30% of the total cost of construction.



Figure 3. Asphalt and Concrete Slabs Used for Slope Protection

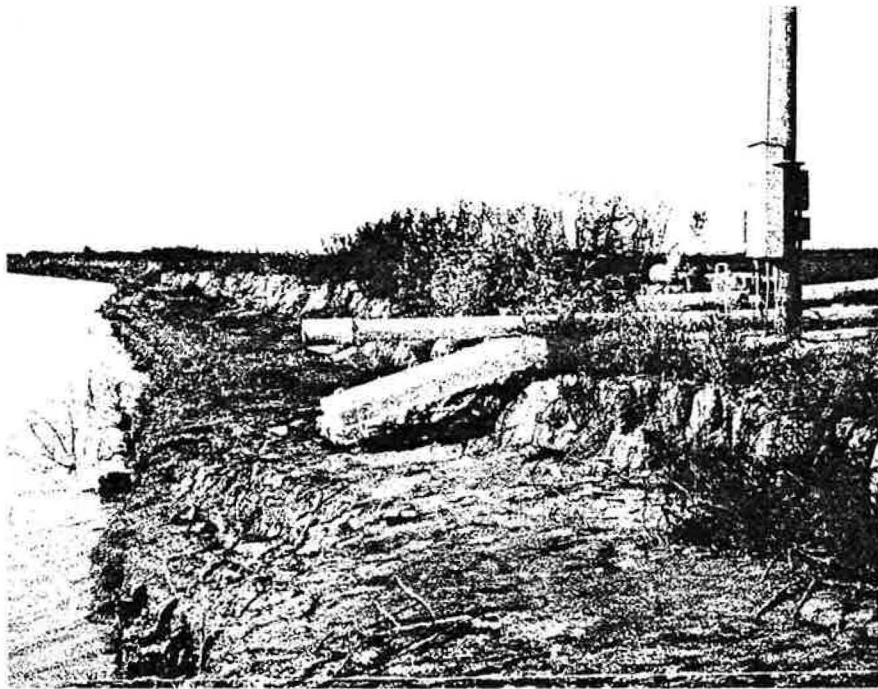


Figure 1. Progressive Wave Damage to an Irrigation Dam



Figure 2. Salvaged Brick Used for Slope Protection

protection system was installed on three sections of the dam subjected to wave erosion. The erosion experienced on sections without protection was monitored at three locations adjacent the sand pillow sections. Fourteen profiles within these unprotected sections were surveyed at regular intervals.

2. Model Study. The objectives of the model study were to determine the effect of certain wave parameters on the stability of the sand pillow slope protection system, to monitor the erosion resistance offered by the sand pillows and to formulate design criteria for the system based on soil and local wind conditions. The main wave parameters investigated were wave height and wave period. The effects of scaling (viscosity effect), wave steepness, relative wave runup on the sand pillows and embankment slope angle were also investigated. A proposed design equation for determining the average weight of the individual sand pillows to be used on full scale projects was established based on the data obtained in this study. The design weight of the filled bag is a function of wave height, embankment slope angle, soil properties, wave period and scaling effects.

II. ENGINEERING USE OF FABRICS

Synthetic filter fabrics have been utilized for various engineering applications. Woven and non-woven fabrics have been incorporated in designs over weak soils, drainage structures, and water-front applications as well as other structures requiring filter systems. The first application of a synthetic filter fabric in a civil engineering structure occurred in Florida during 1958. A plastic filter cloth was placed beneath a concrete block revetment to prevent waves from eroding the sand which supported the blocks. One of the first uses of a filter fabric on the West Coast occurred in 1963. A filter cloth was used to retain medium-grained sand behind a quarry stone seawall. The gradation of the sand and protective stone was such that a 6 foot (1.83 m) multi-layer granular filter system was required.

B. SCOPE OF THE REPORT

The purpose of this study was to analyze a new synthetic fabric in the form of sand pillows to be used as slope protection for irrigation dams. The project was to be performed in two phases. The first phase of the program consisted of an actual installation and evaluation of a full scale protection system. Phase two of the program was a medium-scale model study of the pillows in a controlled laboratory wave tank equipped with a wave generating device.

1. Field Study. The objective of the field study was to determine the feasibility of placing the bags (pillows) with equipment and resources available to a typical farmer, to monitor the erosion protection offered by the system and to compare the performance of various irrigation dams near the project site with the study site. The durability and soil retention characteristics of the fabric were also evaluated.

A full-scale field installation was used to evaluate the placement requirements and erosion protection offered by the sand pillow system. Inspection of several irrigation dams near the project site provided information regarding the relative performance of the system. Laboratory tests were performed to evaluate the resistance of the fabric to field exposure and to evaluate the soil retention characteristics of the fabric.

The slope protection system was installed on an operational irrigation reservoir using farm equipment available on a typical Missouri farm to handle the soil material and to fill the bags. Tractors were used to transport the filled bags to the upstream slope of the dam and to provide the electric power required to operate a hand-held sewing machine used to close the bags.

The effectiveness of the slope protection system has been evaluated by monitoring the performance of test sections on the dam. The fabric slope

In addition to the cost and construction difficulties of such a filter the limited easement at the site did not permit such a thick filter and a fabric material was substituted. Dallaire (1977) reports that thirteen years after construction the seawall is in excellent condition, with no evidence of loss of the supporting sand material. Since these first applications over 5000 projects utilizing filter fabrics have been successfully completed. Installations in all 50 states and 26 foreign countries attest to the widespread acceptance of fabric filter systems.

Filter fabrics offer several advantages over conventional granular filters. The filter fabrics' primary advantage is one of economics. The savings due to the ease of installation and inspection of a filter fabric system is a major factor in the cost effectiveness of such a system. Filter fabrics are much easier to place than traditional granular filters. Even in areas with locally available granular filter material, filter fabrics have been used extensively. Dallaire (1977) notes that in the Memphis, Tennessee area filter fabrics are used due to cost savings and ease of placement. This is a region of the country with ample supplies of well-graded aggregate.

The need for an engineering fabric capable of resisting outdoor exposure conditions stimulated interest in acrylic fabrics. Nylons and polyesters offer great strength and abrasion resistance, but are adversely affected by sunlight. Acrylic fabrics are resistant to sunlight, weathering, soil burial and deterioration from other causes such as mildew and insect attack.

Resistance to deterioration by sunlight and weathering is a must in fabric products used for sandbags. The resistance of acrylic fabrics to these agents has been documented by Monsanto and other fabric producers, the U.S. Government and various universities. One field test of acrylic fabric sandbags took place on the banks of the Tennessee River near Decatur,

Alabama. As the river level fluctuated the bags were sometimes submerged and at other times exposed to a variety of weather conditions. After 36 months of exposure the acrylic sandbags showed no loss of strength.

Acrylic fabrics have excellent resistance to the various micro-organisms encountered in soil burial tests. Three recent evaluations performed by Monsanto showed no loss in strength due to soil burial of up to one year. Acrylic fabrics are not eaten by insects encountered in nature however, certain types of insects will cut their way out if imprisoned within the bags. For more information concerning acrylic fabrics reference is made to "Acrylic Sand Pillows: A New Approach to Erosion Control" (1976). This special presentation to the U.S. Department of the Army is available from the Monsanto Textiles Company.

Recently, synthetic fiber fabrics have been introduced as a means of slope protection. There are a variety of materials advertised and their shapes and sizes are many. One such product is manufactured by Erosion Control, Inc., and is under the trade names of Dura-bags* and Perma-bags* (Erosion Control, 1976). Dura-bags are made of a synthetic fiber material, coated with polyvinyl chloride for sun protection, and are designed to be hydraulically filled by sand in place. Perma-bags are similarly made of synthetic fiber but are uncoated and are filled with concrete or grout. Although both have been in limited use to date, the manufacturer has reported effective use in structures such as groins, revetments, seawalls, and breakwaters (Figure 4). Because of the large size and weight of the bags, 3.0 cu. yds. (2.3 m^3) and 8,500 lbs. (3855.5 kg) filled, they are generally considered uneconomical for small lakes and local erosion problems.

On a smaller scale, Monsanto Textile Company has developed the acrylic sand pillow made of a synthetic fiber manufactured under the trade

*Registered trade name of Erosion Control, Inc.

CHANNEL EROSION CONTROL

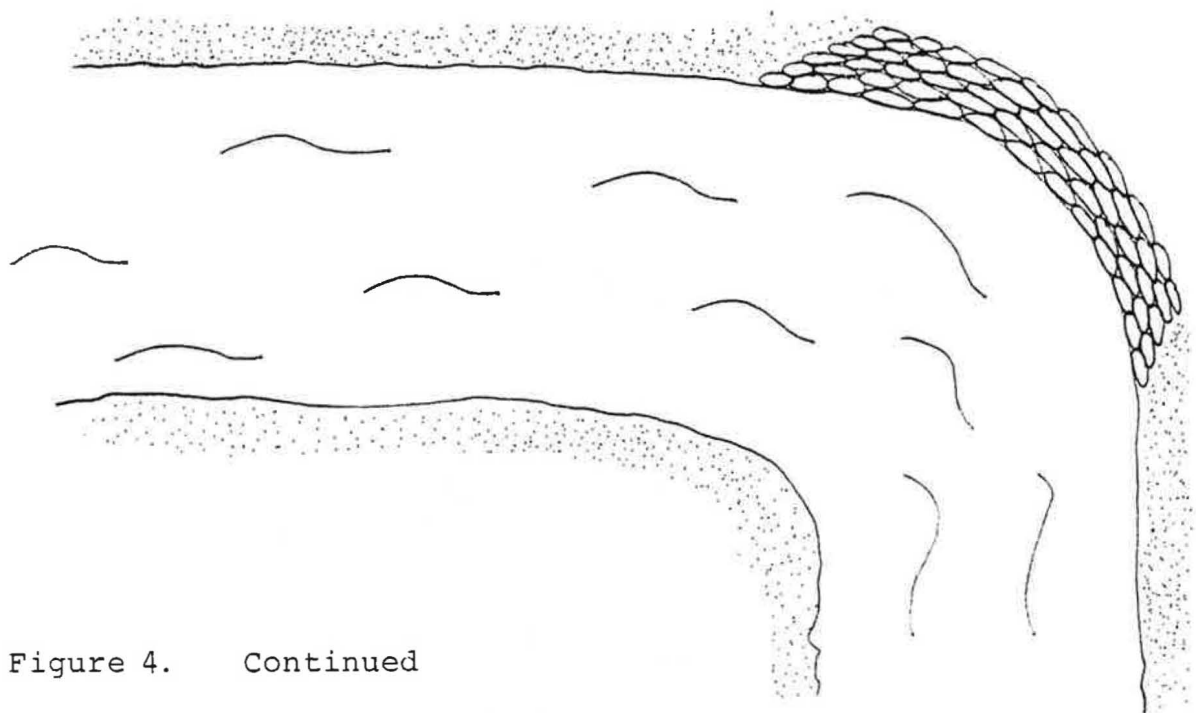


Figure 4. Continued

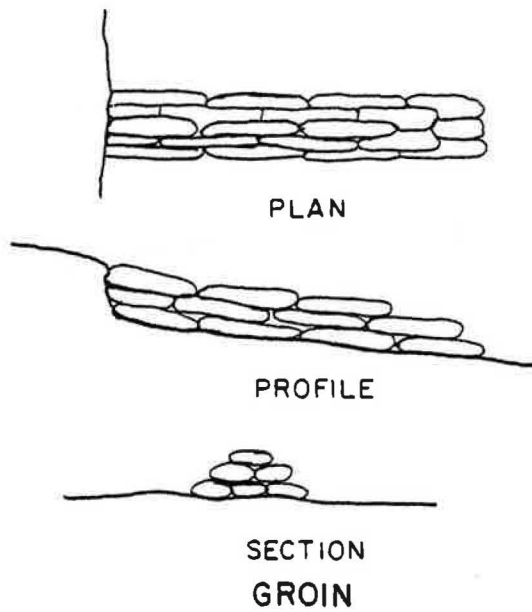
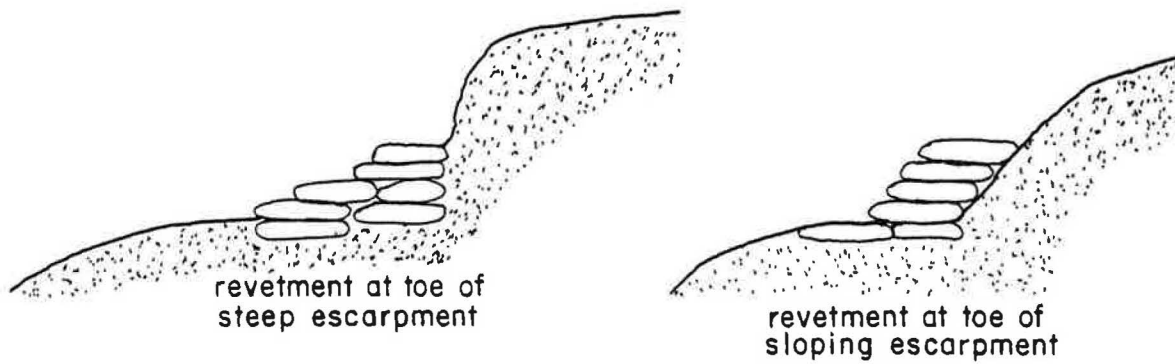


Figure 4. Typical Dura-bag and Perma-bag Structures, (Erosion Control, 1976)

The tensile tests were performed utilizing a Tinius Olsen Testing apparatus in the 0-200 pound (p.889.6 n) testing range. After experimentation it was possible to produce failures within 20 ± 3 seconds.

2. Results. The physical characteristics of the fabric used for the sand pillow slope protection system were evaluated. The strength of the fabric governs the ability of the system to resist wave forces. The resistance of the fabric to deterioration by various natural agents was also evaluated. The life expectancy of the sand pillow slope protection system is a major factor in the economics of such an installation. The ability of the fabric to retain fill material when subjected to repeated wave action has been evaluated since the ability of the bags to retain fill material will control the erosion resistance of the system. The bags must retain fill material during the repeated attack of waves.

The ability of the acrylic fabric to withstand various elements of field exposure will determine the life expectancy of such a system. Table I shows the results of one-inch raveled strip tests performed on the original fabric. Samples were tested in a dry condition and after soaking in water for a period of 24 hours. These results show the original strength properties of the fabric. Table II shows the results of one-inch raveled strip tests performed after the fabric slope protection system had been exposed to the environment for a period of seven months. Samples were taken from bags that remained below the water surface during this interval and from bags that were exposed to unrestricted sunlight. The fabric slope protection system was exposed on the southern face of the dam and therefore the maximum sunlight exposure for this portion of the state. Table III shows the results of tensile tests performed after one year of exposure to the environment. Due to the lowering of the reservoir level as irrigation water was used the first set of results represent bags submerged for

name of Acrilan. This product is the main subject of this study and has been discussed in previous sections of the report. A primary use of acrylic sand pillows is where an erosion control product is needed that has great durability, ease and economy of installation, and attractive cost/benefit relationships. The first large scale use of this product is on the Red River at Morameal near Shreveport, Louisiana.

III. FABRIC TESTING PROGRAM

A. RESISTANCE TO DETERIORATION

1. Testing Method. Tensile strength tests were performed to evaluate the resistance of the fabric to deterioration. The tests were performed after intervals of exposure to the environment. The strength of the fabric after exposure was compared to the results of tensile tests on the original fabric. Two types of field exposure were tested. Samples of the fabric were obtained from bags that remain exposed to direct sunlight and weathering agents. Additional tests were performed on fabric samples from bags that remained submerged at the normal reservoir level. These tensile tests were performed according to the ASTM 1 inch (25.4 mm) Raveled Strip Method. This test is recommended for fabrics with a minimum of 20 yarns per inch that may be readily raveled. The test method is described in ASTM D1682-64 (Reapproved 1970) "Breaking Load and Elongation of Textile Fabrics." The raveled strip test is one of several standard strength tests applicable to fabrics. The strength obtained from the raveled strip test reflects the resistance of a specific width of fabric to rupture. The fabric samples are cut to a width of 1 1/2 inch (38.1 mm) or 1 inch (25.4 mm) plus 20 threads, whichever is the larger. The sample length was at least 6 inches (152.4 mm). This sample is then raveled so that the tested specimen has a width, excluding fringe, of 1 inch (25.4 mm).

TABLE I
RESULTS OF TENSILE TESTS ON THE ORIGINAL FABRIC

Fabric Condition	Rupture Load	
	Pounds	(Newtons)
Wet	62	276
	64	285
	60	267
	60	267
	64	285
	60	267
	63	280
	60	267
	61	271
	66	294
	Mean	62
Standard Deviation	2.2	9.8
Dry	62	276
	60	267
	64	285
	62	276
	62	276
	66	294
	63	280
	60	267
	64	285
	61	271
	Mean	62.4
Standard Deviation	1.9	8.4

TABLE II
 RESULTS OF TENSILE TESTS ON THE FABRIC
 AFTER SEVEN MONTHS OF EXPOSURE

Fabric Condition	Rupture Load	
	Pounds	(Newtons)
Submerged	70	311
	60	267
	62	276
	64	285
	64	285
	59	262
	60	267
	62	276
	66	294
	60	267
	Mean	62.7
Standard Deviation	3.4	15.1
Fully Exposed	64	285
	62	276
	66	294
	62	276
	60	267
	61	271
	64	285
	62	276
	60	267
	64	285
	Mean	62.5
Standard Deviation	2.0	8.7

approximately eight months and exposed to direct sunlight for four months. These test results indicate that the fabric has effectively resisted deterioration during the first year of exposure. Statistical analysis (t-test) indicates that with less than a 5 percent chance of error the tensile strength tests were performed on samples with the same mean.

B. SOIL RETENTION CHARACTERISTICS OF THE FABRIC

1. Immersion Tests. To determine the ability of the synthetic fabric to retain its fill material when submerged repeatedly in water, a dunking apparatus was designed and built. This test was designed to simulate the constant wave action attack upon prototype sand pillows.

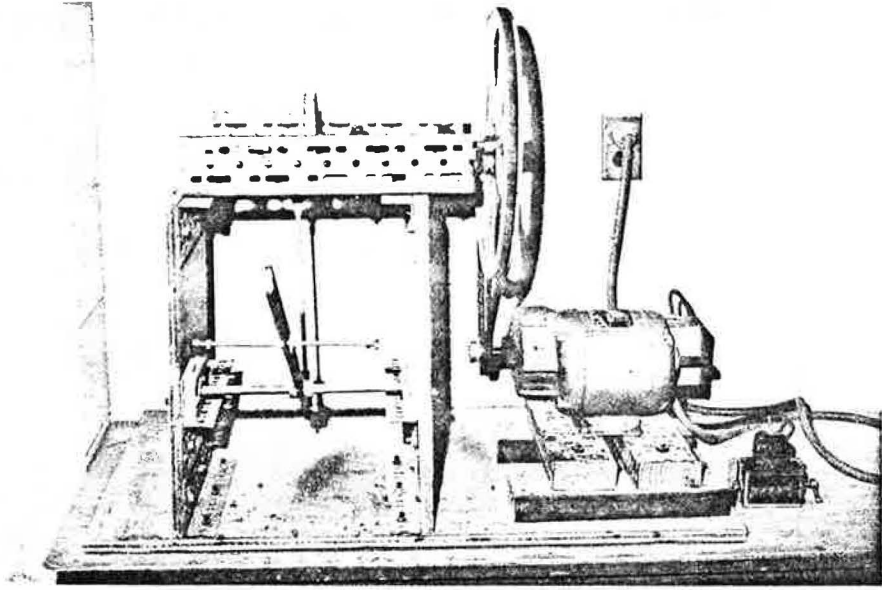
a. Apparatus. The equipment used for this test is shown in Figure 5. It consists of an electric motor-operated rocker arm with a vertical displacement of approximately 10 in. (254.0 mm) set at a speed of 37 cycles (or dunks) per minute. Two 10,000 ml plexiglass cylinders were used as water containers.

Sixteen inch (406.4 mm) diameter retainers were made from a representative piece of the fabric. These bags were filled with the material to be dunked and were wired shut at the top to prevent any loss of soil (Figure 6). With this method, any soil lost during the test would be filtered directly through the fabric and not through the seams that were on two sides of all bags used in previously performed tests.

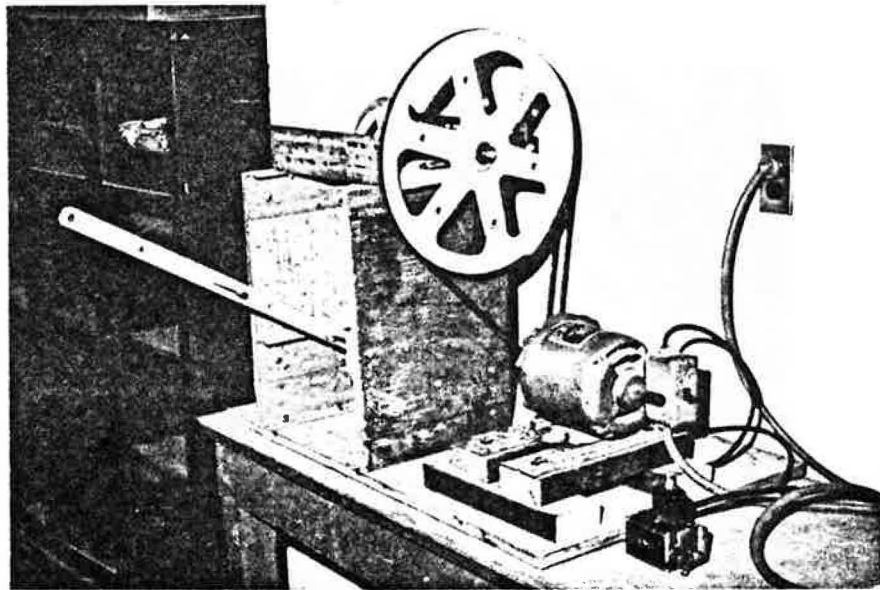
b. Testing Material. Two types of soil were used for fill material during the dunking tests. The first material tested was the previously described Mexico clay. The second type of soil tested was obtained from near Quincy, Illinois. This soil, herein referred to as Quincy loess, is a brown, silty-loessial soil that is quite common in that Illinois region. It has a specific gravity of 2.68 and a grain size distribution as shown in

TABLE III
RESULTS OF TENSILE TESTS ON THE FABRIC
AFTER ONE YEAR OF EXPOSURE

Fabric Condition	Rupture Load	
	Pounds	(Newtons)
Partial Submergence	60	267
	62	276
	62	276
	64	285
	60	267
	64	285
	64	285
	60	267
	61	271
	64	285
	Mean	62.1
Standard Deviation	1.8	8.0
Fully Exposed	63	280
	62	276
	60	267
	66	294
	64	285
	62	276
	61	271
	60	267
	66	294
	62	276
	Mean	62.6
Standard Deviation	2.2	9.9

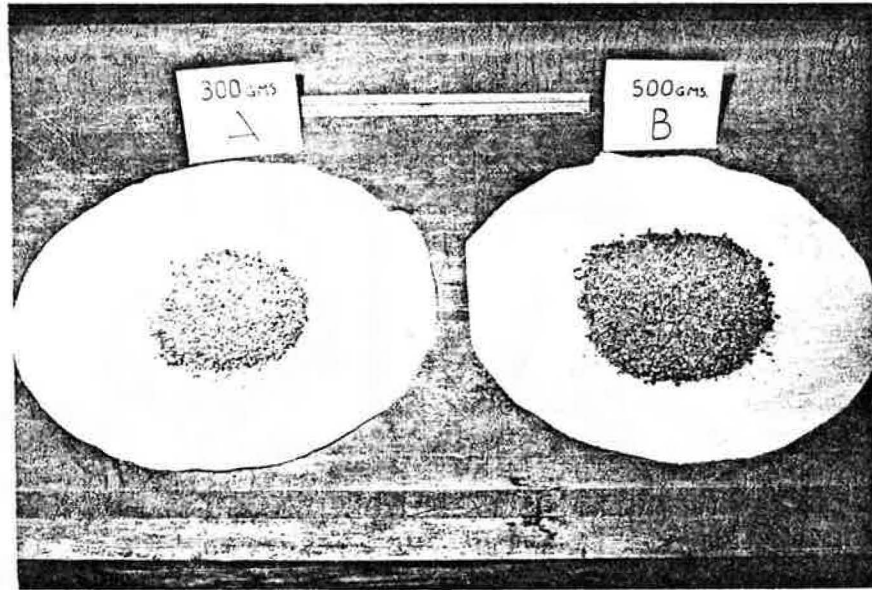


a. Front View

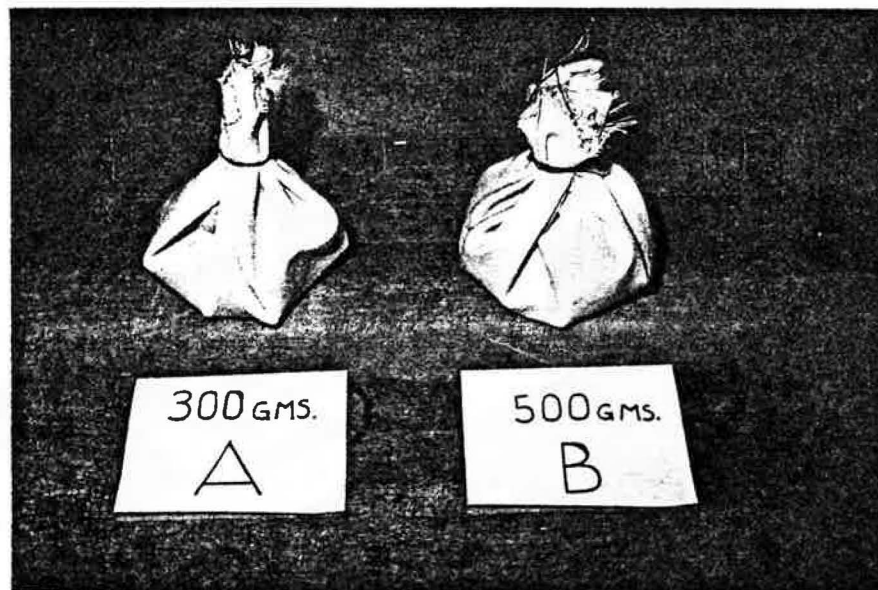


b. Side View

Figure 5. Front and Side View of Dunking Apparatus



a. Before Closing



b. After Closing

Figure 6. Test Soil Bags

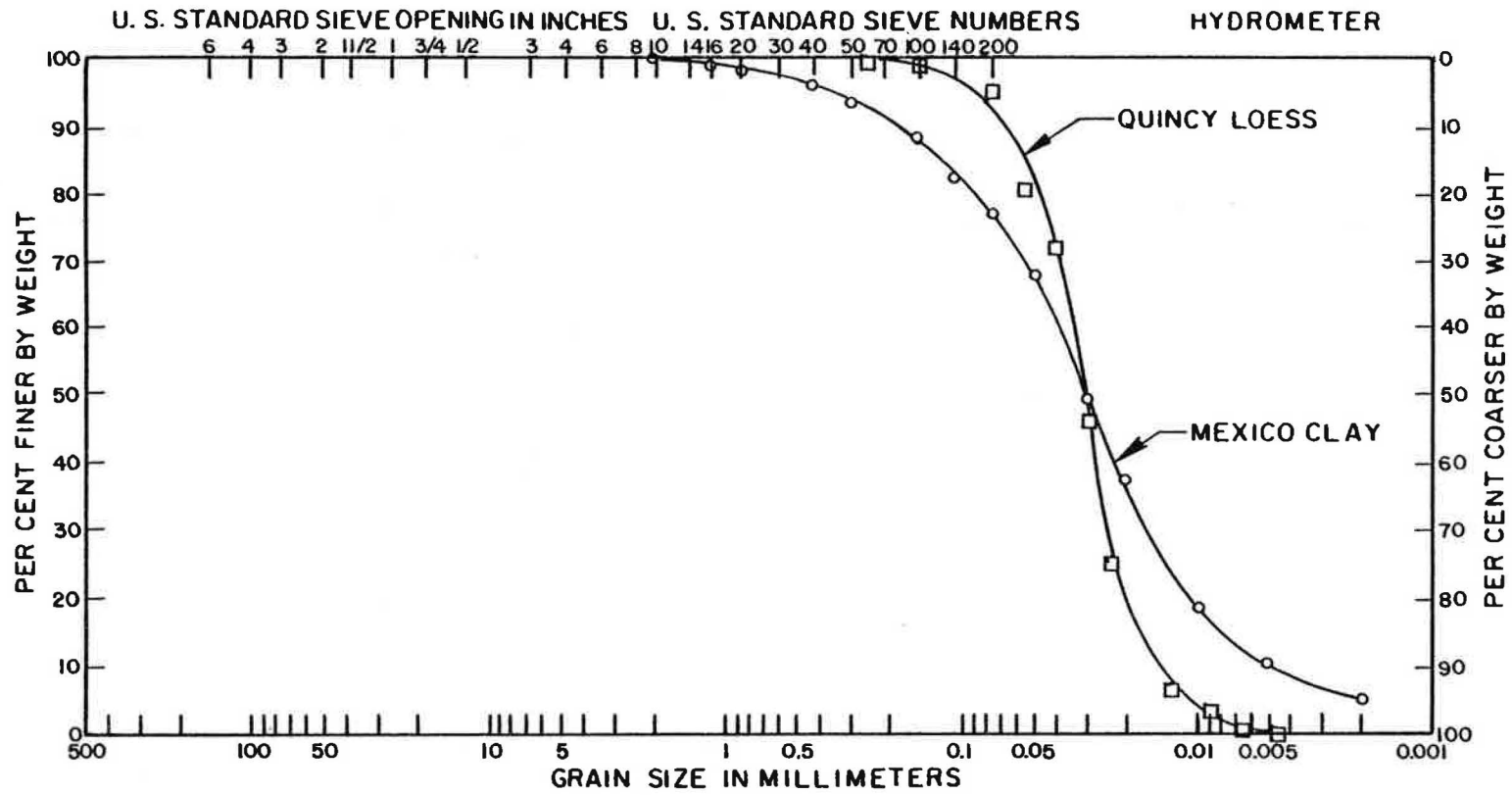


Figure 7. Grain Size Distribution Curves of Tested Soils

Figure 7. (Note that again the term Quincy loess is not the agricultural soil name but is used in this study as reference to the soil's location).

c. Procedure. Oven-dried samples of Mexico clay were passed through a No. 4 sieve to eliminate gravel and to obtain some uniformity in the tested soils. Two samples, one weighing 300 ± 1 g (0.66 lb), and the other weighing 500 ± 1 g (1.10 lb), were placed in separate circular pieces of fabric, the material wired shut and suspended from the rocker arm. The equipment was designed so that two tests could be conducted simultaneously.

Approximately 4,000 ml (1.06 gal.) of water were placed in each cylinder and the cylinders were placed so that when the rocker arm was at its highest position, the suspended bags cleared the water by approximately 7 in. (178.0 mm). This distance prevented the tops of the bags from becoming completely submerged and yet allowed the soil in the bags to be submerged (Figure 8).

After the bags had been immersed and removed from the water 1000 times, the apparatus was stopped with the rocker arm at its highest point. The bags were allowed to hang from the rocker arm until dripping had stopped.

The water and soil mixture was carefully poured into a pre-weighed tare and oven-dried until all water had been evaporated and only the dried soil remained. The oven-dried soil was weighed and recorded as soil lost during dunking.

The dunking test was repeated with the Mexico clay by increasing the number of dunks to 3000, 5000, 7000, and 10,000 dunks. The entire sequence of tests was repeated so that a total of ten 300 g samples (0.66 lb) and ten 500 g (1.10 lb) samples were tested for a combined total of twenty tests.

Oven-dried samples of Quincy loess were used for the next series of testing and the procedure followed was as described for the Mexico Clay except for the following:

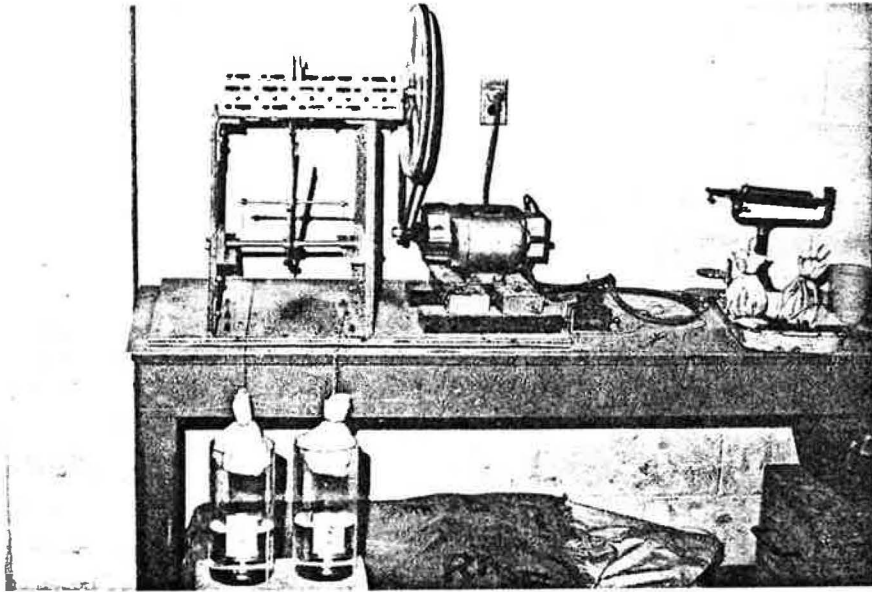


Figure 8. Samples Ready for Testing

1. All bags were filled with 300 g (0.66 lb) of loess,
2. Six tests each were performed at 1000, 2000, 5000, 7000, and 10,000 dunks for a total of thirty tests.

Splashing and bag vibration were considered by varying the depth that the bags were submerged in the water. Bags of Quincy loess were submerged 100%, 75% and 50% of their length and the results compared.

2. Grain Size Distribution Analysis. Another series of dunking tests was conducted using the previously described apparatus and procedures, in order to determine the ability of the synthetic fabric to act as a filter material. The soils used as fill material in these tests were again the Mexico clay and the Quincy loess.

Initially, three combined grain size and analyses for each soil were conducted on the Mexico clay and Quincy loess (U.S. Army, Corps of Engineers, 1970). The three tests for each soil were averaged and the results plotted to form grain size distribution curves (Figure 7). One exception to the standard testing procedure was that due to the fine nature of the soils and their tendency to form hard lumps upon drying, the representative soil samples used for each test had to be initially wet sieved through a No. 200 sieve before testing. This was to insure proper distribution of the fines when sieved.

Two oven-dried 300 g (0.66 lb) samples of Mexico clay were submerged and immersed 10,000 times using the equipment and procedure described above. Upon completion of the dunking, the bags were allowed to hang until dripping had stopped. The material remaining in the bags was carefully removed and the inside of the cloth was thoroughly washed to remove particles that might have been caught in the fabric. This soil was wet sieved over a No. 200 sieve and the material coarser than the No. 200 was oven-dried and a standard grain size analysis was performed. The soil that was

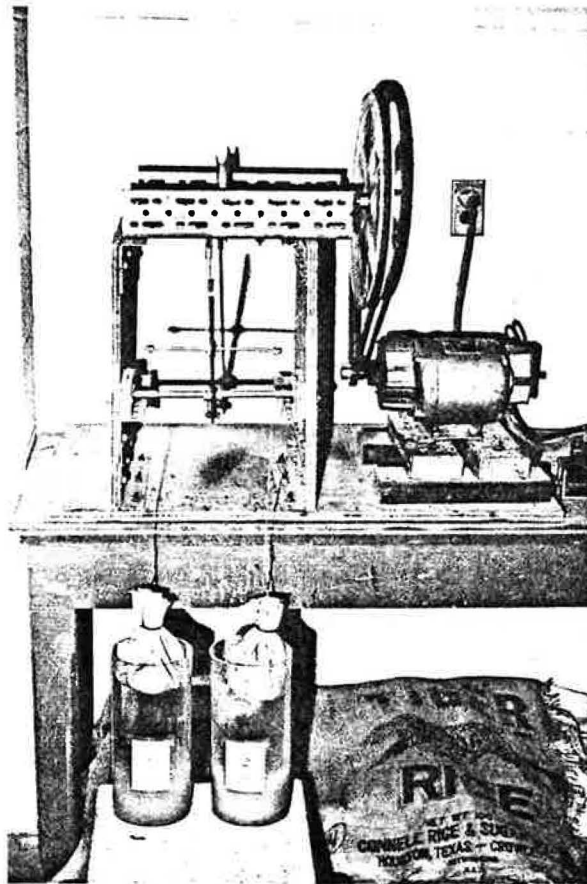


Figure 9. Typical View of a Completed Immersion Test

finer than the No. 200 sieve was air-dried and a representative sample was obtained for use in a hydrometer test. The combined results of the grain size analysis were based on the original 300 g (0.66 lb) of soil placed in the bags before dunking.

This sequence of testing was repeated for two 300 g (0.66 lb) samples of Quincy loess. Since there is considerable variation in the amount of material lost through the fabric due to vibration while dunking, it was decided that the dunking test on the Quincy loess should be performed such that only 50% of the bag should be submerged and excessive splashing eliminated. This would give loss of fill percentages on the order of that determined for the Mexico clay.

3. Soil Loss Results. The measurement of the amount of soil lost through the fabric by continued wave action was achieved by the use of a laboratory immersion device previously described. Figure 9 shows a typical photograph of a completed test before the determination of the amount of soil lost through the bag was made.

In every test the weight of fill material lost from each bag was calculated by using Equation

$$\text{Loss of fill, g} = W - T \quad (1)$$

where

W = weight of tare plus oven-dried fill, g

T = weight of oven-dried fill, g.

The percent of fill lost from each bag was calculated by using Equation (2)

$$\text{Percent loss of fill, \%} = \frac{(W-T)}{W_0} \times 100 \quad (2)$$

where

W_0 = weight of oven-dried fill originally placed in the bags.

TABLE IV
SOIL LOST THROUGH FABRIC FOR MEXICO CLAY

Number of Dunks	Trial 1		Trial 2		Average		Combined Average (%)
	Bag A ¹	Bag B ²	Bag A	Bag B	Bag A	Bag B	
1000	1.70	3.12	1.98	1.54	1.84	2.33	2.09
3000	4.25	3.62	3.95	3.88	4.10	3.75	3.93
5000	5.08	5.32	4.00	5.48	4.54	5.40	4.97
7000	6.28	7.23	4.98	6.89	5.63	7.06	6.35
10000	9.16	6.30	8.52	8.74	8.84	7.52	8.18

Note:

¹ Bag A weighs 300 g (0.66 lb)

² Bag B weighs 500 g (1.10 lb)

The first series of immersion tests was conducted on Mexico clay samples. Two samples, one weighing 300 g (0.66 lb) and the other weighing 500 g (1.10 lb), were tested with the number of immersions varying from 1000 to 10,000. Table IV gives a complete listing of all test results for the Mexico clay. Figure 10 shows the results of the average percent soil loss for Bag A and Bag B. Figure 11 gives the average result of the curves from Figure 10.

Both the 300 g (0.66 lb) bag and the 500 g (1.10 lb) bag showed the same general trend of increasing percent loss with increasing number of dunks. Figure 10 also shows that when tested under the same condition, the weight of the bag has no significant effect on the amount of soil that will be retained.

The second series of immersion tests was conducted on the Quincy loess with the same apparatus as previously described. However, after conducting a few preliminary dunking tests it became apparent that the amount of soil lost was very much a function of the amount of vibration or submergence that occurred during the test. Therefore, thirty tests were performed with the amount of submergence or vibration being altered from completely submerged to 75% submerged and finally 50% submerged. The testing was performed with a series of dunkings ranging from 1000 to 10,000 immersions. Table V gives a complete listing of the test results. Figure 12 is a graphical presentation of the average percent loss found in Table V.

In all three cases, the percentage of soil lost increases with the number of dunks, as would be expected. However, the average percent loss increase is not constant for all three cases of vibrations with the most vibration case losing 85.7% of its soil after 10,000 dunks.

MEXICO CLAY
COMBINED AVERAGE PERCENT SOIL LOSS
VERSUS
NUMBER OF DUNKS

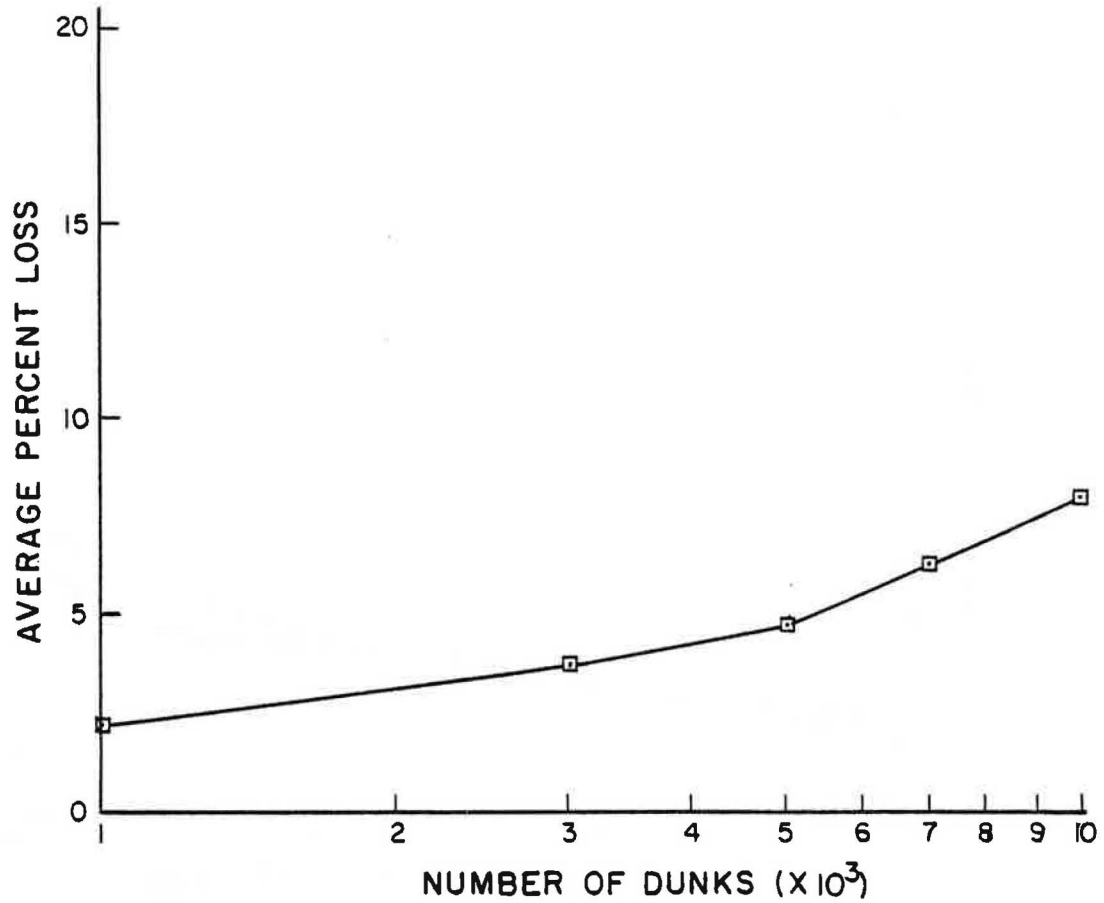


Figure 11. Combined Average Percent of Soil Lost for Mexico Clay Samples

MEXICO CLAY
AVERAGE PERCENT SOIL LOSS
VERSUS
NUMBER OF DUNKS

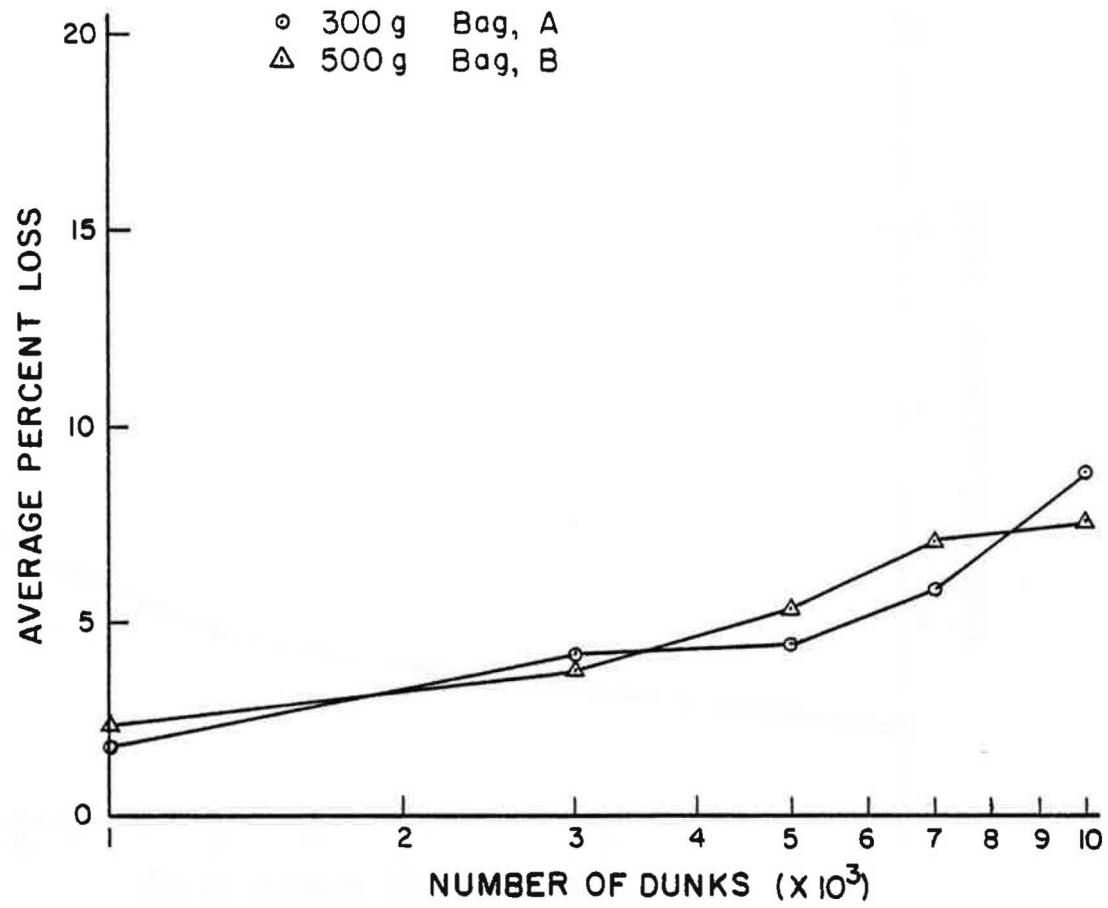


Figure 10. Average Percent of Soil Lost for Mexico Clay Samples

TABLE V
EFFECT OF VIBRATION ON QUINCY LOESS

Number of Dunks	Test No. 1 ¹		Test No. 2 ²		Test No. 3 ³		Avg. Test No. 1	Avg. Test No. 2	Avg. Test No. 3
	Trial 1	Trial 2	Trial 1	Trial 2	Trial 1	Trial 2			
1000	12.6	7.8	7.2	7.0	4.1	2.3	10.2	7.1	3.2
2000	14.4	23.6	12.3	7.9	3.6	4.2	19.0	10.1	3.9
5000	35.3	41.5	22.3	17.7	7.6	7.4	38.4	20.0	7.5
7000	73.6	77.2	33.8	38.6	11.2	9.4	75.4	36.2	10.3
1000	90.0 ⁴	81.4	45.1	42.3	12.9	11.1	85.7	43.7	12.0

Notes:

¹Test No. 1 = completely submerged

²Test No. 2 = 75% submerged

³Test No. 4 = 50% submerged

⁴All values are expressed as a percent of soil lost during dunking

QUINCY LOESS
AVERAGE PERCENT SOIL LOSS
VERSUS
NUMBER OF DUNKS

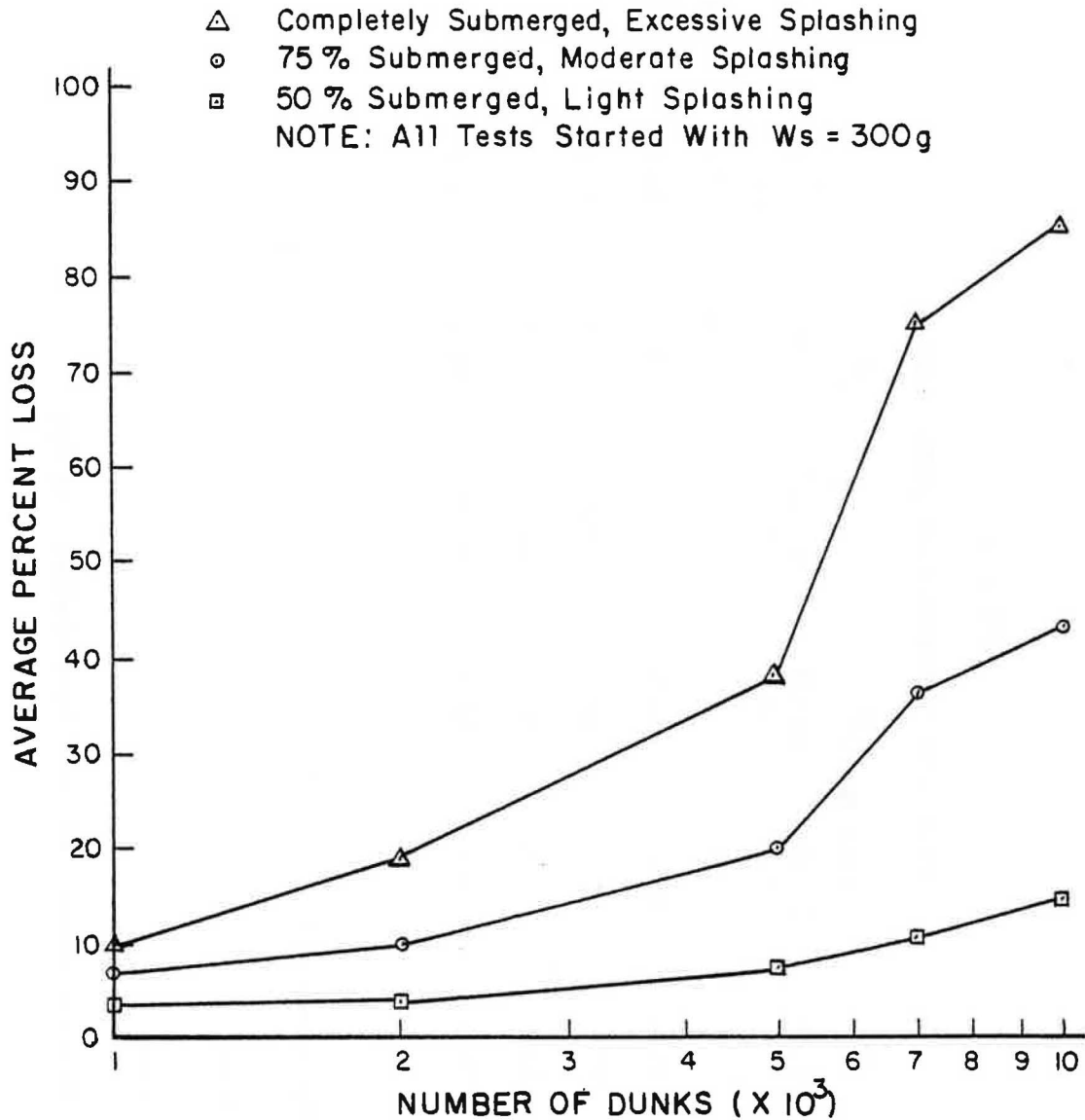


Figure 12. Average Percent Soil Loss as a Function of Vibration for Quincy Loess

cohesionless material. Excessive vibration while submerged simply accelerates the leaching process by constantly rearranging the particles and thereby permitting faster saturation of the particles.

Although the above is a highly oversimplified description of the actions of clays and loess when in contact with water, the general reasoning could be one explanation as to why loss of loess was a function of vibration while immersed and the clay apparently was unaffected.

4. Grain-Size Distribution Results. To observe what percentage of fines was lost through the fabric when subjected to repeated wave action, wave action, a series of immersion tests was conducted on Mexico clay and Quincy loess samples.

The initial grain size distribution curves for three clay samples and three loess samples were obtained before dunking and are shown in Figures 13 and 14 as the average of three clay and three loess samples,

The initial grain size distribution curves for three clay samples and three loess samples were obtained before dunking and are shown in Figures 13 and 14 as the average of three clay and three loess samples, respectively. Two 300 g (0.66 lb) samples of each soil were dunked 10,000 times using the procedure and apparatus previously described. The soil retained in each test was used to obtain another grain size distribution curve for the "after dunking" soil. The total combined weight of these last curves was based on the original 300 g (0.66 lb) weight before dunking. The after dunking curves are shown as the average of the two samples of clay and loess in Figures 13 and 14 respectively.

From these curves it appears that some fine material was lost during each test as would be expected. Both soils lost some fines that were smaller than 0.06 mm, but the clay began losing fines initially that were

To fully understand the reasons for the extremely different actions of clay and loessial soil when in contact with water, a basic understanding of the physical properties of the two soils is needed.

Practically all clay minerals are sheet-like in structure. The sheets are characterized by an arrangement of atoms leading to a negative electrical charge on the flat surface, but with either positive or negative charges on the edges, depending primarily on the environment.

Pure water consists primarily of molecules of H_2O , but a few molecules always dissociate into hydrogen ions (H^+) and hydroxyl ions (OH^-). With impurities present, as in most water, the impurities also tend to dissociate into positively charged cations and negatively charged anions. Since the plane surface of the clay mineral is negatively charged, the hydrogen ions of the water and the cations of the impurities are attracted toward the surface of the clay particles. Various clays adsorb widely different amounts of cations. The water adjacent to the mineral itself tends to undergo alterations and may actually become adsorbed and form a structure of its own. The adsorbed ions plus the adsorbed water make up what is called the adsorption complex. Therefore, depending on the amount of impurities in the water and in the clay (e.g, the amount of silt), when water is added to clay, the particles will tend to group closer together and their cohesion will usually increase to a certain degree.

Loess on the other hand is a wind-laid soil which consists mainly of angular and subangular quartz grains that are only slightly cemented together. Cohesion in the loess is due to thin films of a slightly soluble cementing agents that cover the individual particles.

When loess becomes submerged it is likely to become very unstable because of the leaching effects of submergence. Leaching removes the cementing agent around the particles and the soil becomes an almost

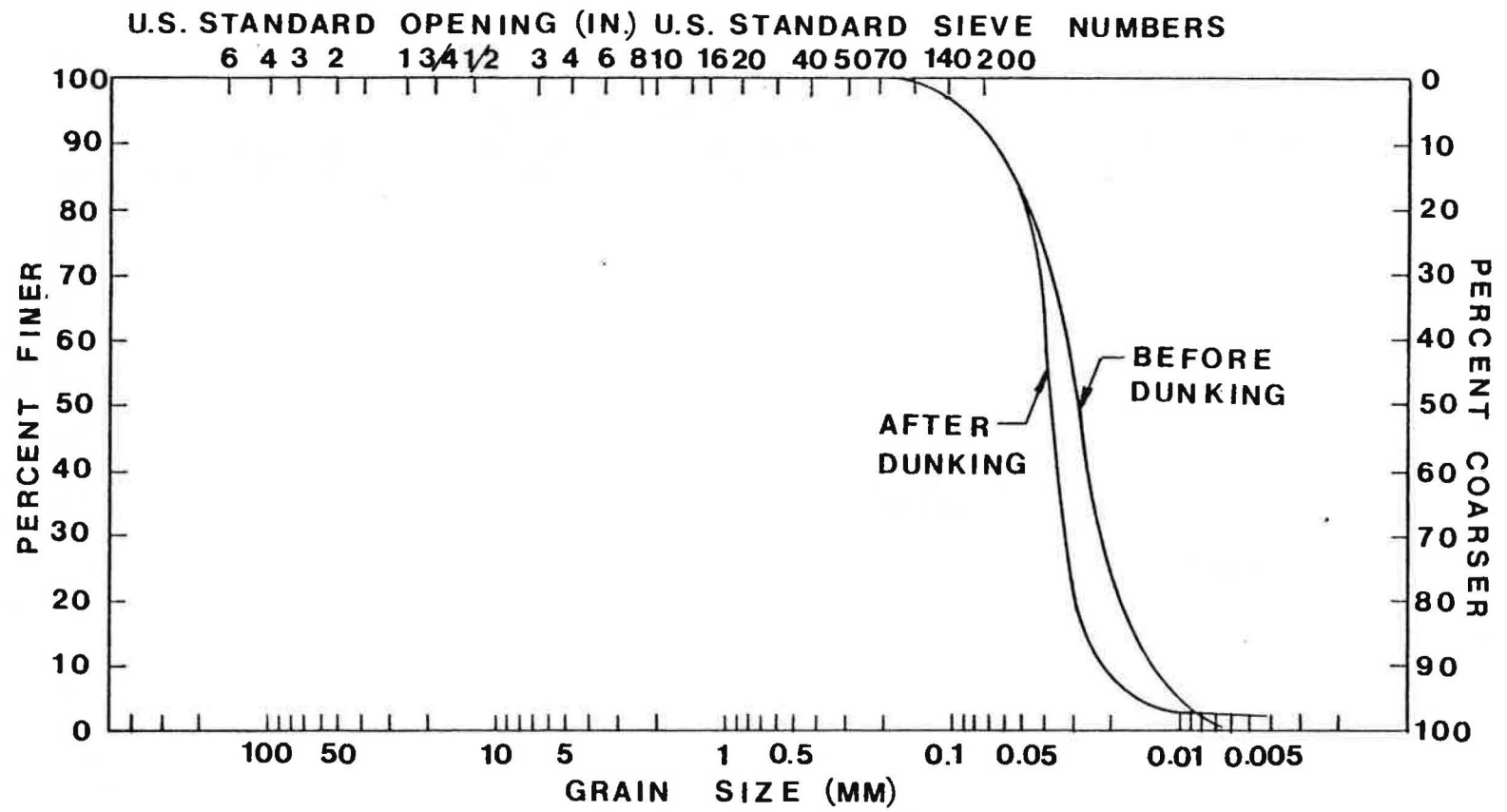


Figure 14. Comparison of Grain Size Analyses for Quincy Loess

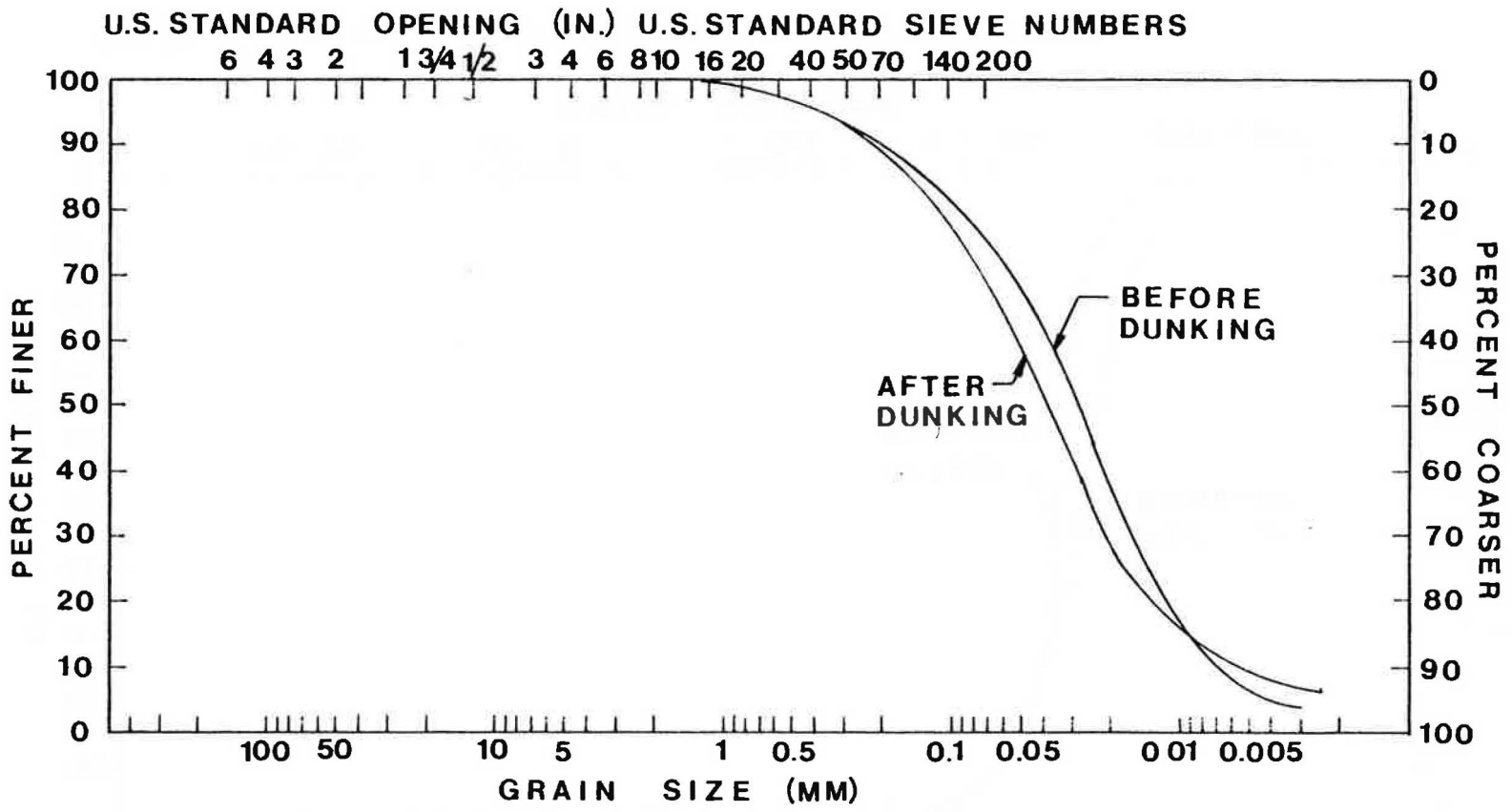


Figure 13. Comparison of Grain Size Analyses for Mexico Clay

equipment and resources available to a typical farmer. The performance of this slope protection system has been monitored by means of test sections established on the dam. The relative performance of the test site was compared to the performance of various slope protection systems at several irrigation dams near the project site.

B. FIELD EVALUATION OF THE SLOPE PROTECTION SYSTEM

1. Introduction. Four possible project sites were inspected in Audrain County, Missouri. Audrain County was selected for study because of the availability of dams undergoing significant erosion problems. Two types of dams are in general use in Audrain County. Where topographic conditions are favorable a dam across a natural drainage feature provides a most economical reservoir. However, Audrain County is located in the east central glaciated area of the state and many portions of the county are relatively flat without significant relief. Therefore at these sites, natural drainage ways do not carry significant flows. For these conditions a second type of reservoir is constructed and is referred to as a pump-in, due to the necessity of pumping into the reservoir all the water required for irrigation. The dams surveyed for the project are situated in a manner such that the water surface is located south and/or west of the upstream slope of the dam. Dams situated in such a manner are subjected to waves generated by the strongest prevailing winds in this portion of the state. A pump-in reservoir has their upstream slopes subjected to wind generated waves from any direction.

The dam, chosen for this field investigation, is the pump-in irrigation dam owned by Mr. Jake Freyer of Laddonia, Missouri. The dam is located 12 miles (19.31 km) east of Mexico, Missouri, approximately 1/2 mile (.80 km) west of U.S. Highway 54. The dam, completed in December of

smaller than a No. 70 sieve, i.e., 0.21 mm. It is possible that this difference could have occurred due to the aggregation of the clay soil before dunking and particle separation during dunking.

The difference in the percents finer by weight of the before and after dunking test of the clay samples is approximately 4% at a grain size of 0.1 mm. Since this difference is so small, it is possible that when the soil was initially wet sieved on a No. 200 sieve, some of the clay particles were not properly separated. When a grain size analysis was performed on the sample, the aggregated particles increased the amount retained on the lower numbered sieves, thus shifting the distribution curve upward. During the dunking phase, the clay particles separated and filtered through the cloth, the grain size distribution curves shifted downward.

Because of the difference in results in the two soils tested, no substantial conclusion as to the maximum size of particles that can be filtered through the fabric could be reached. It is therefore recommended that more fine-grained soils with a wider range of particle sizes be tested using this method of immersion so that perhaps a limiting particle size of soil can be established for use as a fill material in the sand pillow slope protection system.

IV. FIELD TESTING OF SAND PILLOWS FOR EROSION CONTROL

A. INTRODUCTION

A field evaluation of the acrylic sand pillow method of slope protection has been conducted on an irrigation dam near Mexico, Missouri. The slope protection system was installed on the upstream slope of an irrigation dam where wave erosion was anticipated. The field study deals with the feasibility of filling, closing and placing the bags with



Figure 15. East-West Portion of the Project Site--
November 1977



Figure 16. North-South Portion of the Project Site--
November 1977

1976, experienced very little wave erosion during 1977. Figures 15 and 16 show two views of the crest of the dam in November of 1977. These views reflect the almost unaltered condition of the upstream portion of the dam which was designed to have a slope of 1V on 3H. This is the steepest upstream slope recommended by the Soil Conservation Service. The dam is L-shaped with a total crest length of 1340 feet (408.43 m) and reaches a maximum height of 25 feet (7.62 m) in the north-east corner of the reservoir. Figure 17 shows the shape of the dam and the location of the water surface with respect to the dam. The surface area is 13.7 acres (55442 m²) and approximately 212 acre feet (261500 m³) of irrigation water is impounded.

2. Installation of the Slope Protection System. It is essential for the economical utilization of this slope protection system that a farmer be able to fill, close and place the bags with equipment and resources available to him. Elaborate equipment capable of filling and closing 500 bags per hour, as used on the Corps of Engineers Red River levee project, is not practical for a small irrigation dam. After some study, it was determined that a fertilizer cart used to spread dry fertilizer on farm fields could be modified to fill the bags. The cart normally utilizes a chain belt to remove fertilizer from the bin on the cart. The fertilizer then falls onto a fan which disperses it over the field. The chain belt and fan are normally powered by the revolutions of the wheels as the cart is pulled across a field. For the bag filling operation the cart was placed on blocks and the fan apparatus removed to allow easy access to the flow of soil material from the bin. The power takeoff shaft of a tractor was then attached to power the chain. This allowed variation of the belt speed and

therefore the flow rate of the material from the bin as required to fill the bags. The power take-off shaft was very carefully sheathed to avoid entangling loose clothing of the workers. Figure 18 shows the fertilizer cart and tractor used to fill the bags. A tractor with a front end loader was used to place stockpiled material into the bin. One worker with a shovel was stationed in or on top of the cart to maintain a flow of material to the chain. This was necessary due to the cohesive nature of the on-site material used to fill the majority of the bags. The remainder of the bags were filled with a cohesionless sand material. The sand flow required almost no supervision to maintain continuity. A bulldozer was used to stockpile the on-site material due to the frozen soil conditions when the majority of the bags were filled. Under more favorable conditions the bulldozer would not be required. Figure 19 shows a bag being filled. Upon filling, the bags were placed on a pallet behind one of two tractors. Figure 20 shows an overview of the filling operation with bags being placed on the pallets. The tractors were capable of carrying 15-20 bags per trip between the filling site and dam.

Another tractor was used on the dam to operate a generator to produce electricity to power a hand-held sewing machine used to close the bags. The hand-held sewing machine is the only specialized equipment required for the project. Figures 21 and 22 show the closing operation.

The local high school chapter of the Future Farmers of America provided assistance in filling and placing the bags on the dam. With a small amount of supervision and the assistance of 15 to 20 high school students it was possible to fill and place approximately 250 bags per hour. Figures 23 and 24 show the placement operation. Seven rows of bags were placed on the slope, two rows under the water surface and the remaining five rows on the portion of the slope subjected to wave action.

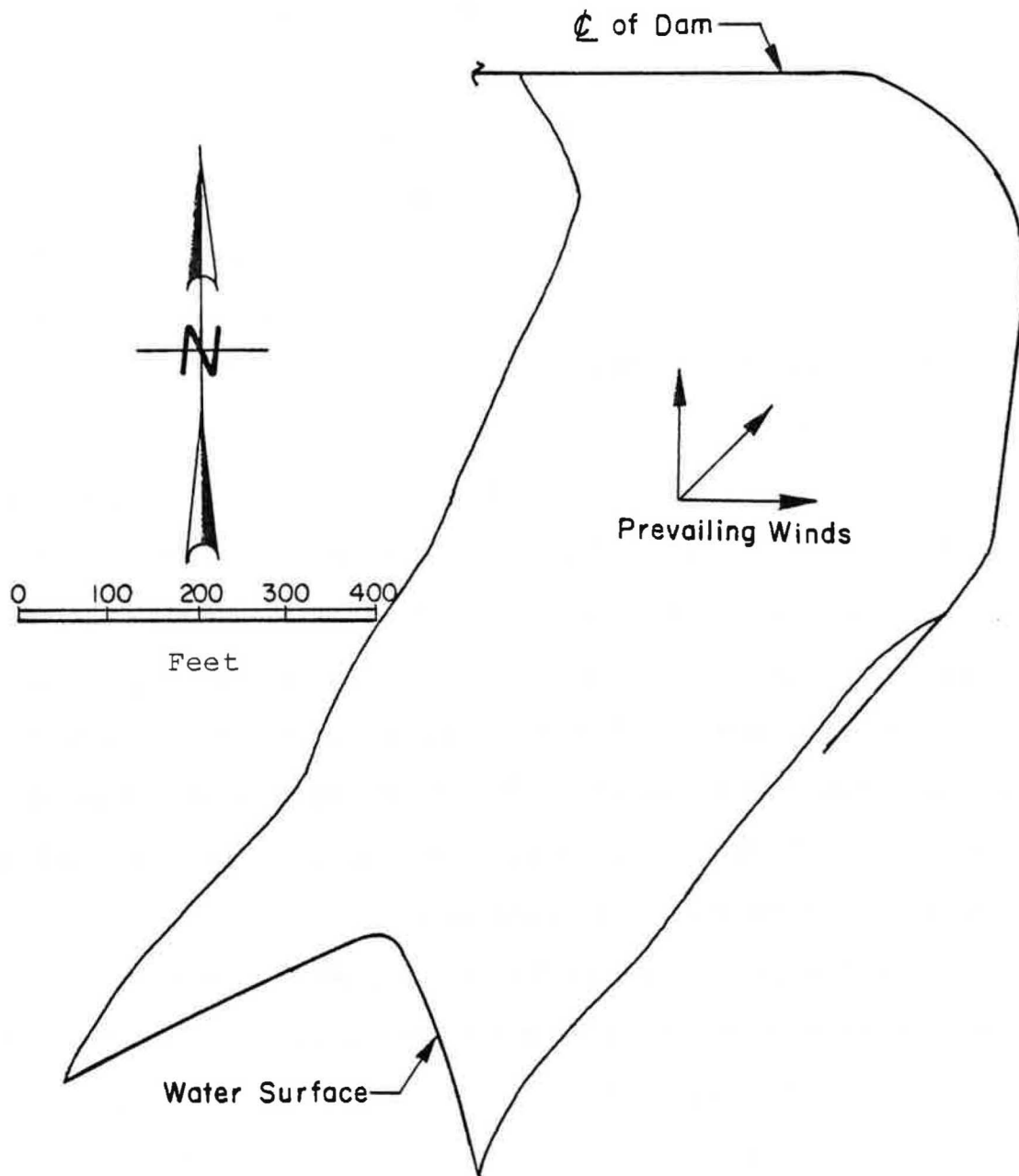


Figure 17. Configuration of the Project Site



Figure 19. Bag Being Filled



Figure 18. Fertilizer Cart and Tractor Used to Fill Bags



Figure 21. Sewing the Bag



Figure 20. Overview of the Filling Operation



Figure 22. Finishing the Seam .



Figure 23. Positioning the Bags on the Dam



Figure 24. Positioning the Slope Protection System

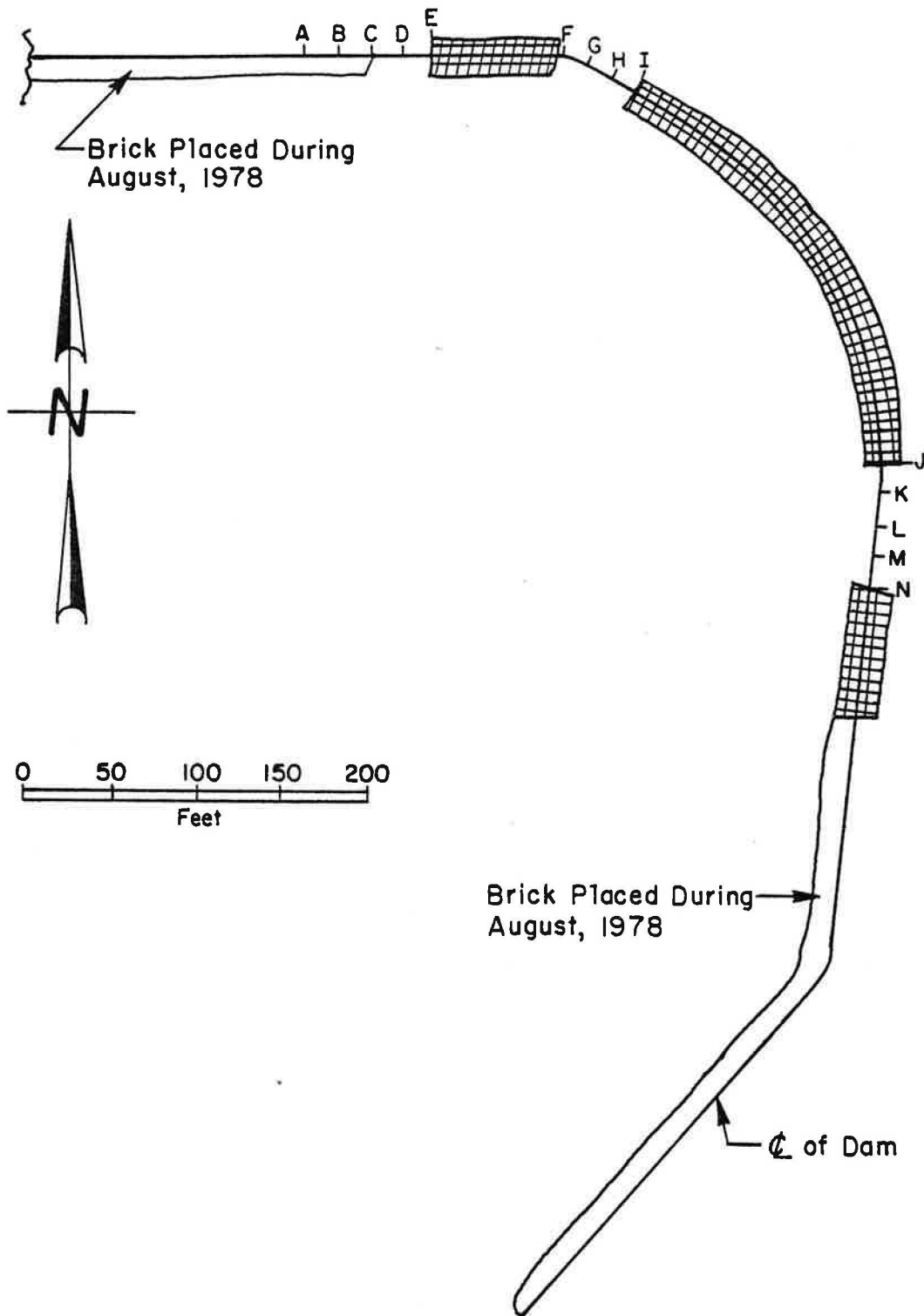


Figure 25. Location of the Test Sections of the Dam

3. In-Situ Monitoring of the Slope Protection System. The performance of the sand pillow protection system is being monitored by means of surveying test sections on the dam. Figure 25 shows the location of the sand pillow protected sections and unprotected sections. Two sections, 75 feet (22.86 m) in length, are located on the North and East upstream slopes of the dam. The third section, 45 feet (13.72 m) in length, is located in the northeast corner of the dam. These sections will receive direct wave attack from the prevailing wind directions of south, southwest and west. The sections contain evenly spaced profiles that are surveyed at regular intervals. These profiles, designated A-N, are located as shown in Figure 25. A benchmark was established in a 12 inch (30.48 cm) thorn tree approximately 225 feet (68.58 m) west of the reservoir. Three steel fence posts 6 feet (1.83 m) long were driven into the downstream slope of the dam. These posts provided turning points and a check at the end of each survey. The profiles are surveyed on 2 foot (.61 m) intervals down the slope. The distance to the break in the slope was measured and the elevation on each side of the break recorded. Three profiles, A-C, were covered during August of 1978 when the owner placed salvaged brick on the remaining exposed upstream slopes of the dam.

4. Results

a. Field Performance of the Slope Protection System. The performance of the acrylic fabric slope protection system has been evaluated on an operational irrigation dam. These results have been analyzed to provide specific data on the properties and requirements of this slope protection method. This data will facilitate the evaluation of this slope protection method as an economical solution to erosion control on additional irrigation dams.

bags. The cart offers a very stable and durable method of filling the bags. After filling the bags the cart can be used for various tasks on the farm. For this or subsequent projects a rental arrangement with a fertilizer distributor could be used to procure a cart for the short time required to fill the bags necessary for a typical installation.

The system was easily installed by personnel unfamiliar with the procedure. Simple instructions and supervision enabled high school students to place the bags upon the slope in a uniform and consistent manner. This produced a competent slope protection system without weak areas. Weak portions of typical slope protection systems have led to the progressive failure of such systems. The sand pillow system conforms easily to the shape of the dam. Vertical or horizontal curves present no installation difficulties.

The installation procedure required no special equipment after the bags were closed with a hand-held sewing machine. The closing operation proved to be the critical stage of the entire operation. One sewing machine was not adequate for the closing operation. Although part of the delays due to the closing operation resulted from the inexperience of the machine operator, the weakness of the thread used to sew the bags during the initial filling operation was the primary factor. The original thread did not have sufficient strength for the heavy fabric and sometimes soiled condition of the bags. Using a thread with a minimum tensile strength of 15 pounds (66.72 n) eliminated the problems caused by the original thread. With the equipment and personnel available to fill the bags additional sewing machines would be required to avoid delays. Four sewing machines with adequate thread would be required to keep pace with the filling operation. This would allow two separate closing stations on the dam with two sewing machines at each station.

The irrigation dam used for the project is constructed of a silty clay typical to Audrain County. The liquid and plastic limits of the material were 50 and 19 percent respectively. These fall well within the typical ranges of 40-70 percent for liquid limits and 15-25 percent for plastic limits for Audrain County soils.

In-situ density tests were performed at various locations on the upstream slope of the dam. The in-situ dry density of the dam material varied from 80.5 to 104.0 pcf. These results were expected due to the lack of field control during the construction sequence. The maximum dry density (Standard Proctor Method ASTM) of the on site dam material is 105 pounds per cubic foot. The optimum water content is 20 percent. The dry density tests performed at the project site represent a typical range of the dry densities found on the other irrigation dams.

i. Feasibility of Installation on Farm Irrigation Dams. The ability to efficiently install this method of slope protection on a typical farm irrigation reservoir was a major aspect of this study. The time and labor required to fill even the relatively small number of bags required for a typical irrigation dam would be prohibitive without mechanical assistance. Several alternate systems were considered as possible methods of filling the bags. An auger or conveyor belt was one possible means of providing a flow of fill material to the bags. Such an arrangement would necessitate the construction of a bin to direct the fill material to the auger or conveyor belt. The durability of such a makeshift bin would control the success of such a system.

Because a fertilizer cart is normally available at a farm, such a cart was modified for the project. This cart combines a steel bin to hold fill material and a chain belt to dispense the material into hand-held

approximately 2 square feet (0.186 square meters) of slope when filled. The cost of the fabric is then \$1.55 per square foot (0.093 square meter). The sand material required to fill the bags, if not freely available, would cost \$.08 - \$.10 per bag. A slope protection system capable of resisting typical wind-generated waves would require at least an equivalent 6 inch (15.24 cm) bedding layer of sand. The time and expense required to install the fabric slope protection system for this project was nominal. With the equipment and personnel available the slope protection system was installed at a rate of 250 bags per hour. Approximately 8 man hours per 100 bags were required to fill, close and place the bags on the dam. The cost of the labor was nominal. The F.F.A. Chapter provided the necessary labor in exchange for tools and equipment. However if the labor was charged out at \$3.00 per hour, the installation cost would be \$0.12 per square foot. The final approximate cost per square foot of the soil pillow system would be on the order of \$1.75 per square foot (0.093 square meter) not considering freight and other miscellaneous site dependent costs.

The availability of riprap materials capable of resisting anticipated wave forces will determine the cost effectiveness of using a sand pillow slope protection system. The cost of dumped riprap is on the order of \$1.20 per square foot (0.093 square meter), approximately 70% of that of the sand pillow system. If the cost of acquiring slope protection material for a dam exceed \$1.75 per square foot (0.093 square meter) of slope, the use of a sand pillow system may be justified. The costs of alternate slope protection methods must be evaluated for each particular irrigation dam.

ii. Erosion Resistance of the Slope Protection System. The ability of the sand pillow system to resist the erosive forces of wind generated waves has been evaluated. The test sections were monitored from January,

The sand pillow slope protection system may be installed at the convenience of the farmer. Weather conditions did not hinder the successful filling and placement of the bags on the dam. Figures 23 and 24 show the frozen condition of the reservoir when the majority of the bags were placed. The bags were filled with a wet, cohesive soil material during the middle of January. The adhesion of the soil to the steel walls of the cart hindered the flow of material to a minor degree. The fact that the soil tended to stick together in clumps enabled the chain belt to provide a faster flow of material than expected.

The crest of the dam was rutted due to the repeated tractor trips hauling filled bags to the upstream slope. These loads were small compared to the loading which would result if truck loads of riprap had been placed on the slope. The distance from an adequate road to the project site or almost any other irrigation reservoir in Audrain County would necessitate excellent weather conditions to successfully deliver riprap. The fact that the slope protection system may be installed during a relatively slack period of the year is a major advantage of the system.

The slope protection system was installed with the reservoir at its maximum level and placement of the bags below the water surface was easily accomplished. The bottom row of bags was placed initially. Subsequent bags were offset with respect to the previous row of bags. The fact that the sand pillow system is easily installed without the necessity of lowering the reservoir level is still another advantage of this slope protection method.

The cost of the acrylic fabric slope protection system will limit the locations where such an installation is practical. The bags presently cost \$3.10 each at the manufacturing location. Each bag will protect

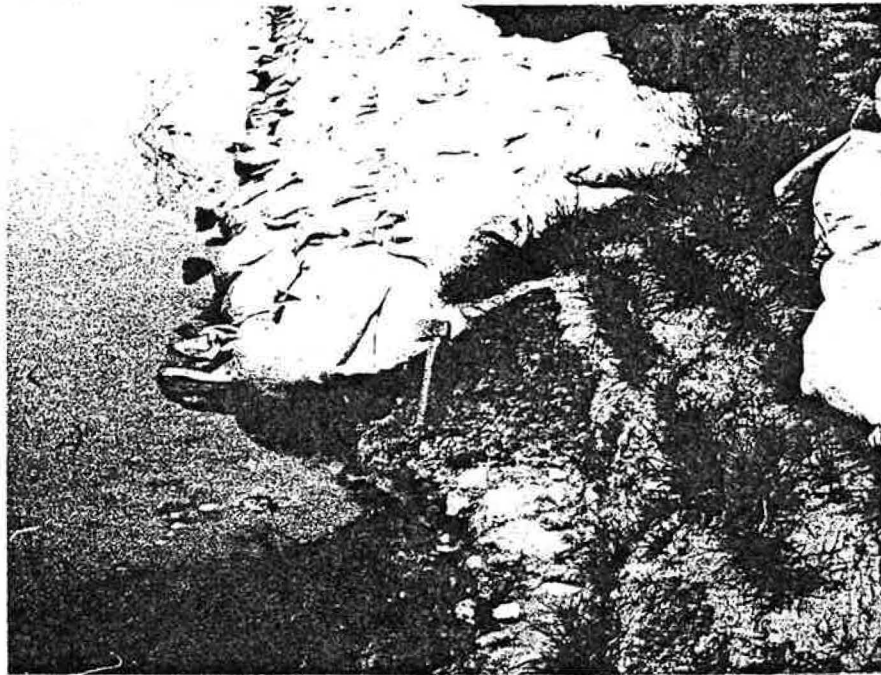


Figure 26. View of the Unprotected Slope Versus the Protected Slope

1978 until June of 1979 for a total of eighteen months. During this period the protected sections of the dam have remained unaltered.

Figure 26 shows a view of the slope protection system during the summer of 1978. The sand pillow slope protection system did settle and adjust slightly as various natural forces acted upon the slope. The sand pillow system remained intact during these minor disruptions and provided complete protection for the slope.

In contrast to the protected sections, the unprotected sections showed acute erosion. Profiles D through N are shown in Appendix C. Profiles A, B, and C are not shown because of the accidental covering of these profiles with brick during August, 1978. As shown by these profiles, the rate and amount of erosion depends greatly on the time of year. The greatest erosion occurred between the months of April and May for both 1978 and 1979 which is usually the time of the highest wind velocities and duration for the year as well as the highest water levels in the reservoir. The amount of slope deterioration over a 12 month period from April 1978 to April 1979 varied from about 1 foot (0.30 m) of erosion for profile K to about 2 feet (0.61 m) for profile G. It is noted from Figure 25 that profile G is located in the section over which the longest effective fetch occurs and in the direct path of the prevailing winds for that section of the state.

Profiles G, H, and I are good examples of the problems that can be encountered on unprotected reservoir embankments during periods of high winds. Between April, 1979 and May, 1979 these three profile sections eroded an average of 1.3 feet (0.40 m) with profile I eroding about 1.5 feet (0.46 m).

The process by which this large amount of erosion occurs can be more readily understood by referring to Figure 27 and 28, and by referring to the profiles shown in Appendix C. From the profiles, it is evident that

the erosion of the embankment slope is slowly decreasing the horizontal distance from the crest to the normal water level while at the same time increasing the vertical distance from the water level to the top of the break, i.e., the point on each profile where the slope becomes vertical. During periods of normal water level, these vertical cuts will be slowly undercut by wave action as can be seen in Figure 27. As a result of this undercutting and the fact that vertical cuts in silty clay are generally unstable, what little stability existed at the toe of cut before wave action began is removed and the cut begins to slump as shown in Figure 28. The slumped material will soon be broken up by the constant pounding of the waves and the process of undercutting and slumping will continue.

The longer the vertical cut, the more unstable the embankment becomes and therefore the more slumping that can occur with smaller amounts of undercutting. As noted from Appendix C, the vertical cuts become longer with time. This could explain the large amount of erosion that took place on profiles, G, H, and I. After a year of almost constant erosion, these profiles may have reached a stage where the vertical cuts were large enough to cause accelerated slumping. Since this occurred during the period of high winds, the problem was amplified considerably.

Because the slumping in these three profiles had resulted in a drastically reduced horizontal distance from the top of the crest to the water level, it was recommended that some repair work was necessary to prevent any further deterioration of the embankment. The owner of the reservoir was instructed to place as many sand pillows filled with sand in the unprotected northeast section as he thought necessary in order to prevent any further erosion. To date, the sand pillows placed in the section have performed adequately and have apparently stopped all erosion of the embankment at this section.



Figure 27. Undercutting of Vertical Cut Due to Wave Action



Figure 28. Slumping of Embankment Slope Due to Undercutting by Wave Action

$$F \doteq MLT^{-2}$$

where the symbol \doteq means dimensionally equivalent but not necessarily numerically equal.

Murphy (1950, pp. 4, 17) states that the theory of similitude is "developed by dimensional analysis which is based on our concept of measurements..." and that dimensional analysis is based on two axioms:

Axiom 1. "Absolute numerical equality of quantities may exist only when the quantities are similar qualitatively."

Axiom 2. "The ratio of the magnitude of two like quantities is independent of the units used in the measurement, provided that the same units are used for evaluating each."

The first step in establishing a dimensional analysis is to write the pertinent variables in a general form that can be developed into dimensionless quantities. The general form can be one of many with the most common form being

$$A \doteq C_{\alpha} F^{c_1} L^{c_2} T^{c_3} \quad (4)$$

where

C_{α} , c_1 , c_2 , c_3 are developed constants. By developing any one of a number of dimensionless terms and substituting in each dimensionless term's place the Greek symbol Pi (π) each term can be manipulated with much more ease than the original dimensionless groupings or terms. This process is known as the Buckingham Pi Theorem (Murphy, 1950; p. 36) which, in equation form, is

$$s = n - b \quad (5)$$

The completely submerged pillows filled with on-site material lost much of their fill through the fabric due to wave action. In some instances this resulted in complete removal of the pillows down the slope. These displaced pillows were generally located in the lower two rows of pillows. However, when these displaced pillows were replaced with pillows filled with sand, they remained intact and are to date still offering excellent protection.

V. MODEL STUDY INVESTIGATIONS OF SAND PILLOWS FOR SLOPE PROTECTION

A. GENERAL MODEL THEORY

To evaluate the effectiveness of the various slope protection methods, and to determine under what set of conditions these methods were most applicable, the need for controlled testing became obvious. Controlled conditions were achieved by constructing scaled models of the slope and protection material and simulating natural wind waves by forcing wind over water in closed flumes (Johnson and Rice, 1951) or by producing waves generated by a paddle (Grantham, 1953; Saville, 1953; Ahrens, 1975; and U.S. Army Corps of Engineers, 1942, 1957).

The need for defining at least three qualitative factors in model study has been known for centuries with distance or length, L, time, T, and force or weight, F, being generally chosen as the three factors, not because they are basic parameters, but because they are usually the simplest to use (Groat, 1932, U.S. Army Corps of Engineers, 1941; and Murphy, 1950). These quantities are interrelated through Newton's Second Law of Motion, namely,

$$F = Ma \tag{3}$$

or dimensionally,

plywood panels and was made air-tight by placing modeling clay on the joints. Air was forced over the water to produce the desired waves. The purpose of this experiment was to determine the relationships that existed between wave height, length, and period. These tests were later modified to study fetch length and water depth.

Numerous model studies on breakwaters and riprap on different slopes were conducted shortly after Johnson and Rice's investigations by Saville (1953), Grantham (1953), and Hudson (1961). Ahren (1975) worked with dumped stone in a tank 15 ft. (4.57 m) wide, 20 ft. (6.10 m) deep, and 635 ft (193.6 m) long with a still water level of 15 ft. (4.57 m). By varying wave height, embankment slope, riprap weight, and wave period, Ahren was able to study the most damaging combination of wave and slope, and the resulting zero-damage waveheight (H_{zD}), i.e., the highest wave height that will produce no riprap movement. It was concluded that the largest variability of riprap stability is related to wave period with the shorter-period wave having higher stability. The slope of the embankment generally influences the point of wave breakage, and therefore, influences riprap stability, with the steeper slopes causing the most damage. The previously discussed stability number, N_s , was used exclusively to form the relationship between slope angle, θ , and stability coefficient,

$$K_{rr} = \frac{(N_s)^3}{\cot \theta} \quad (6)$$

Perhaps the most complete study of model laws and of riprap stability under wave action, has been by Thomsen, Wohlt, and Harrison (1972) for the U.S. Department of the Army and the Missouri River Division. In this study, dimensional analysis using the Pi Theorem was used to establish the sets

where

s is the number of Pi terms,

n is the total number of quantities involved, and

b is the number of basic dimensions involved.

The use of the Pi Theorem is greatly facilitated where the dimensionless terms in the equation become too cumbersome to handle with ease. By multiplying, dividing, adding or subtracting Pi terms, the once cumbersome terms can be reduced. The only restrictions placed on Pi terms are that they must be dimensionless and independent.

B. MODEL STUDIES. In some early tests, Johnson (1948, p. 671) defines the model laws for wave generation in deep water:

1. "The wave motion is controlled by gravity and is not affected by viscosity or surface tension,
2. Normal and tangential forces exerted on the water surface by the wind are proportional to the squares of the velocities or velocity differences."

He concluded from his studies of windwaves on Clear Lake, California, that in order to develop dynamically similar model-prototype conditions, wind velocity and duration should play the most important role for laboratory wind generated waves. He further concluded that the flume should be designed such that only gravity waves will exist over most of the fetch, i.e., insure that the lower limits of the wave periods be 0.27 seconds (this will vary with size and shape of flume).

Johnson and Rice (1952) made several laboratory investigations using the wave channel located in the Fluid Mechanics Laboratory of the University of California-Berkeley. The wave channel was 1 ft. (0.30 m) wide, 3 ft. (0.91 m) deep, and 60 ft. (18.3 m) long. It was covered with

$$N = \frac{H_o}{(W/\gamma)^{1/3}(S-1)} \quad (9)$$

which is a form of the stability number for deep water waves, and the Reynolds Number into

$$R_N = \frac{\gamma_f}{\mu} \frac{W}{\gamma}^{1/3} \frac{H_o}{g}^{1/2} \quad (10)$$

by using the Pi Theorem's transformation functions.

Three different sizes of wave tanks were used with wave heights varying from 6.0 ft. (1.83 m) high to 0.1 ft. (0.03 m) high. Each tank was equipped with a main piston-type wave generator and an alternate flap-type generator for wave heights below 2.0 ft (0.61 m). The slope protection material tested was dumped stone, placed stone, dumped tribars, and placed tribars. Each slope was constructed with a filter material placed as bedding followed by the armor material.

Progressively larger waves were run over the slopes to simulate wave action expected on a dam before a storm arrives, after which the "design wave" becomes the critical wave. In each analysis, the highest wave in each burst of approximately 100 waves was considered the effective wave because of its ease in measurement and because this wave will most likely cause the worst damage during any given wave train.

Wave damage was measured by movement of armor, namely, by superimposing before and after profiles on each other (Figure 29) and measuring the dimensionless damage,

$$B = \frac{JD}{b} \quad (11)$$

of dimensionless parameters. Variables measured and controlled in this study were: wave height, H_0 ; wave period, T ; wave depth, d ; weight of armor (or stone) unit, W ; unit weight of armor unit, γ ; embankment slope, α ; unit weight of fluid, γ_f ; absolute viscosity, μ ; and gravitational acceleration, g . Since W , γ , and g were easy to measure accurately, they were chosen as the repeating (independent) variables while H_0 was chosen as the dependent variable. For a complete listing of the dimensionless parameters chosen, refer to Thomsen, et al., (1972; Table 1).

Dynamic similarity was demonstrated in this study since it was assumed that the forces of fluid viscosity, inertia, and gravity are in the same ratio in model and prototype. The Froude Number,

$$N = \frac{\text{inertia forces}}{\text{gravity forces}} = \frac{\rho_f D^2 V^2}{(\gamma - \gamma_f) D^3} \quad (7)$$

and the Reynolds Number

$$R_N = \frac{\text{inertia forces}}{\text{friction forces}} = \frac{\rho_f D^2 V^2}{\mu D V} \quad (8)$$

are simply ratios of these forces and where, by definition,

$$\rho_f = \gamma_f / g$$

$$D = \left(\frac{W}{\gamma}\right)^{1/3}$$

$$V = (gH_0)^{1/2}$$

$$S = \gamma / \gamma_f$$

The Froude Number can be transformed into

where

B = dimensionless damage

J = total number of armor units removed during the test

b = test section width

D = representative linear dimension of an armor unit.

The results of these tests confirmed previous theories on what effect certain wave parameters would have on the stability number or zero-damage wave height, H_{ZD} , and on the limited-damage wave height, H_{LD} (the highest wave that did not remove a significant amount of underlayer material). Some of the conclusions obtained from this report were that underlayer design (filter design) is of no significance to riprap stability, and that underlayer thickness variations did not affect stability. The effects of water depth on zero-damage stability was not determined for the underlayer material.

Two important results obtained from this study were that stability is a function of wave period and embankment slope (Figure 30 and 31). Stability generally increased when wave period decreased and embankment slope decreased ($\cot \alpha$ increased).

The results of this study provided substantial proof of the importance of providing accurately calculated slope protection, based on availability of material, reservoir characteristics, embankment slope, and wind properties. Although many of the results from this study did not exactly agree with previous studies, it should be recognized that some of the parameters and techniques used in this study varied considerably from earlier studies (e.g., differences in Reynold's Numbers accounted for much of the inaccuracies), and that once these differences have been accounted for, the results of past research can be reasonably compared to present studies.

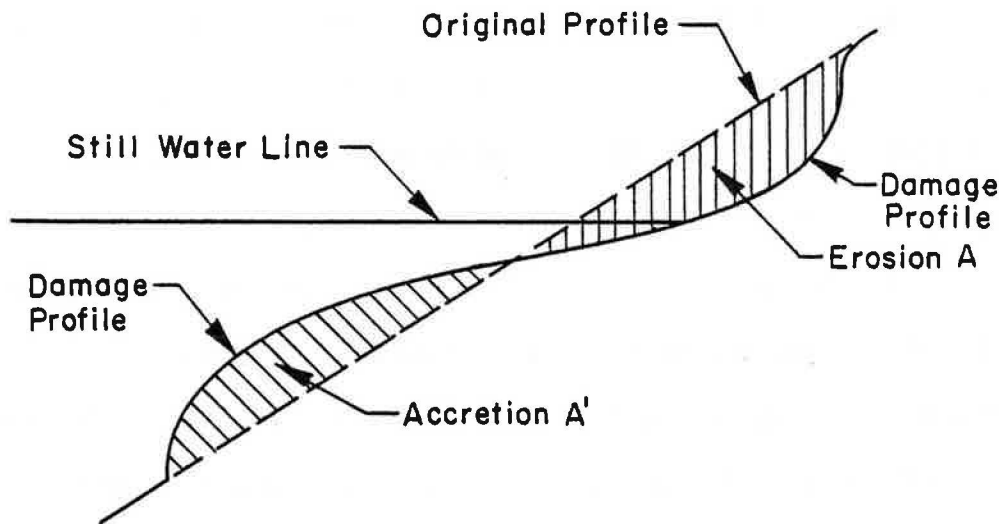


Figure 29. Damage Cross-Section, (Thomsen, et al., 1972)

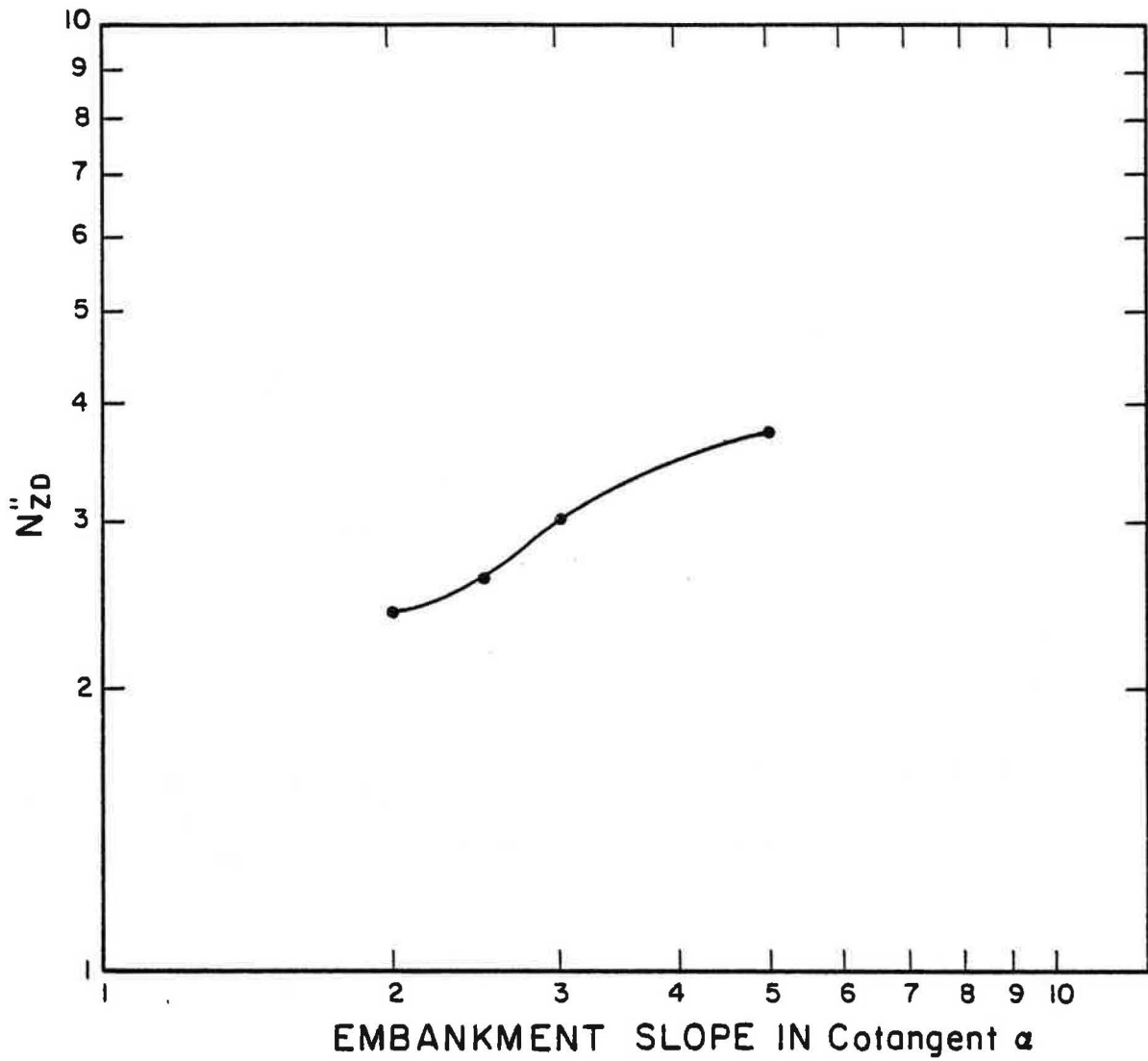


Figure 31. Effect of Embankment Slope on Zero-Damage Stability of Dumped Stone, (Thomsen, 1972)

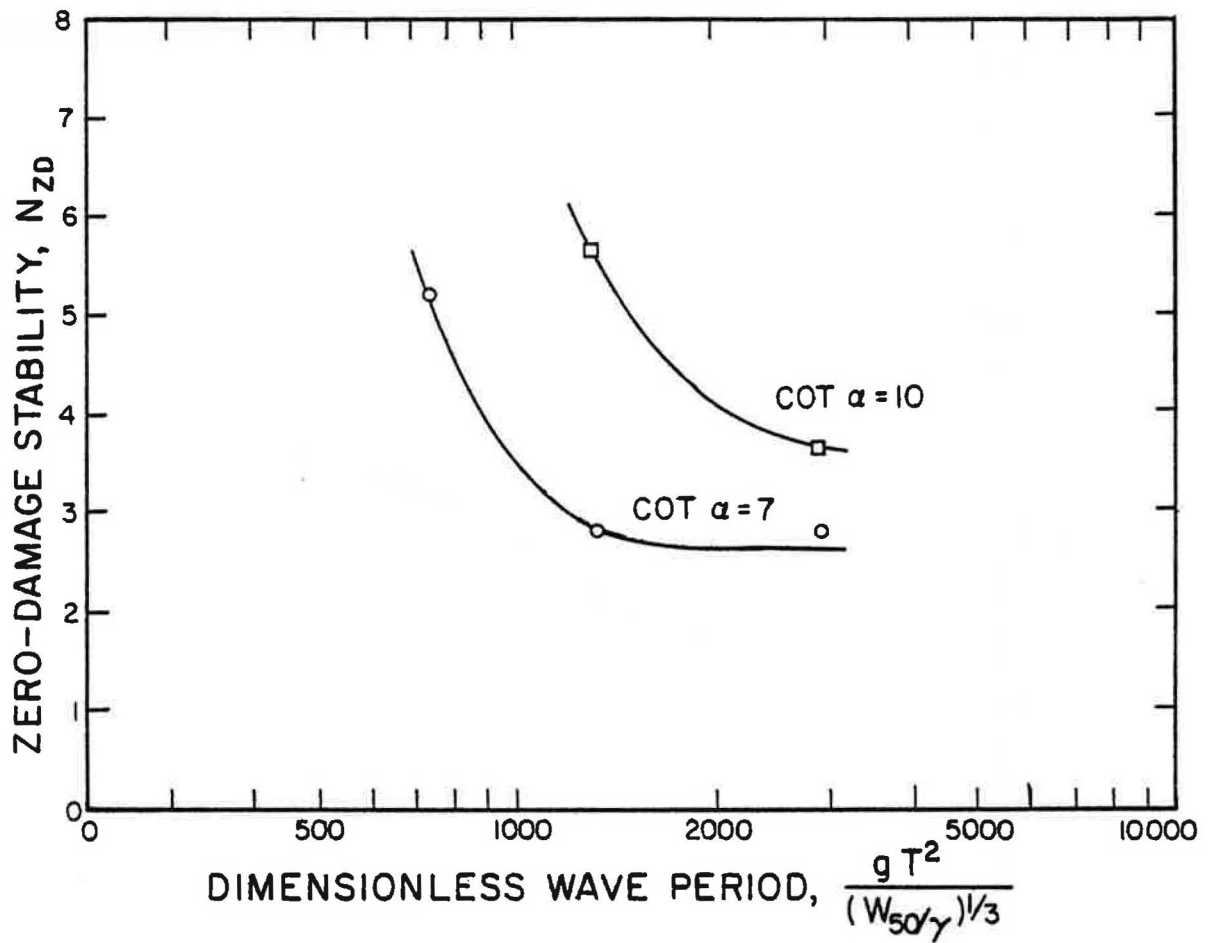


Figure 30. Effect of Wave Period on Zero-Damage Stability of Dumped Stone, (Thomsen, 1972)

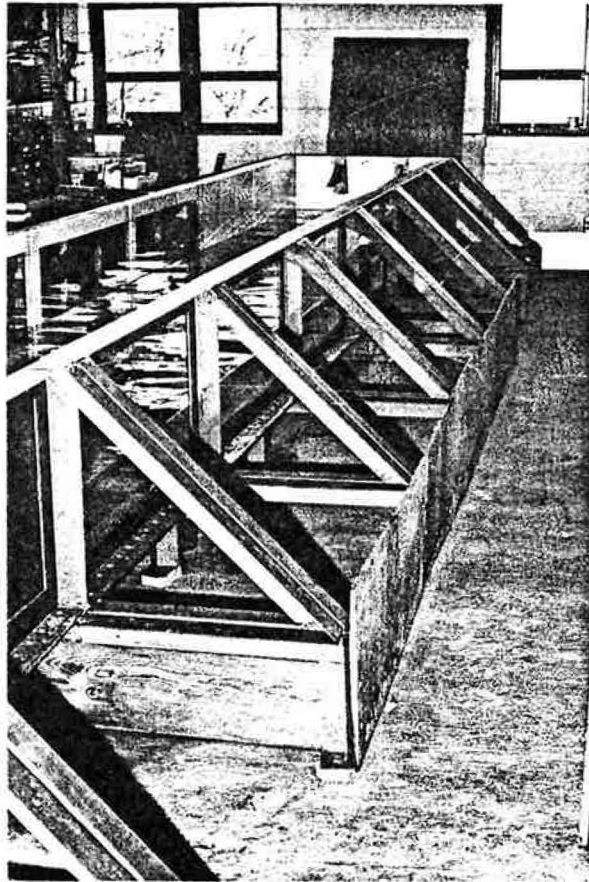


Figure 32. Right Side of Wave Tank

Further reference to model study behavior is made to Creager, Justin, and Hinds (1945), and Brasfield (1973).

C. TESTING EQUIPMENT AND PROCEDURES

1. Introduction. A three phase testing program was incorporated for this study. The three programs included a wave tank model investigation where scaled replicas of the sand pillows were tested, a laboratory testing program where the properties of the synthetic material themselves were tested, and a field evaluation of the synthetic material for use as a slope protection agent was studied on a prototype earth embankment constructed just east of Mexico, Missouri. The prototype embankment site is located in a region where a fine-grained silty clay exists on relatively flat terrain. These three testing programs were conducted concurrently such that any correlation that exists between them could be quickly and efficiently analyzed.

2. Model Testing Program.

a. Wave Tank and Wave Generator Description. A model study of the protection offered by acrylic sand pillows for use as a slope protection method was conducted in a laboratory wave tank located in the Engineering Research Laboratories building at the University of Missouri-Rolla. This wave tank is a rectangular, steel-framed tank that measures 32 ft. (9.75 m) long by 3.5 ft. (1.07 m) wide by 2 ft. (0.61 m) deep. It has four 4-foot (1.22 m) glass plates along each side for viewing (Figures 32 and 33). The wave generation device is the flap-type design consisting of a reinforced plexiglass paddle driven by a 1/2 horsepower variable speed drive motor (Figures 34 and 35).

b. Wave Tank Calibration. The wave tank was initially calibrated to establish the relationships between generator-blade displacement, wave height, wave period, water depth, and motor speed. These relationships

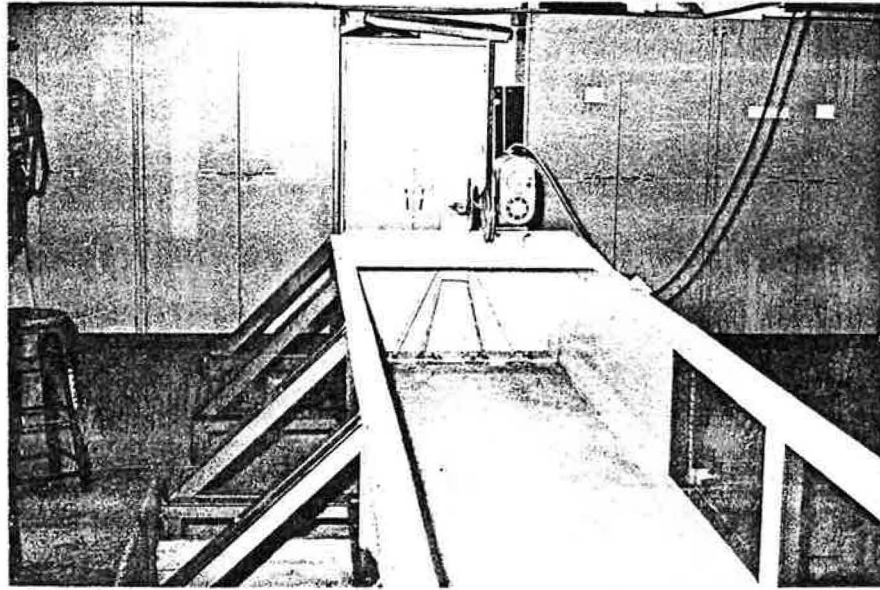


Figure 34. Reinforced Plexiglass Paddle

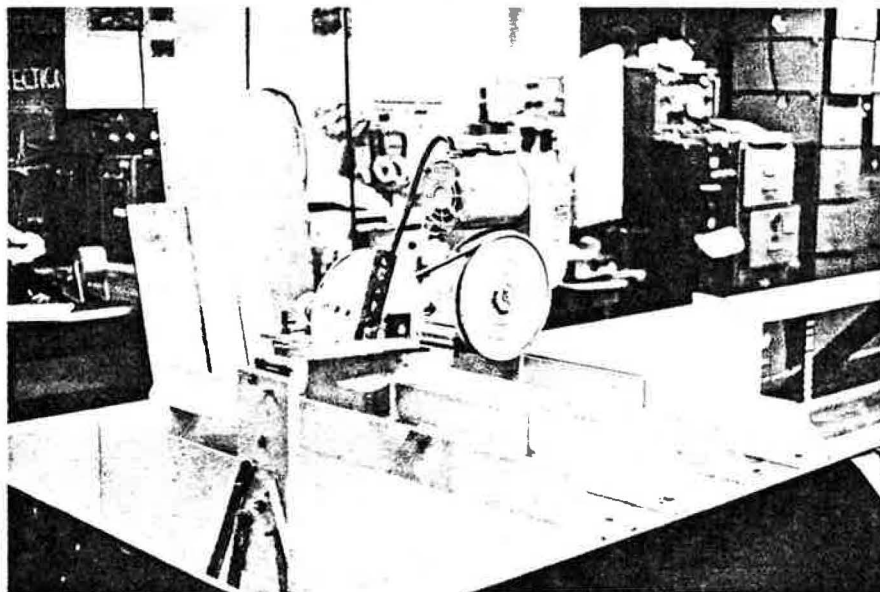


Figure 35. Motor and Pulley Assembly

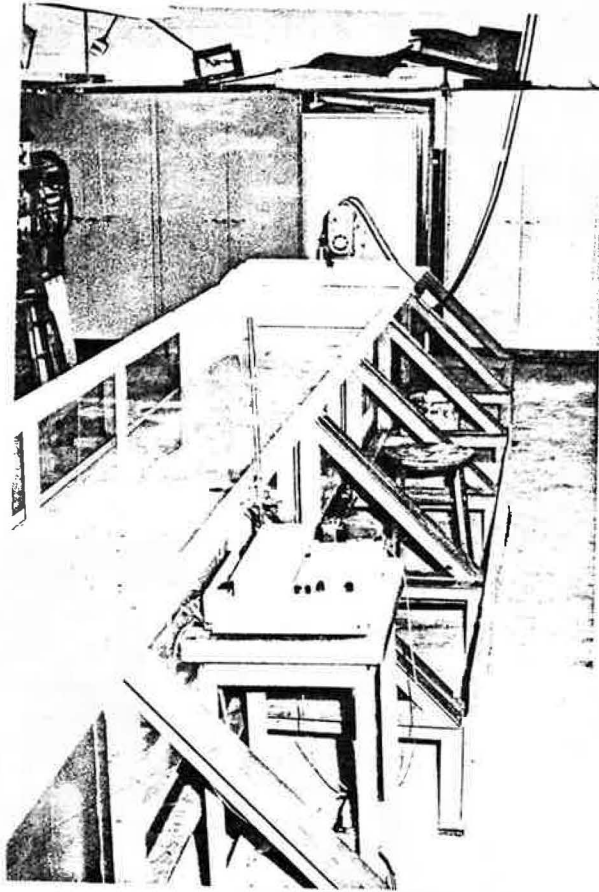


Figure 33. Left Side of Wave Tank Showing Paddle and Motor

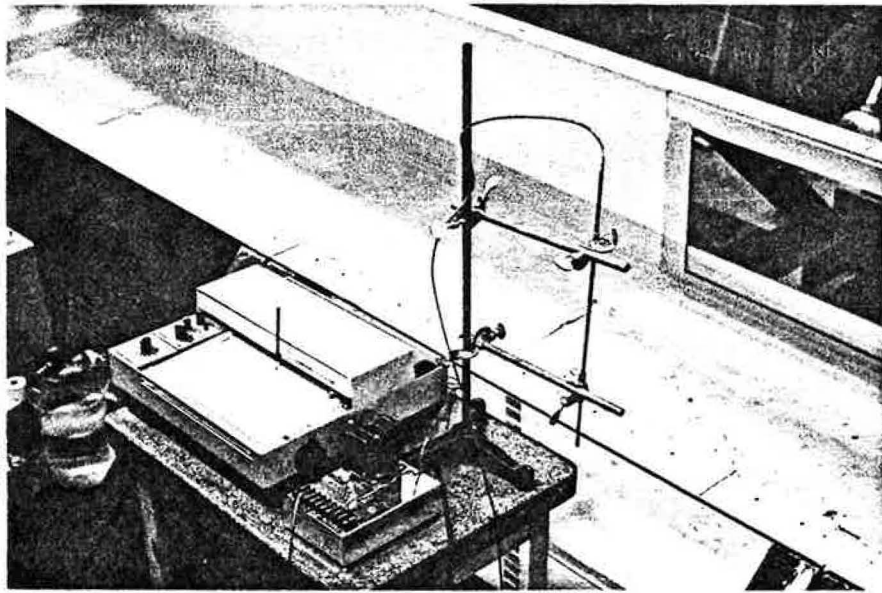


Figure 36. Step Resistance Wave Rod, Power Supply, and Recorder

determined by measuring the wave heights and wave velocities at the location of the toe of the model slope at various magnitudes of blade displacements, water depths, and motor speeds.

The wave heights were measured by a step-resistance gauge designed and built specifically for this study (Figure 36). As water passes over the wave rod, the resistance of the gauge is altered depending on whether the depth of water passing by is increased or decreased. These alterations, measured by means of electrical impulses, were monitored directly by a strip chart recorder. Figures 37 and 38 show placement of the wave rod in the tank and the action of waves as they pass by the rod. Figure 39 shows a typical wave rod recording.

The effective wave height for each wave generator setting and water depth was considered in this study to be the modal wave height, H , of each burst (average height of the waves of fairly consistent height in the center of the burst of waves). The reasons for using the modal wave as the effective wave are:

1. The modal wave is a fairly uniform wave for each wave train.
2. The modal wave is easily reproduced.
3. The modal wave is readily determined for each wave train.
4. The modal wave has been used with good success in previous investigations.

The tank was calibrated for water depths ranging from 152.4 mm (6.0 in.) to 254.0 mm (10.0 in.). The wave velocities were measured by timing a single wave of a given wave group over a known distance. This was repeated with a number of waves from each wave train, then averaging the velocities.

The wave period was calculated using the equation,

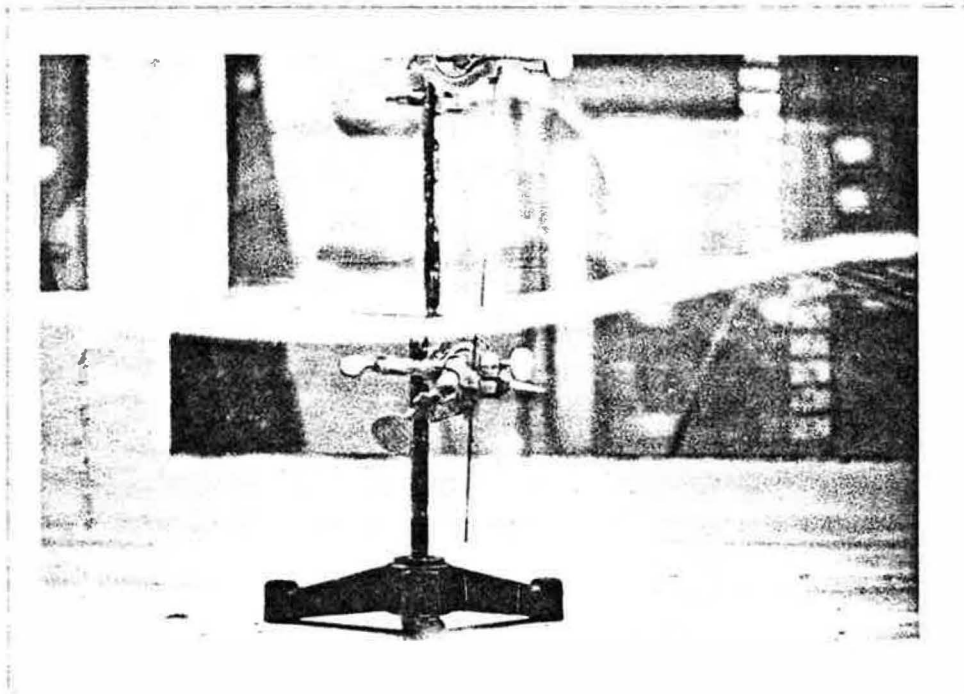


Figure 38. Wave Rod in Water with Wave Passing

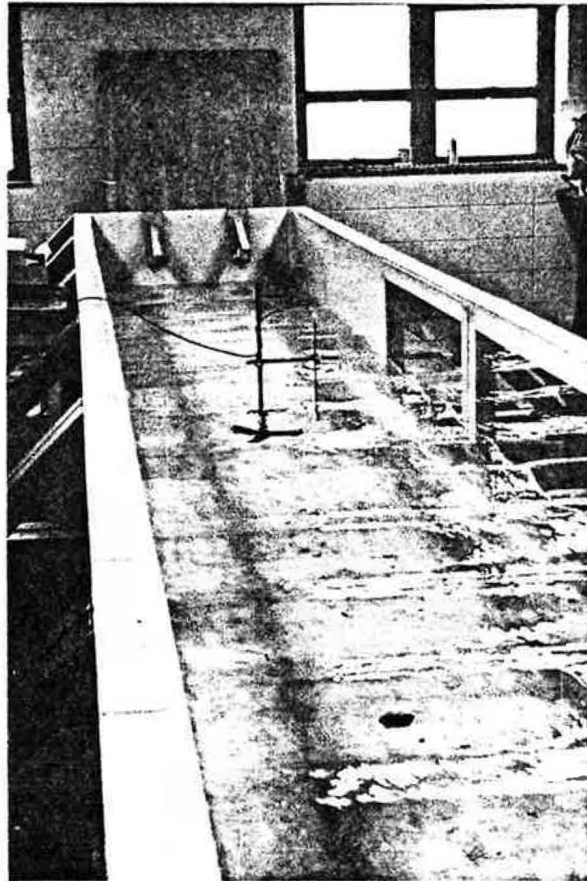


Figure 37. Wave Rod in Water with Approaching Waves

$$T = \frac{2\pi V_0}{g} \quad (12)$$

where

T = wave period, sec

V_0 = wave velocity, cm/sec

g = acceleration of gravity = 980 cm/sec²

This equation applies only to deep water waves.

The wave length was calculated by using the equation,

$$L_0 = \frac{gT^2}{2\pi} \quad (13)$$

where

L_0 is the deep water wave length in cm.

Only the deepwater waves were of interest in this study since they are the most common in irrigation reservoirs. The limiting criteria for defining waves is that used by the Corps of Engineers (1973) who set the values of relative depth (d/L_0) at greater than 1/2 for deep water waves, less than 1/25 for shallow waves and intermediate relative depths were called transitional waves.

c. Survey Equipment. The model slopes were surveyed with a 1 in. (25.4 mm) wide vertically moveable rod that was incremented in centimeters. This rod was mounted on a rail that extended across the tank and rested on the tank walls. This rail could be moved horizontally up and down the slope for surface monitoring. The rod could also be moved laterally along the rail to any position that the slope was to be surveyed. Three positions (left 1/3, center, and right 1/3) were surveyed and an average reading was obtained. Fourteen positions at spacings of 50.0 mm (1.97 in.) each were used for the horizontal movement down the slope. All soundings

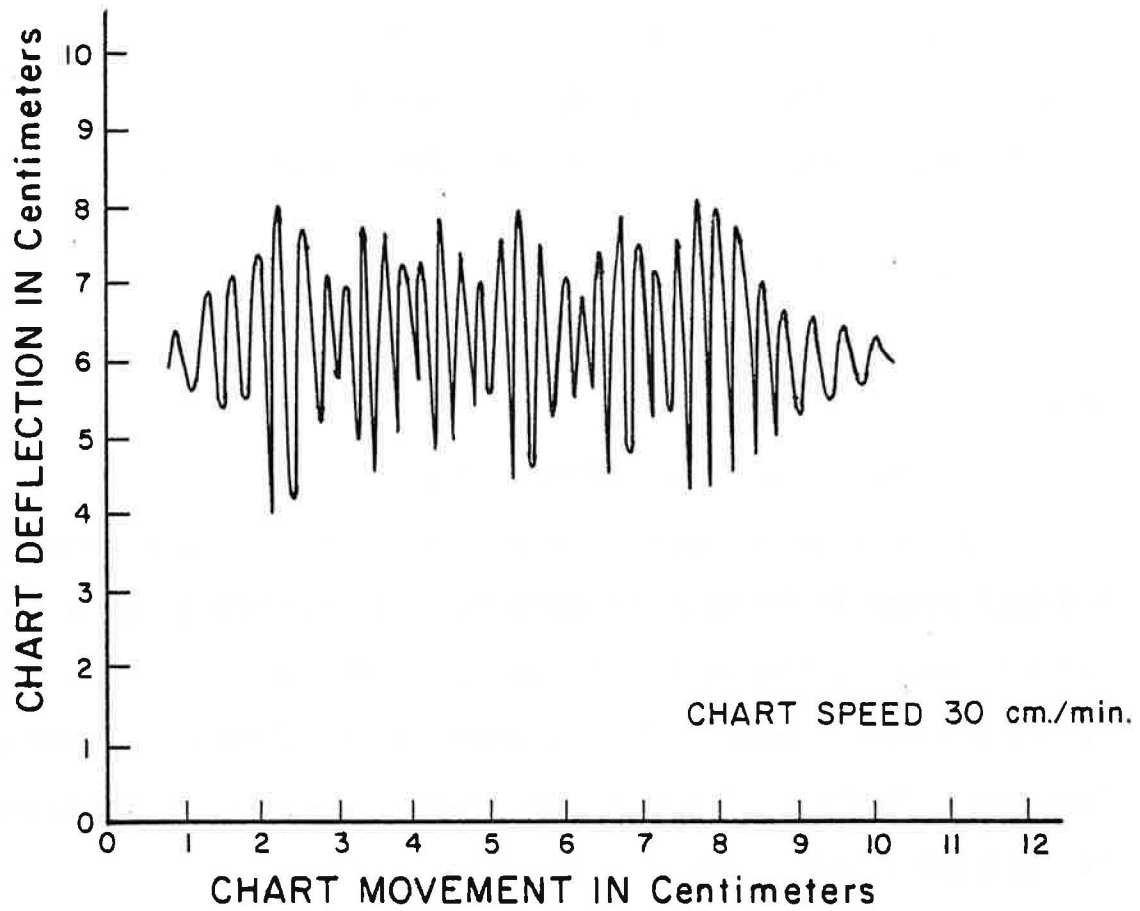


Figure 39. Typical Chart Recording

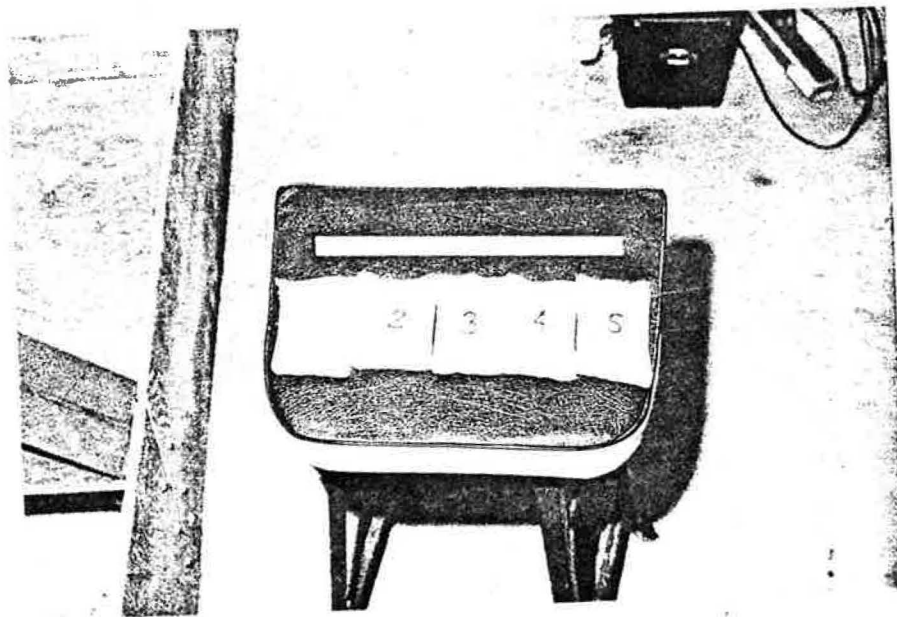


Figure 40. Model Sand Pillows

were located with an accuracy of 25.0 mm (0.98 in.) in the horizontal plane and to 5.0 mm (0.2 in.) in a vertical plane.

d. Testing Material. The soil used for the model slope and for the sand pillows' fill material was obtained from an earth embankment located in northern Missouri. This embankment is part of a field evaluation of the sand pillows and will be discussed in detail under Field Evaluation Program.

The on-site material is a grey, stiff, low plasticity, silty clay with a liquid limit of 37% and a plasticity index of 19.5%. It has a specific gravity of 2.73 and a grain size distribution as shown in Figure 7. When compacted according to ASTM D-698 Standard Proctor, the soil had an optimum water content of 19-20% and a maximum dry density of 104 pcf. This soil, herein referred to as Mexico clay, becomes extremely hard upon drying. It should be noted that Mexico clay is not the agricultural soil name but is used in this report to specify the soil location. The agricultural soil name for the soil is Putnam silt loam.

The model sand pillows for the slope protection system were made of acrylic fabric that is sold under the trade name of Acrilan. These model bags were made 5 in. (127.0 mm) long by 3.5 in. (88.9 mm) wide which represents an area scaling of 1:6 of the prototype sand pillows (Figure 40). In terms of median weights of the slope protection pillows, the model scale was approximately 1:200 for average weight sand pillows and for similar water contents in model and prototype soil.

The model slope consisted of a 3/4 in. (19.0 mm) laminated plywood sheet that had been painted with a waterproof sealant to protect the wood and prevent deterioration. The plywood was 41 in. (1.04 m) wide and 72 in. (1.83 m) long. Beneath the plywood was a portable jack to prevent sagging of the slope due to the weight of soil and water.

The sand pillow were placed on the slope with the unseamed long side facing the oncoming wave attack to minimize soil loss through the seams. The sand pillows were placed 10 across with each pillow overlapping the sealed end of the previous pillow. This again was to reduce the effect of soil loss through the stapled end of the pillows (Figure 41). The numbered pillows were placed such that they were at the still water level (SWL).

After completion of the slope construction, the motor speed and paddle eccentricity were adjusted to develop the desired wave height. Testing began by supplying "seasoning waves", i.e., small waves that might cause some settlement and adjustment but no removal of the armor units. If none of the sand pillows were displaced after approximately 2000 waves had passed over them, the motor speed and paddle eccentricity were modified to obtain the next higher wave height and the testing continued.

After the initial seasoning waves, the following wave heights were allowed to pass over the slope longer so that it could be determined what effect larger waves had on the stability of the slope with longer durations.

Generally, the first waves that moved some of the sand bags only reoriented some of the less stable ones. If, after some movement, the model withstood at least 1000 waves without further movement, the slope was considered stable for that particular wave height. The wave height was again increased to the next higher amount and the procedure repeated.

The increasing of the wave heights continued until a wave height was reached that caused excessive removal of the sand pillows down the slope. The number of sand pillows that had been moved was recorded. The sand pillows were removed from the slope and the slope was surveyed and photographed. A moisture content was obtained from the submerged sand pillows

e. Testing Procedure. The soil used in the model bags was initially air-dried and passed through a No. 4 sieve to assure uniformity and prevent gravel inclusions. The soil was then oven-dried for at least 24 hours, cooled and placed in the model bags and the bags were stapled shut. This method of sealing was quick and much more efficient than sewing. Also, since most of the bags were to be reused, staples could be quickly removed. The entire bag, plus soil and staples, was then weighed with a Sartorius electronic scale to the nearest 0.01 g.

The base soil to be used for slope construction was initially air-dried and ground into medium coarse particles. A moisture content at approximately the optimum was desired to ease the compaction effort that was needed for the slope construction. Since the air-dried moisture content was 3.8%, it was calculated that 1.56 lb (2.07 kg) or approximately 700 ml of water should be added per 10 lb (4.53 kg) of soil to obtain the desired moisture content of 20%.

The moist soil was then placed on the wooden slope and compacted by hand to a density of approximately 100 pcf (1.76 g/cm^3). No core or filter material was placed on the slope since the typical irrigation reservoir built in northern Missouri consists only of excavated in-situ soil with very little attempt made at complying with minimum embankment specifications, such as compaction requirements or layering requirements.

The soil was placed on the slope with an approximate thickness of 3 in. (76.2 mm). Approximately 100 lb (45.4 kg) of dry soil were needed per slope.

After construction of the slope, the tank was filled with water to a depth of 10 in. (254 mm) and the soil was allowed to become saturated by soaking overnight. The slope was then initially surveyed and photographed.

and several of the pillows that were directly attacked by the waves were used in the determination of the percentage of soil lost through the synthetic material due to wave pounding.

The remaining pillows were emptied, washed and allowed to dry. After drying, they were again filled to the desired weight with oven-dried Mexico clay and stapled shut (to be used in another model slope test).

During model testing, progressively larger wave were applied without rebuilding or repairing the model slope between wave heights. This expedited the testing, and was not inconsistent with prototype wave action. It is unlikely that large waves of the "design" wave height will be experienced in the prototype before a number of smaller storms have occurred, or that the "design" storm will generate the "design" wave before many other smaller waves have reached the slope.

Judgment was required to decide when to change the wave height and to determine how much damage was "excessive" such that the test should be terminated. Generally, the test was terminated after at least six sand pillows were totally removed and the remaining submerged pillows were being constantly reoriented. This criteria was intended to make the testing consistent.

An additional aspect that was investigated on the models was the determination of the relationships between wave runup on flat surfaces, soil surfaces, and sand pillow surfaces for various slope angles and wave height. The runup was measured during each test for every wave height and slope. Runup was recorded as an average of at least ten different readings.

D. RESULTS OF MODEL TESTING PROGRAM

1. Wave Damage. The ability of the model sand bags to resist displacement due to increased wave heights was monitored for every model test.

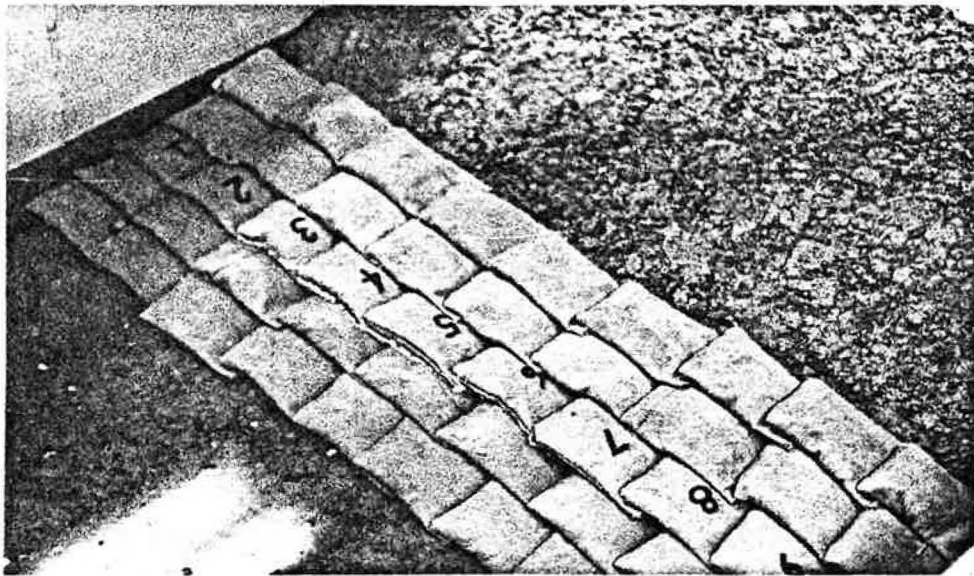


Figure 41. Typical Sand Pillow Configuration on a Model Slope

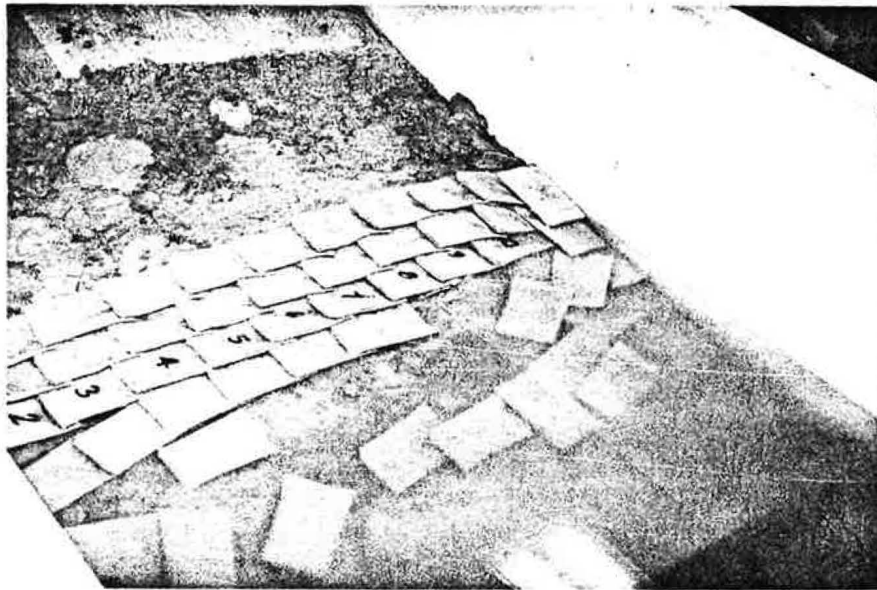


Figure 42. Typical Model Failure, Slope: 1 on 4, Test No. 9.

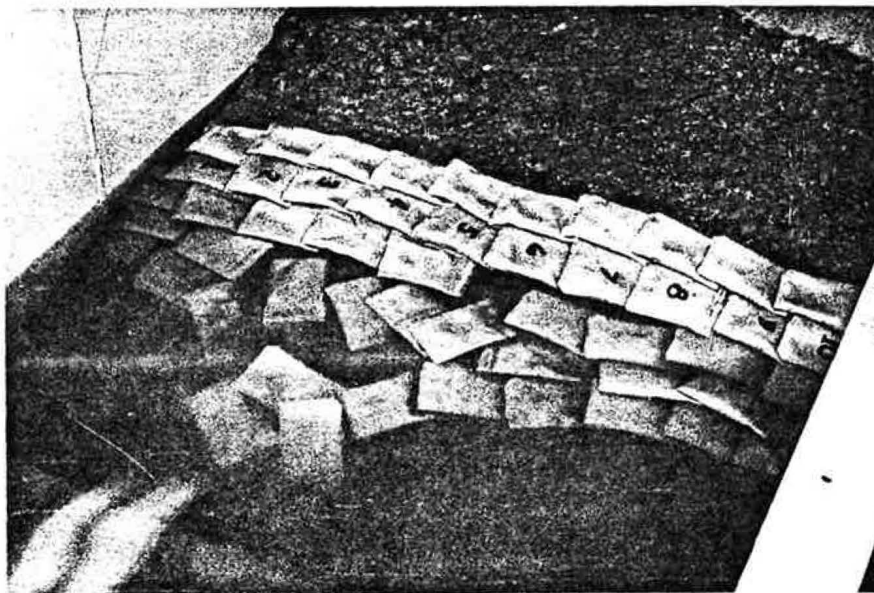


Figure 43. Typical Model Failure, Slope: 1 on 3, Test No. 1

The number of bags displaced or moved was recorded for each wave height until sufficient movement or damage had taken place to cause failure of the protection material.

Figures 42 through 44 show typical failures that occurred at the end of each test. In all cases the first movement started in the bottom row of bags, usually near the center of the model. Once a few of the lower bags were removed, progressive failure generally proceeded upslope and laterally with the greatest removal occurring in the center of the slope. Figures 45 through 47 show the typical progressive failure of a model slope.

To allow comparisons of damage and damage rates of each model, regardless of weight or bag size, damage is expressed in dimensionless terms. Dimensionless damage, D_J , was determined in previous tests (Thomsen, et al., 1972) to be the average number of armor units removed or displaced from a unit test section measured parallel to the tank walls. When applied to model sand bags Equation 11 becomes:

$$D_J = \frac{JD}{b} \quad (14)$$

where

D_J = dimensionless damage

J = the total number of armor units removed

D = least distance traveled to cause displacement, i.e., the bag width (88.9 mm)

b = test section width (1.04 m).

The dimensionless damage, D_J , was determined for each wave height and was plotted as a function of wave height for each test. Figure 48 shows

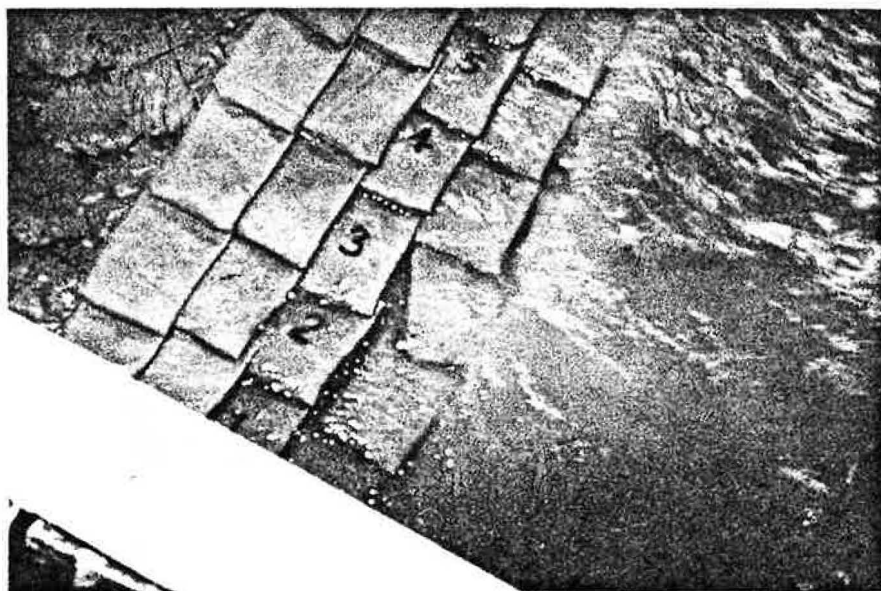


Figure 45. Start of Model Failure, (Test No. 10)

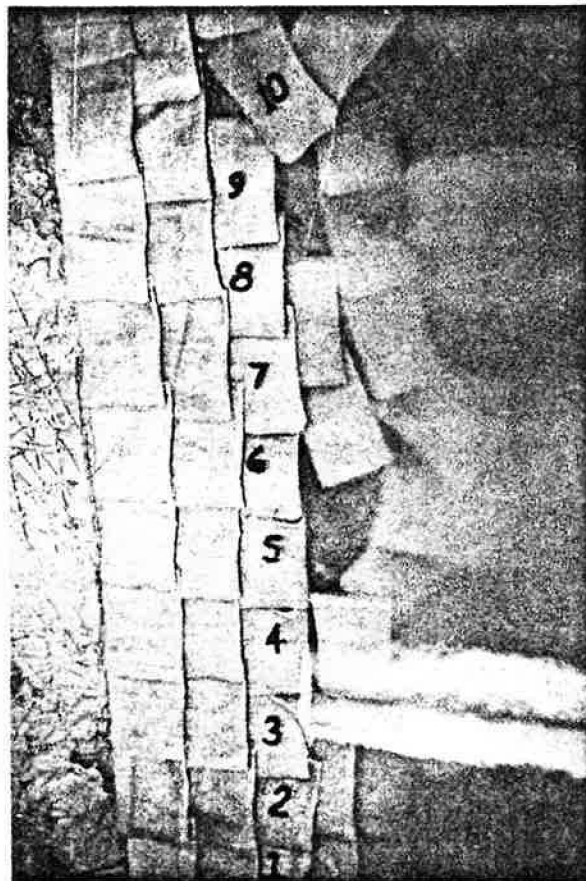


Figure 44. Typical Model Failure, Slope:
1 on 5, Test No. 13

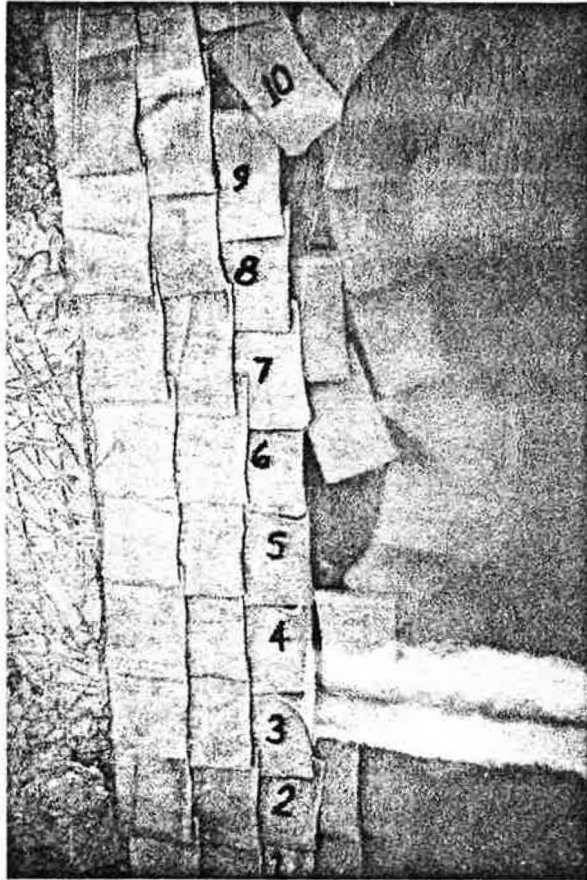


Figure 47. Completed Failure of Model Slope,
(Test No. 10)

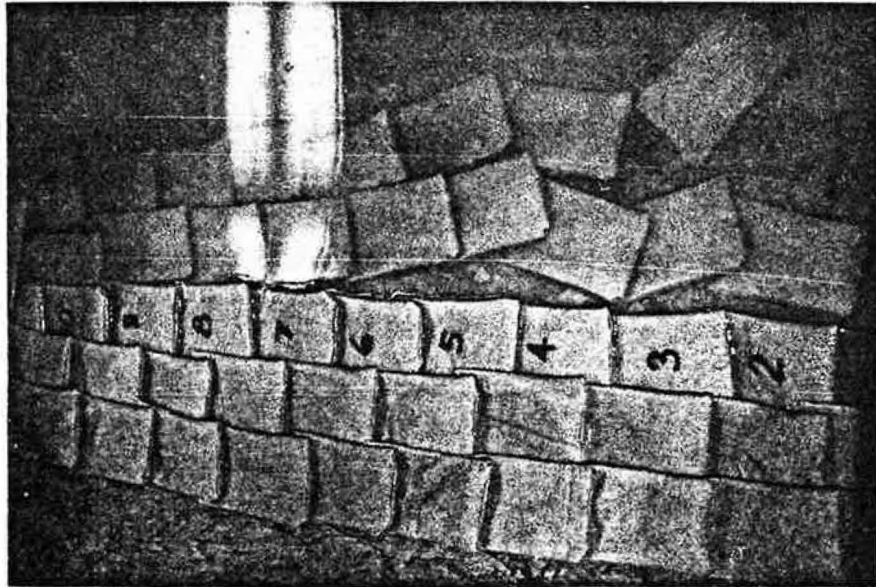


Figure 46. Progressive Failure of Model Slope (Test No. 10)

two typical damage curves while Appendix B gives the damage curves for all sixteen tests. Each point on these figures represents the maximum damage that may occur with that particular wave height. In other words, if more waves of each particular wave height had attacked the slope, further damage would have been negligible. The validity of this statement can be shown by Figure 49. The number of bags lost is plotted in Figure 49 as a function of the total number of waves that attacked the slope for Test No. 10. The modal wave height, shown at the top, was kept constant until the amount of damage reached equilibrium and the damage rate became nearly zero, i.e., the number of bags removed remained unchanged after more waves attacked the slope. At the time when the modal wave height then was increased, an immediate increase in the number of displaced bags was noted. This increase soon leveled off at some given number of lost bags after which the wave height was again increased. For the purpose of demonstrating the equilibrium damage phenomenon, Test No. 10 was taken past failure.

For each test, the condition of stability known as the zero-damage wave height, H_{ZD} , (the highest wave during a test that did not cause any removal of bags from the slope) was determined by the extension of straight lines through the points on the damage curves (Appendix B) to the zero-damage ordinate. In most cases, the point of intersection was easily located by the extension of the straight line through the one or two points that were away from the ordinate. However, in a few cases, the movement of one or two bags indicated an initial insignificant damage rate and the intersection of two straight lines was used to locate the zero-damage wave height. One line represented the "real" damage while the other line drawn through the initial few points represented the

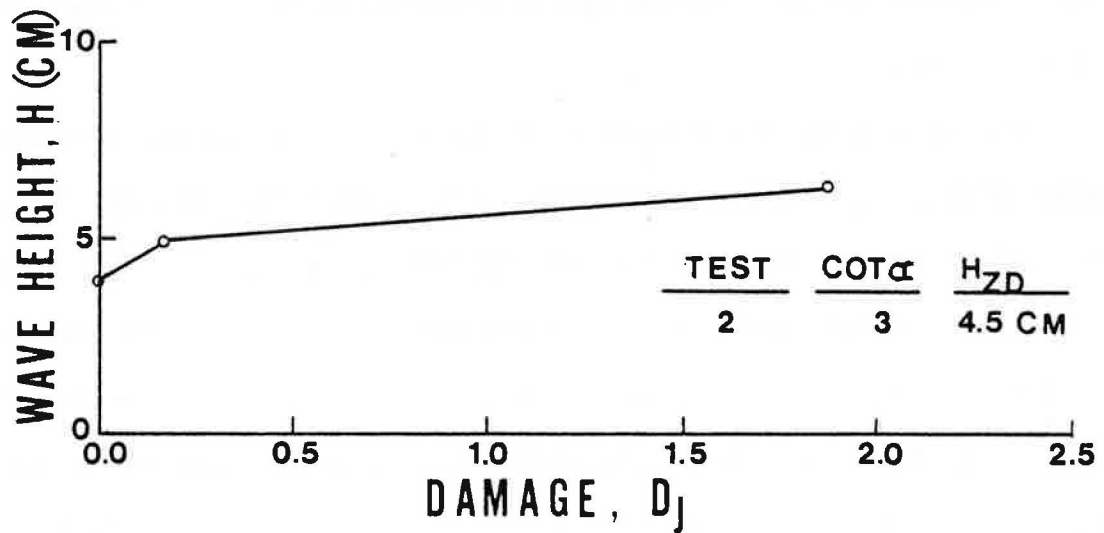
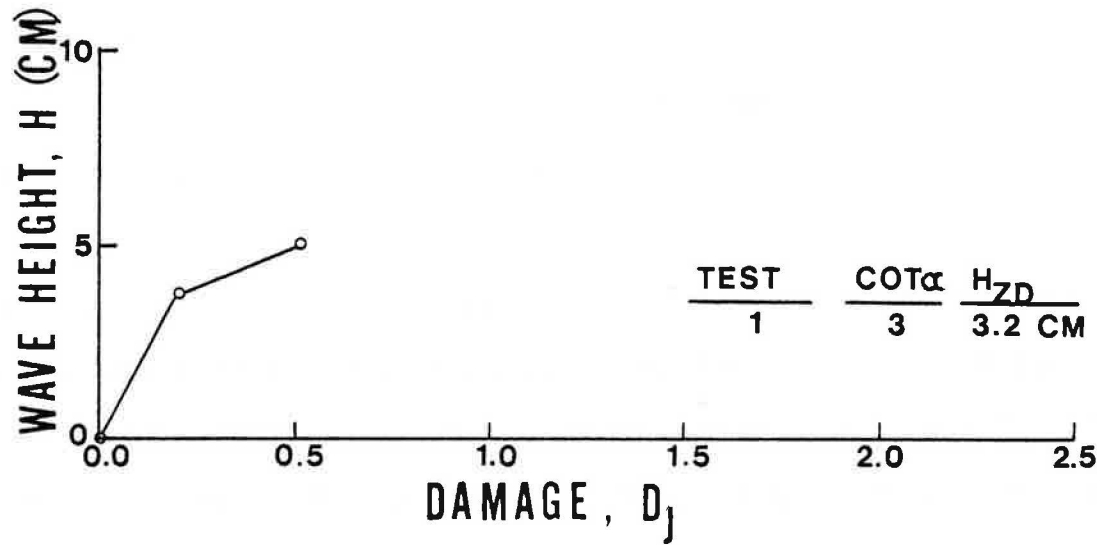


Figure 48. Typical Damage Curves

insignificant damage, as in the case of Test No. 3 (Appendix B). Table VI gives a complete listing of each test with its corresponding H_{ZD} , wave period, and area damage.

The amount of soil lost from each model slope by wave erosion between the sand bags was measured by superimposing cross-sectional areas of damage of original surface profiles on the average surface profile of the slope after completion of the test. Figures 50 through 58 show typical damage profiles for each slope. The cross-sectional area of erosion, measured in square centimeters, was taken as the average of three damage profiles for each test, and was measured by means of a Tectronix graphic tablet programmed by Schaefer (1979). This technique could measure the area of erosion to within an accuracy of 0.1 cm^2 (0.02 in.^2). Also shown in each figure is an erosion profile of an unprotected slope. In the case of the unprotected slopes, the area of erosion was approximately 3 to 4 times as much and the rate of erosion was about 200 times that of the protected slope.

Thomsen, et al., (1972) established an area dimensionless damage term to correlate the amount of erosion for various size models and prototype conditions. When applied to sand bags the relationship becomes,

$$D_A = \frac{(1-n)A\gamma_{sat}}{W_{50}} \quad (15)$$

where

D_A = area dimensionless damage

n = porosity

A = cross-sectional area of erosion, cm^2

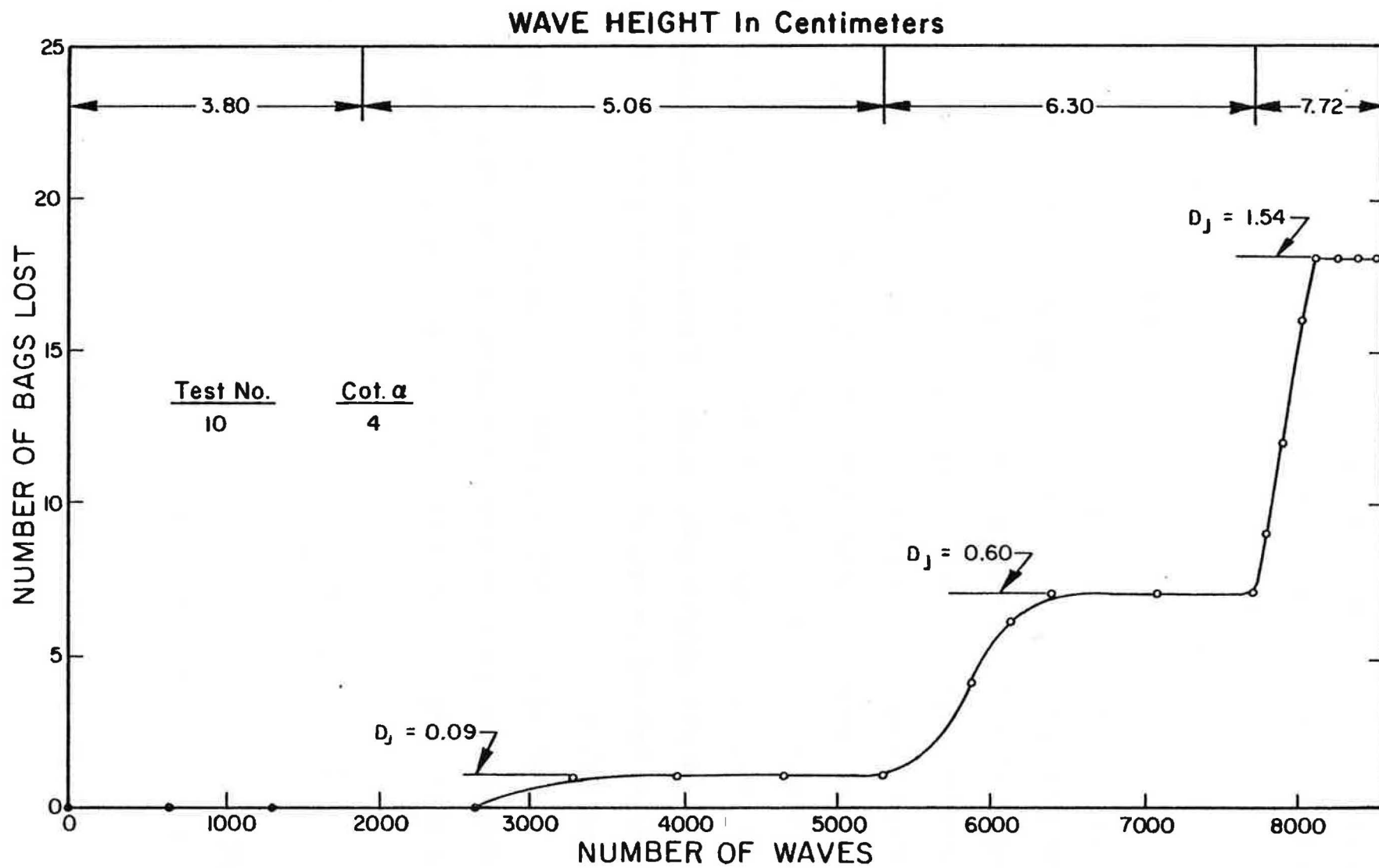


Figure 49. Typical Wave Damage Development

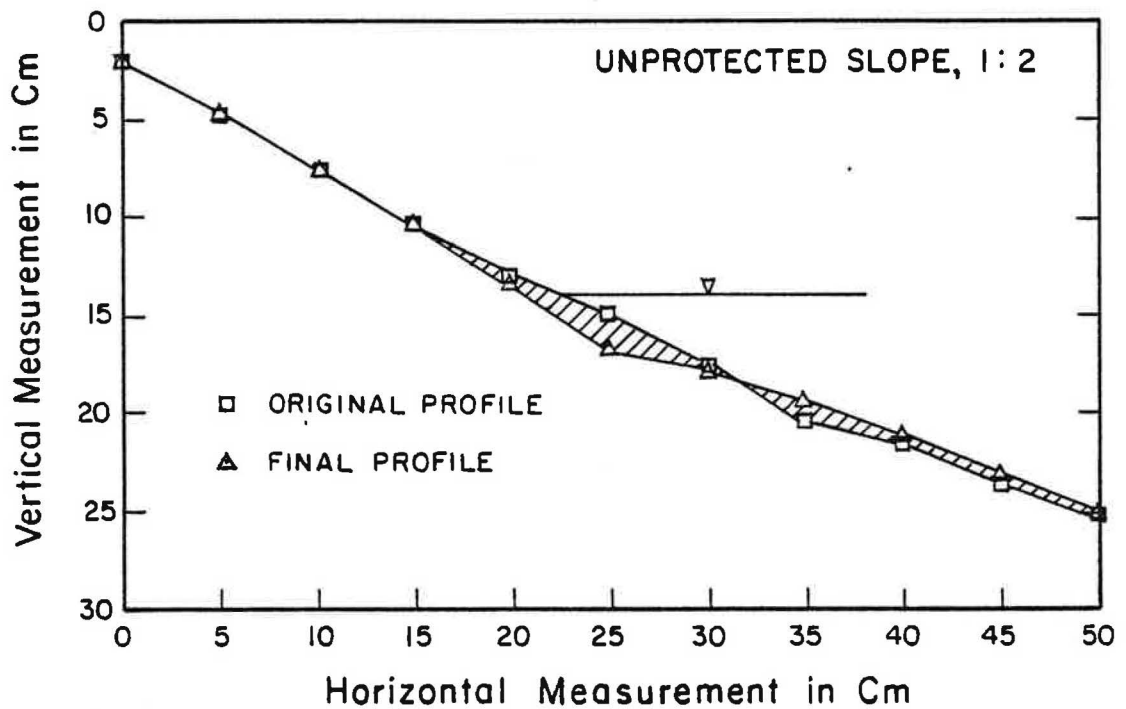
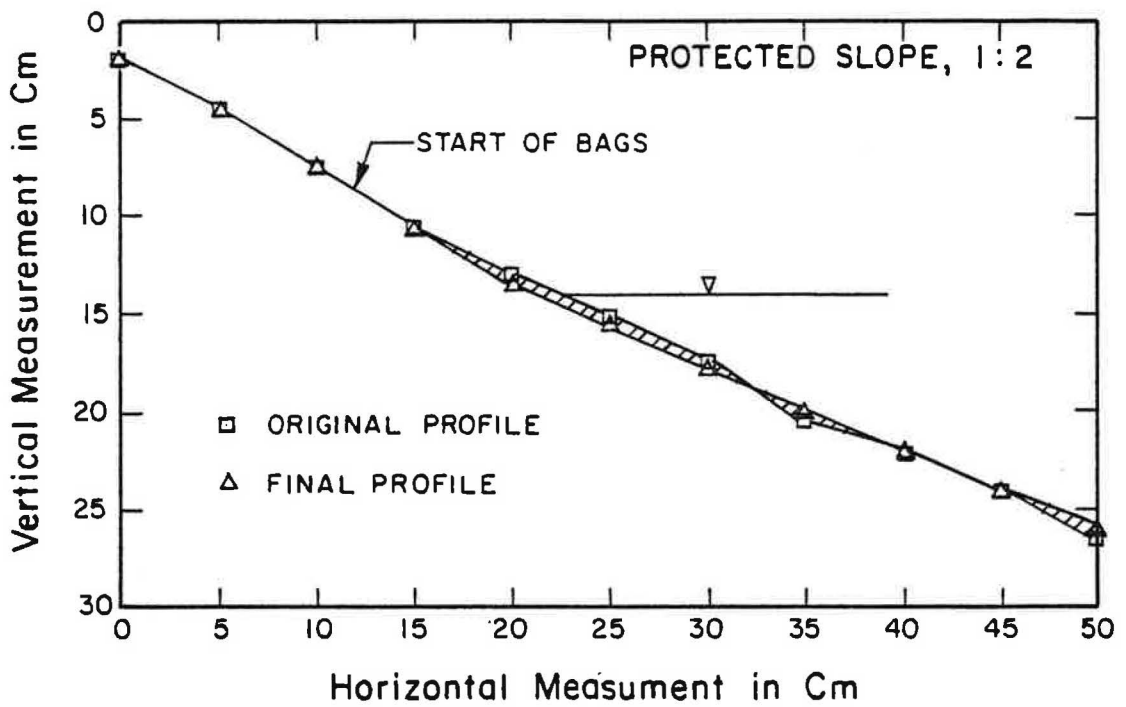


Figure 50. Typical Damage (D_A) Profiles for Protected and Unprotected Slopes, (Slope: 1 on 2)

TABLE VI
MODEL TEST RESULTS

Test No.	cot α	W_{50} ¹ (g)	Area Damage ² D_A	H_{ZD} ³ (cm)	Wave Period, T (sec)
1	3	55	1.00	3.20	0.43
2	3	85	0.53	4.80	0.55
3	3	120	0.44	5.75	0.51
4	3	165	0.20	6.30	0.51
No Bags ⁴	3	---	1.82	----	----
5	2	55	1.39	3.00	0.41
6	2	85	0.68	4.30	0.43
7	2	120	0.53	5.00	0.55
8	2	165	0.28	5.60	0.55
No Bags	2	---	2.84	----	----
9	4	55	0.60	4.20	0.43
10	4	85	0.45	5.20	0.55
11	4	120	0.35	6.00	0.51
12	4	165	0.29	6.75	0.50
No Bags	4	---	1.74	----	----
13	5	55	0.44	4.30	0.55
14	5	85	0.34	5.50	0.55
15	5	120	0.28	6.30	0.51
16	5	165 ⁵	0.27	7.00 ⁶	0.55
No Bags	5	----	1.18	----	----

Notes:

¹ W_{50} = the median weight of the soil plus bag

$${}^2D_A = \frac{(1-n)\gamma AD_{50}}{W_{50}}$$

³ H_{ZD} = Zero-damage deepwater wave height

⁴No Bags = the slope is unprotected and D_A is based on $W_{50} = 55$ g

⁵1 lb = 453.6 g

⁶1 in. = 2.54 cm

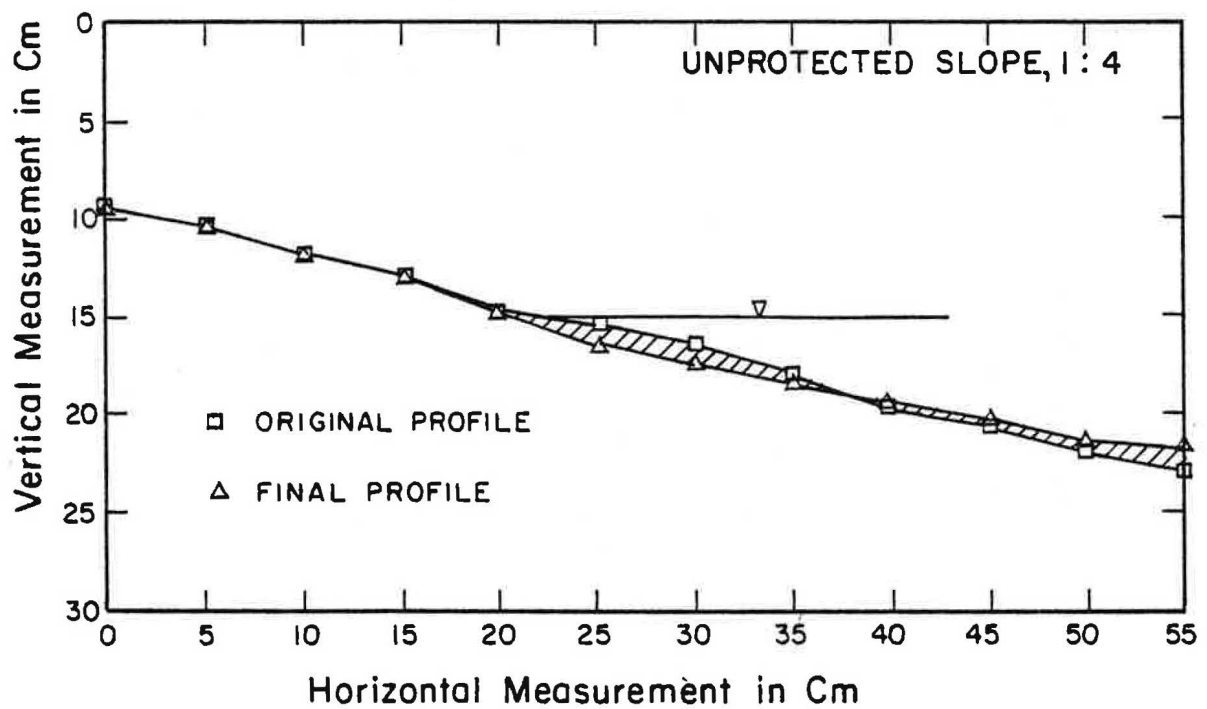
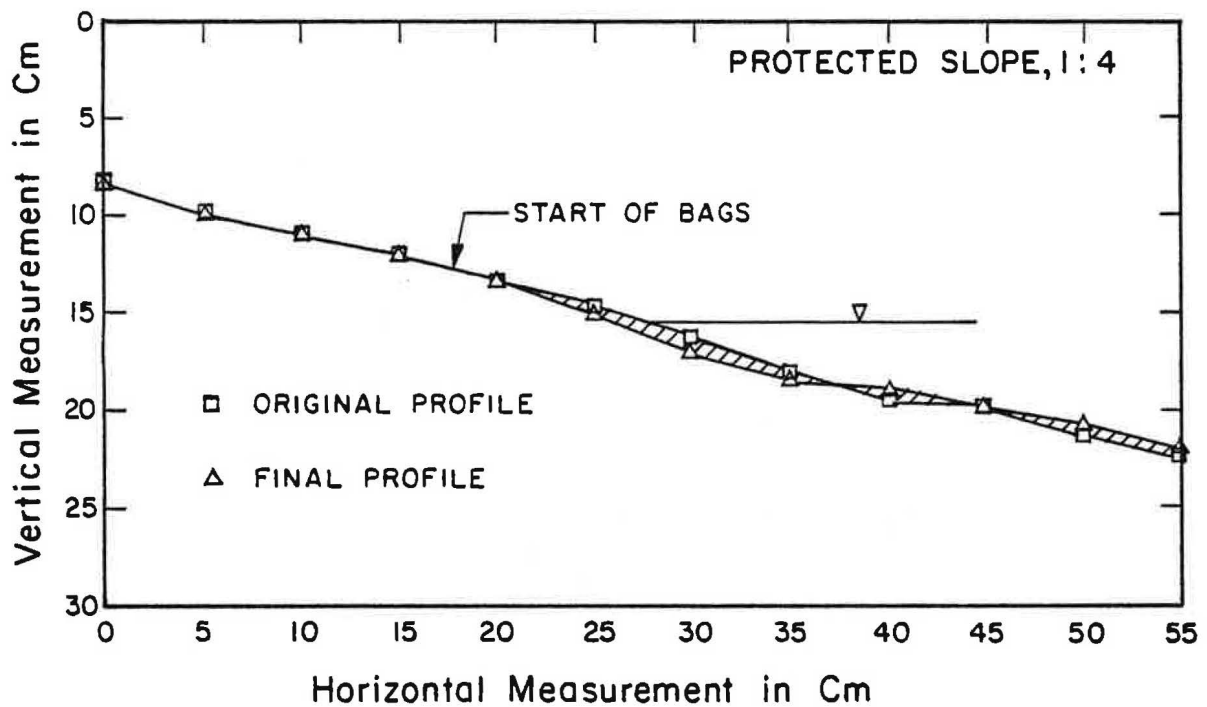


Figure 52.. Typical Damage (D_A) Profiles for Protected and Unprotected Slopes, (Slope: 1 on 4)

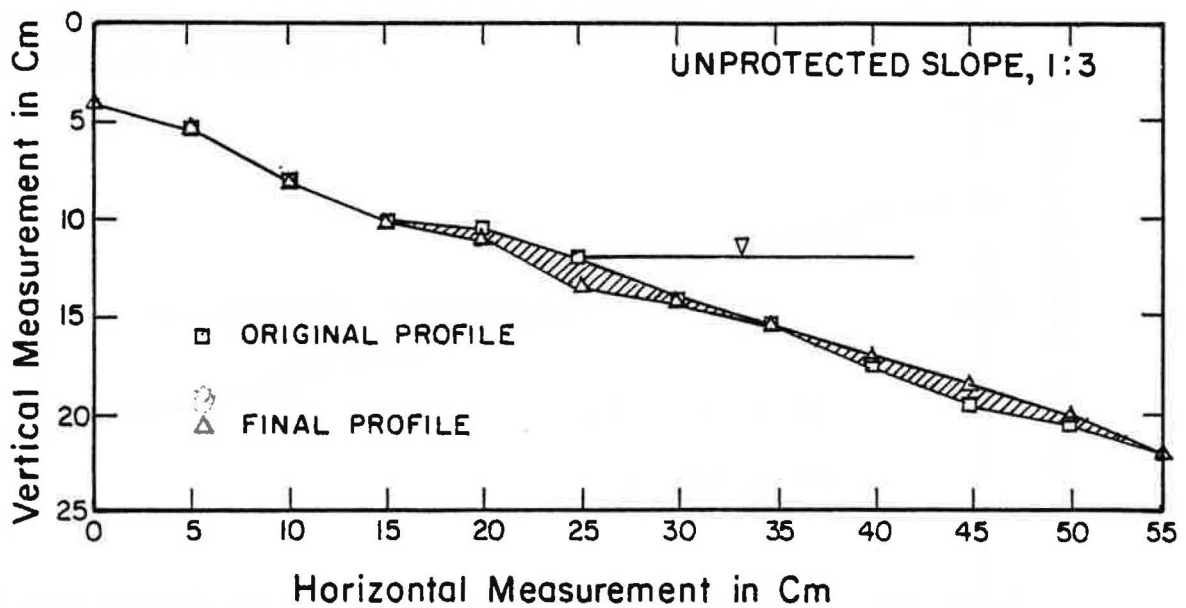
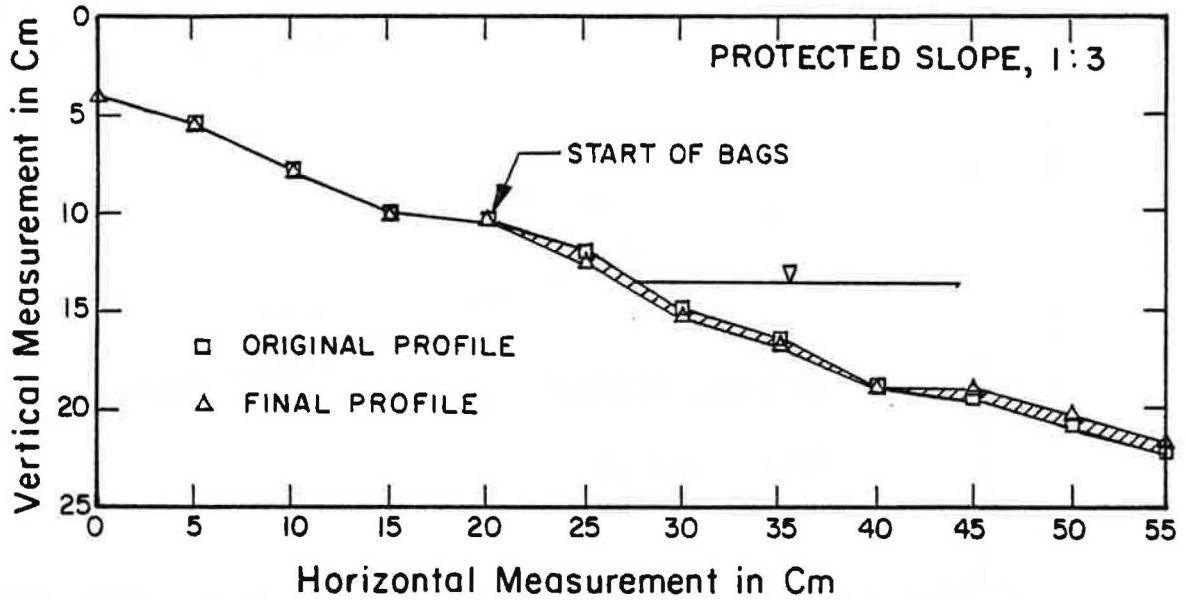


Figure 51. Typical Damage (D_A) Profiles for Protected and Unprotected Slopes, (Slope: 1 on 3)

D = least distance traveled to cause displacement, cm

γ_{sat} = saturated unit weight, g/cm³

W_{50} = median weight of a single bag, g.

By assuming that all the soil below the still water level was saturated and finding the average water content of the submerged sand bags in each test to be 44.0%, the saturated unit weight, γ_{sat} , was calculated to be 1.79 g/cm³ (111.7 pcf) and the porosity, n , was calculated to be 55.0%.

In Figure 54, the area damage, D_A , was plotted as a function of the embankment slope ($\cot \alpha$) and the median weight of the bags (W_{50}). For each slope, it was shown that the damage decreased as the slope angle decreased ($\cot \alpha$ increased) and the weight of the bags increased. Since the area of erosion is directly proportional to the damage, it follows that the area of erosion also decreases with decreasing embankment slope.

From Figure 54, there appears to be a limit at which, with an increasing median weight of bags, the damage remains constant at approximately 0.27. This would indicate that for prototype conditions a maximum size bag could be specified to protect against inner bag erosion. However, since the maximum weight of bag used in these tests was 165 g (0.361b), further testing would have to be conducted at heavier weights to verify this generality.

A complete listing of area damage numbers versus median weights can be found in Table VI.

2. Scaling Effects. From each test the zero-damage wave height was obtained as previously described. A stability number corresponding to each test was calculated based on each H_{ZD} found. This zero-damage stability number, N_{ZD} , can be written in the form

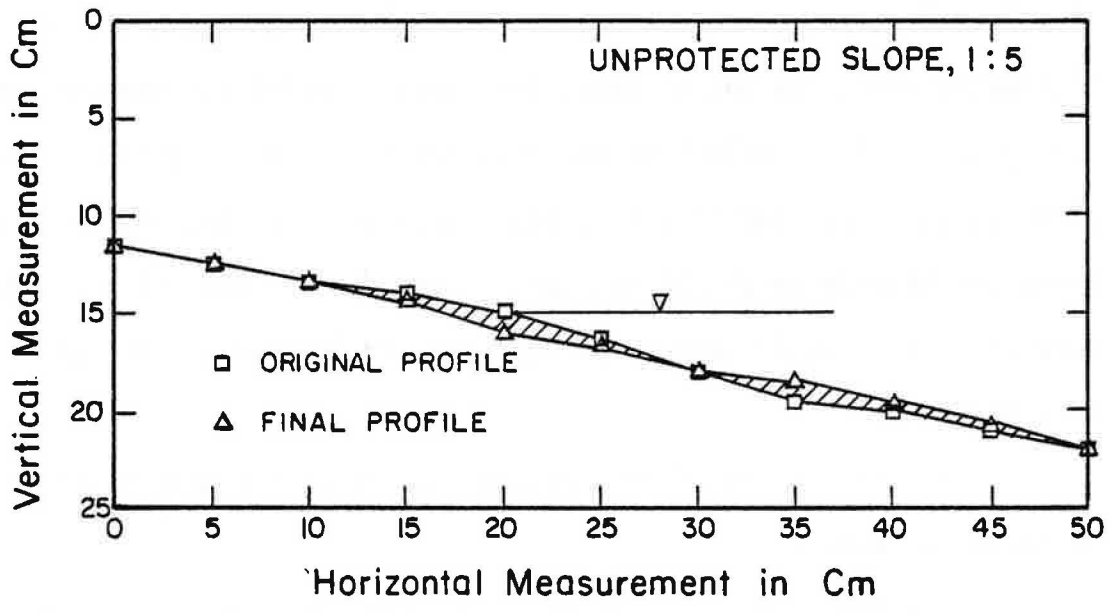
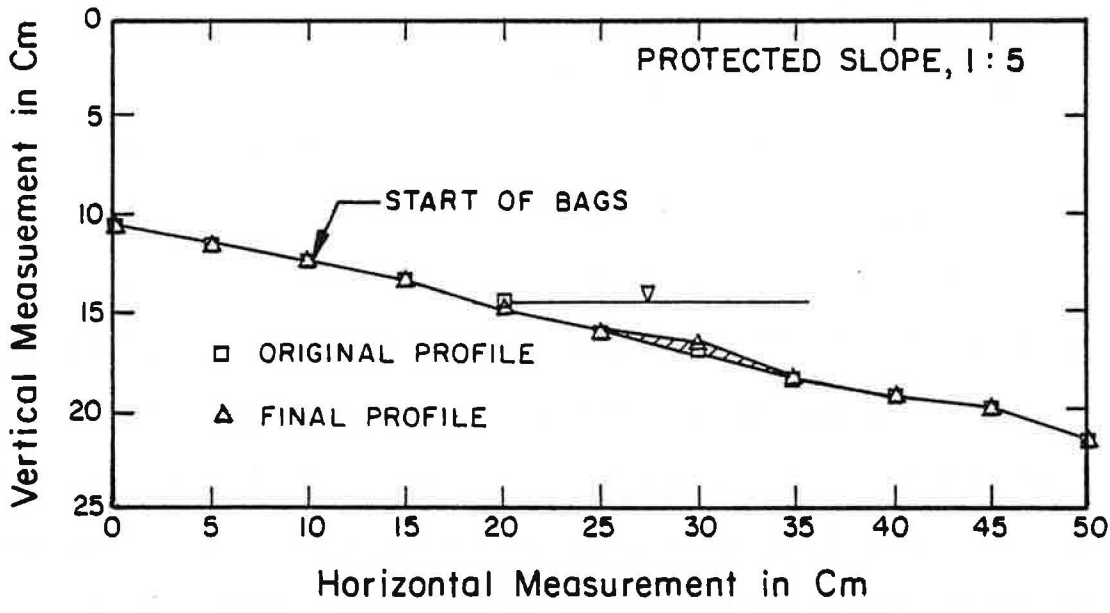


Figure 53. Typical Damage (D_A) Profiles for Protected and Unprotected Slopes, (Slope: 1 on 5)

$$N_{ZD} = \frac{H_{ZD}}{(W_{50}/\gamma_{sat})^{1/3}(G_s-1)} \quad (16)$$

The Reynolds number is also based on the zero-damage wave height and can be written in the form

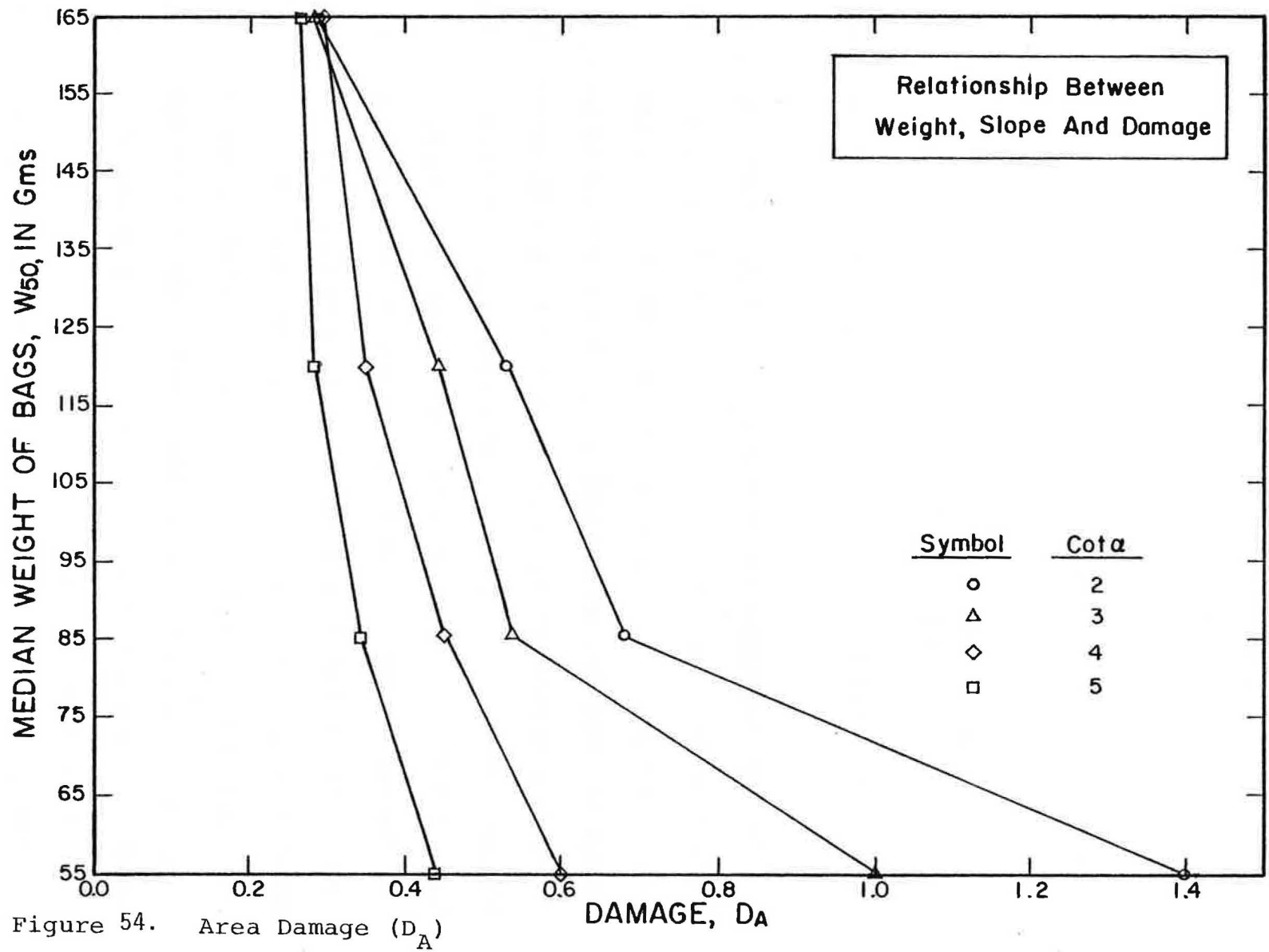
$$R_N = \frac{\gamma_f}{\mu} \cdot \frac{W_{50}^{1/3}}{\gamma_{sat}} \cdot \frac{H_{ZD}^{1/2}}{g} \quad (17)$$

See Appendix A for the development of each equation and Appendix D for variable definitions.

The Reynolds number has been used in the past to correlate scale or viscosity effects for model testing. The effect of viscosity was investigated by analyzing data from this study and comparing it to previous model studies of larger and smaller scales. Since the Reynolds number is primarily a function of viscosity for each test, Reynolds number was plotted against its corresponding zero-damage stability number (Figure 55). Each point is also plotted as a function of embankment slope.

The results were similar for all four plots and showed the same general characteristics developed by Thomsen, et al., (1972). The sand bag stability, expressed as N_{ZD} is low for small Reynolds numbers (small-scale test) and increases with large Reynolds numbers (large-scale test). At $R_N > 3.3 \times 10^4$, stability is independent of the Reynolds number and is therefore independent of scale. Stability is also greater for flatter slopes for a given Reynolds number.

From previous work, it was shown that large-scale testing is confined to $R_N > 2.0 \times 10^5$ and small-scale testing generally yields $R_N < 1.0 \times 10^4$. At the point of constant stability, termed N_{ZD_0} , the tests in this study



are approximating large-scale models with increased scales resulting from increased R_N . However, since all four slopes in this study just begin to approach the constant stability number (the location of each curve in Figure 55 is arbitrarily placed as the constant stability number is approached and its position is based on curve configuration from previous studies) and since $1.0 \times 10^4 < R_N < 2.0 \times 10^5$, the tests conducted for this experiment can be assumed to be medium-scale tests and a need for scale correction becomes apparent. By correcting for scale, small- or medium-scale tests can be used to predict large-scale (or prototype results).

Each N_{ZD} from Figure 55 was divided into its corresponding N'_{ZD_0} value to obtain a factor, $F_R = N'_{ZD_0} / N_{ZD}$. A plot of F_R versus R_N was drawn and is shown in Figure 56. Also shown are some of the results of two other investigations, one for small-scale tests (Thomsen, 1972) and the other for semilarge-scale tests (Ahren, 1975).

All data appear to define a single function for R_N and F_R . From Figure 56, it appears that small-scale and medium-scale stability numbers would have to be increased somewhat to reach large-scale test results. Since the fluid properties, μ and γ_f are the same for all models and prototypes where water is the fluid, variations of R_N depend solely on geometric scale [discounting any temperature variation, which for these tests was constant at 22° C, corresponding to an absolute viscosity of 1.074×10^{-5} g-sec/cm² (2.2×10^{-5} lb-sec/ft²), and $\gamma_f = 1.0$ g/cm³ (62.4 pcf)]. Therefore, F_R can be taken to be a correction factor to convert from medium-scale to large-scale (or prototype conditions). The zero-damage stability number, N_{ZD} , for each model can be adjusted to its equivalent large-scale value by simply multiplying by the correction factor obtained from Figure 56. The new zero-damage stability number is termed N'_{ZD} . (Note that for large-scale tests, $F_R = 1.0$).

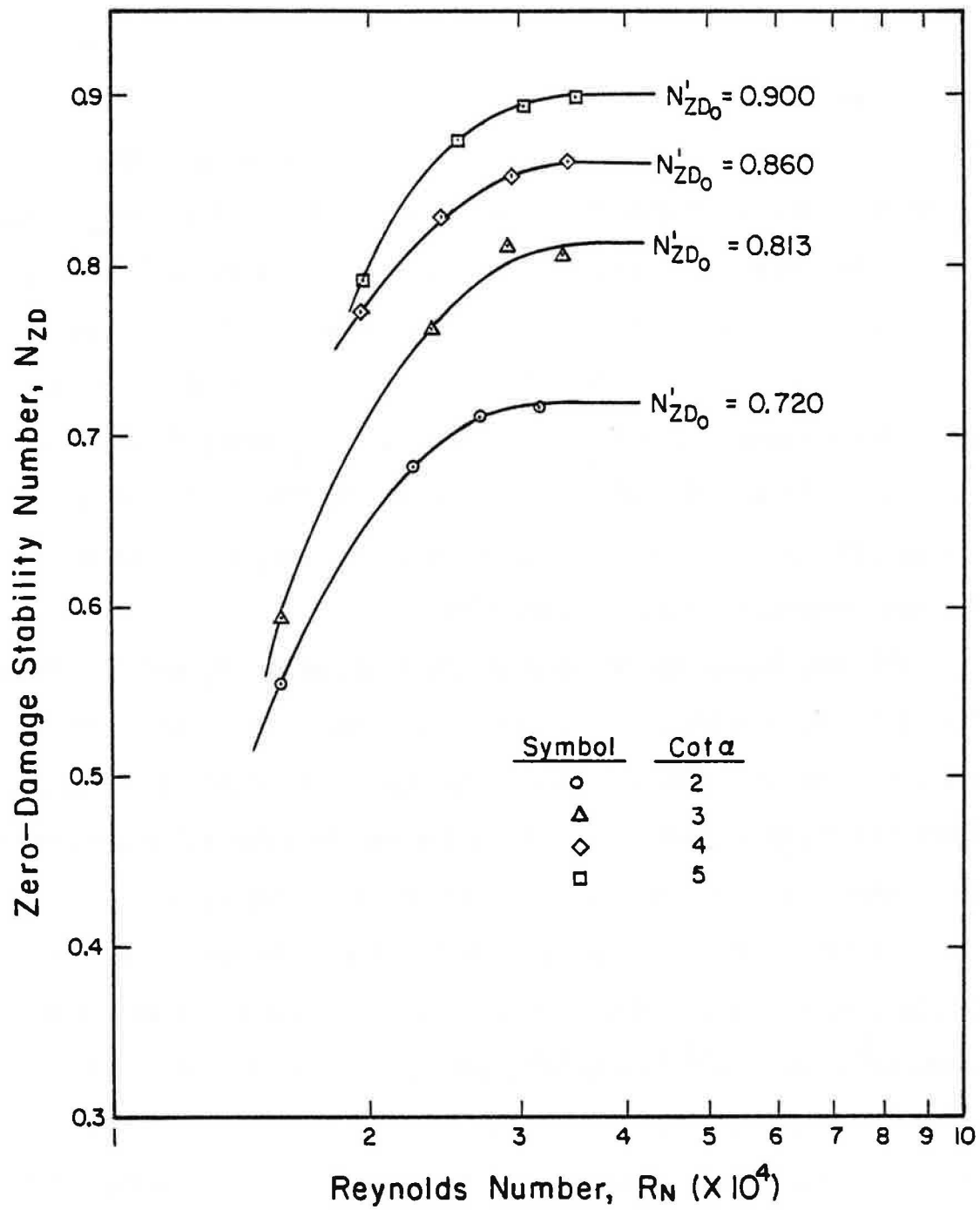


Figure 55. Reynolds Number as a Function of Stability

Table VII gives the calculated stability numbers, Reynolds numbers and zero-damage wave heights for each model test.

3. Wave Period Effect. The effect of wave period on armor stability was investigated for a limited range of periods. However, even with this limited range of periods, it was still observed that zero-damage stability is indeed a function of wave period. By plotting the corrected stability number, N'_{ZD} , against the dimensionless wave period, $gT^2/(W_{50}/\gamma)^{1/3}$, it is seen that stability decreases with increasing wave periods until a constant minimum value of stability is reached which is independent of period (Figure 57). These results are comparable to model tests on dumped riprap which also showed decreasing stability with increasing wave period (Thomsen, et al., 1972). Since the wave parameter $gT^2/W_{50}/\gamma)^{1/3}$ is the ratio of the wave length (Equation 13) to the armor size (the width of the bags), this parameter can be used to compare data from all size tanks and Figure 57 can therefore be used to compare model and prototype testing.

As with Figure 55, Figure 57 also shows that stability increases with decreasing embankment slope ($\cot \alpha$ increasing). The dashed lines are lines of constant deep water wave steepness (H_{ZD}/L_0) which can also be viewed as a relationship between wave height and wave period (Equation 13). They range from 0.10 to 0.20 which is in almost perfect agreement with wave steepness measurements from some inland reservoirs (Johnson, 1948). It is noted from Figure 57 that for wave steepness less than about 0.14, all four slopes are approaching a constant minimum zero-damage stability value. This would indicate that for reservoirs with a wave steepness less than 0.14, the stability of the protection material has reached constant minimum value and is therefore approaching an equilibrium condition. The minimum value of stability termed N''_{ZD} , will be discussed further in the next section.

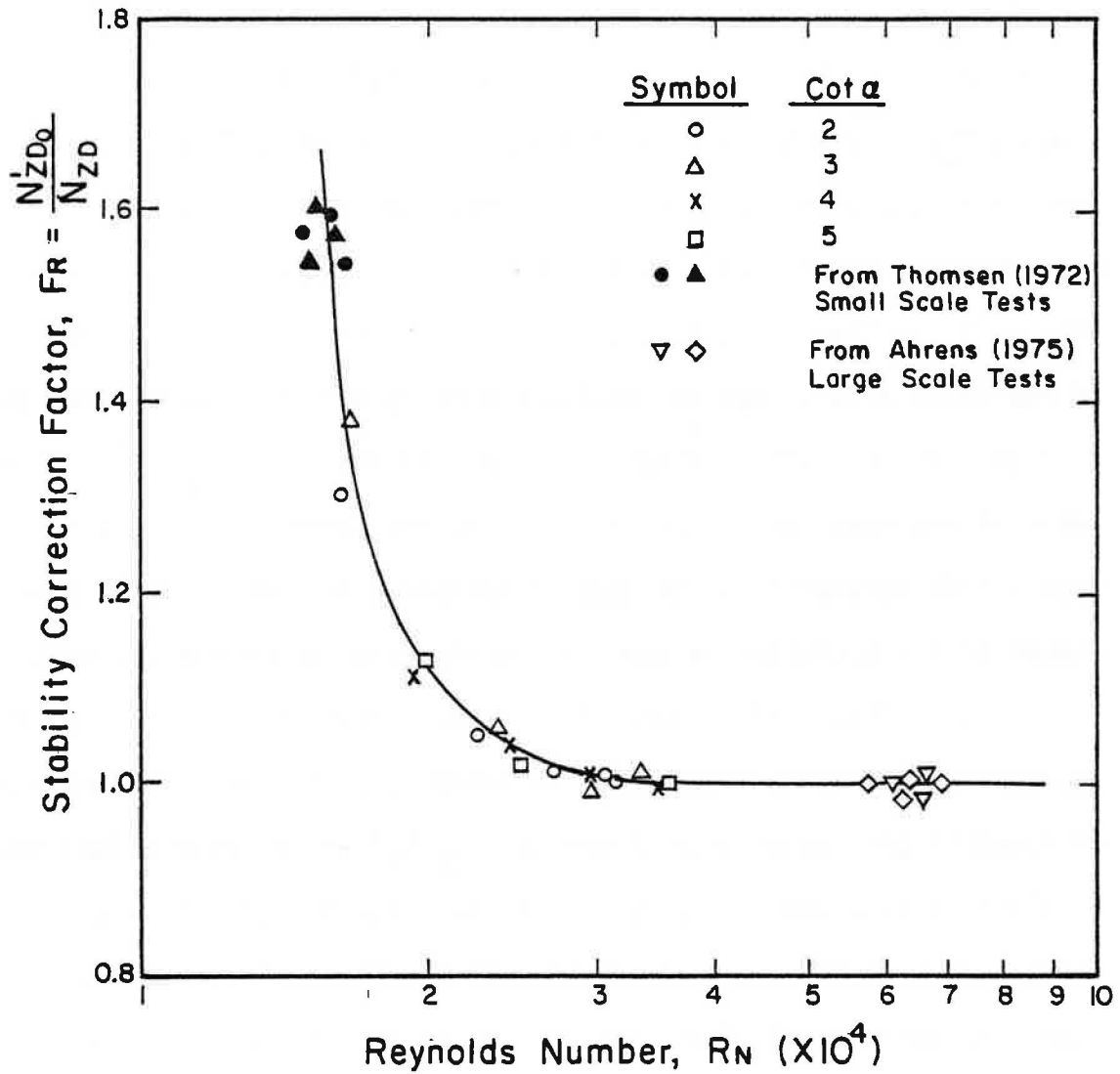
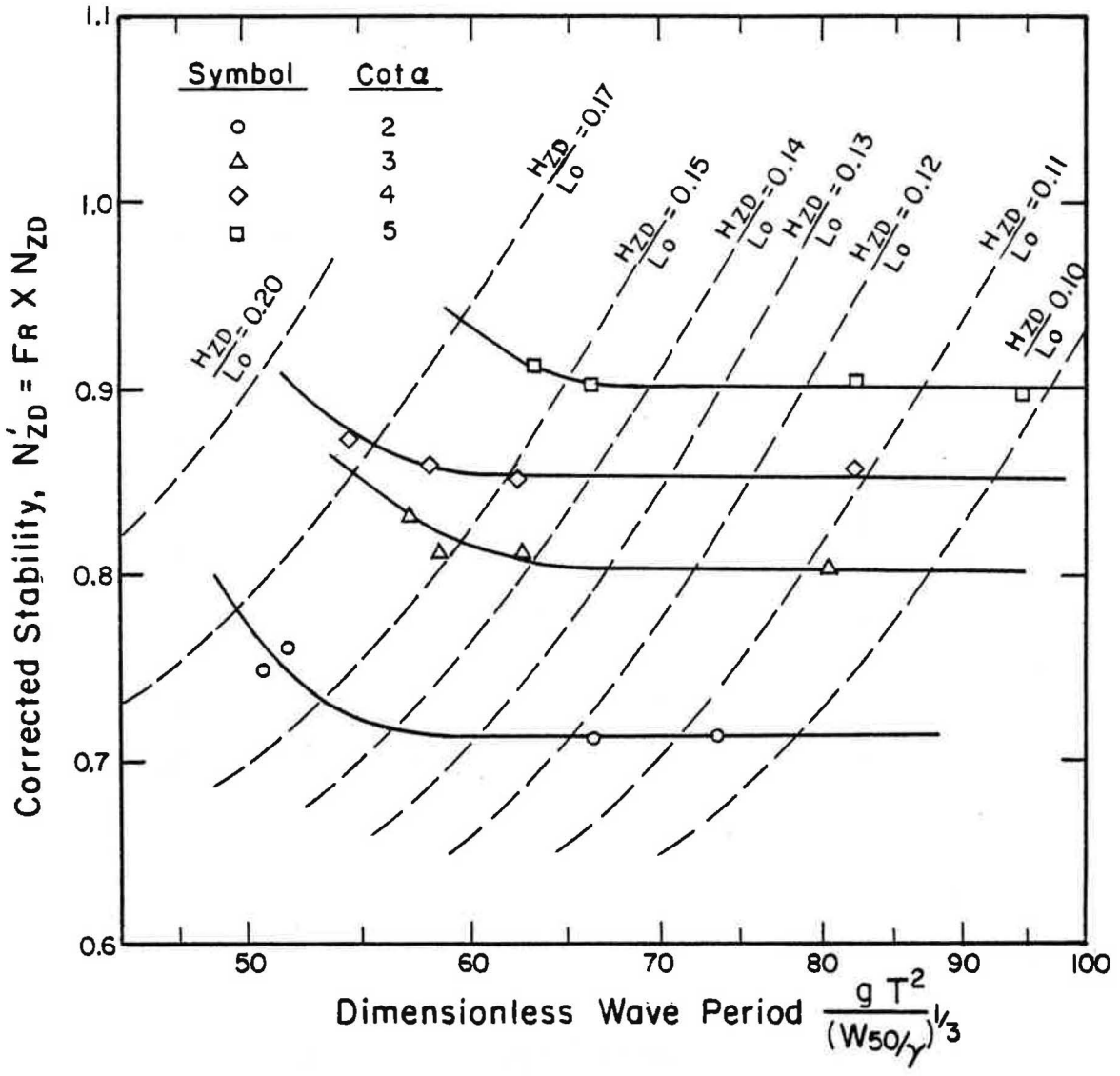


Figure 56. Stability Correction for Scale Effect



$$\frac{H_{ZD}}{L_0} = \frac{N'_{ZD} W_{50}^{1/3} (G_s - 1)}{F_R \gamma_{sat}^{1/3}} = 2\pi (G_s - 1) \frac{\left[\frac{N'_{ZD}}{F_R} \right]}{\left[\frac{g T^2}{(W_{50}/\gamma)^{1/3}} \right]}$$

Figure 57. Stability as a Function of Wave Period

TABLE VII
MODEL TEST RESULTS IN DIMENSIONLESS FORM

Test No.	cot α	H_{ZD}^1 (cm)	Stability Number ² N_{ZD}	Reynolds Number ³ R_N	Period ⁴
1	3	3.20	0.591	16700	57.9
2	3	4.80	0.766	23600	81.9
3	3	5.75	0.818	29000	62.7
4	3	6.30	0.806	33700	56.4
5	2	3.00	0.554	16100	52.6
6	2	4.30	0.686	22300	50.0
7	2	5.00	0.711	27000	73.0
8	2	5.60	0.717	31800	65.6
9	4	4.20	0.775	19100	57.9
10	4	5.20	0.830	24600	81.9
11	4	6.00	0.854	29600	62.7
12	4	6.75	0.864	34900	54.4
13	5	4.30	0.794	19300	94.6
14	5	5.50	0.879	25300	81.9
15	5	6.30	0.896	30300	62.7
16	5	7.00 ⁵	0.900	35600	65.6

Notes:

¹ H_{ZD} = Zero-damage deepwater wave height

$${}^2N_{ZD} = \frac{H_{ZD}}{(W_{50}/\gamma)^{1/3}(G_s-1)} = \text{zero-damage stability number}$$

$${}^3R_N = \frac{\gamma_f}{\mu} \frac{W_{50}}{\gamma}^{1/3} \frac{H_{ZD}}{g}^{1/2}$$

$${}^4\text{Period} = \frac{gT^2}{(W_{50}/\gamma)^{1/3}} = \text{Dimensionless wave period}$$

⁵1 in. = 2.54 cm

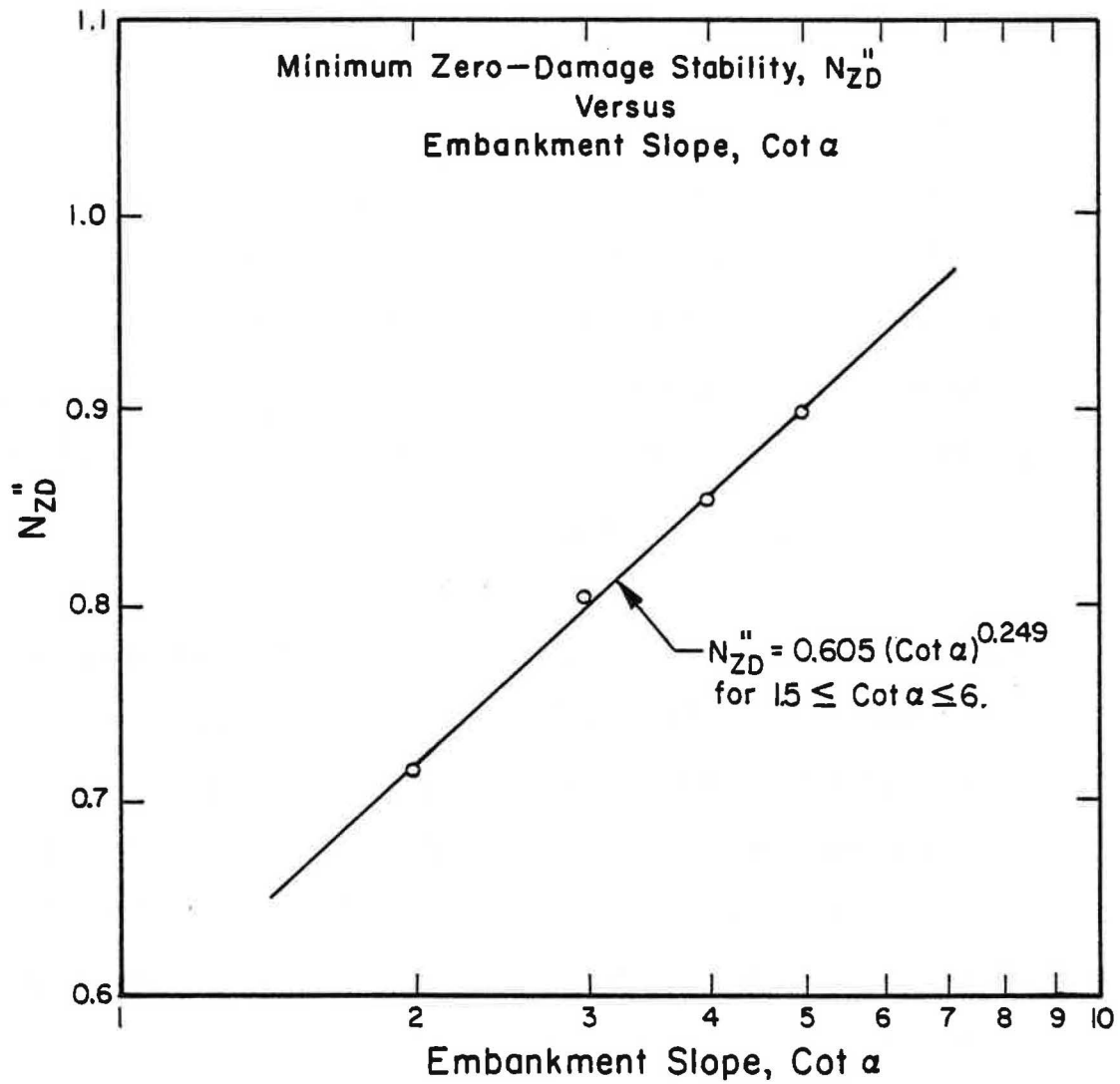


Figure 58. Minimum Zero-Damage Stability as a Function of Embankment Slope

A listing of each dimensionless wave period is shown in Table VII for each test.

4. Embankment Slope Angle Effects. Figure 55 indicated that stability increased with decreased slope angle when plotted as a function of Reynolds number. Figure 57 also showed that stability increased with decreasing slope angle ($\cot \alpha$ increasing) when plotted as a function of dimensionless wave period. By plotting the constant minimum zero-damage stability numbers, N_{ZD}'' , as a direct function of embankment slope for $\cot \alpha$ equal 2, 3, 4, and 5, it is seen that there is a direct relationship between the minimum stability and the embankment slope (Figure 58). Stability increase as the embankment slope decreases. This relationship was determined to be a power curve function in the form, $y = ax^b$, namely

$$N_{ZD}'' = 0.605(\cot \alpha)^{0.249} \quad (18)$$

This equation is valid for sand pillows only and for a range of slopes such that $1.5 \leq \cot \alpha \leq 6.0$. Table VIII shows the more common slopes with their corresponding minimum zero-damage stability value.

With the embankment slope angle known, a minimum stability coefficient can be calculated either from Equation 18 or from Figure 58. This parameter will be seen later to play an important role in the proposed design criteria.

Some other investigations have offered equations to explain the relationship between stability and embankment slope. These are shown in Table IX. Although the constants in each equation are not the same and were not developed for the same type of armor, note that all equations have the same form, i.e., $y = ax^b$.

TABLE IX
COMPARISON OF STABILITY EQUATIONS

Equation	Limits	Reference
$N_{ZD}'' = 0.605(\cot \alpha)^{0.249}$	$1.5 \leq \cot \alpha \leq 6.0$	Equation 18
$N_{ZD} = 1.54(\cot \alpha)^{2/9}$	only for stone	Ahren, 1975
$N_{ZD} = 1.47(\cot \alpha)^{1/3}$	only for stone	Hudson, 1961
$N_{ZD} = \text{constant}(\cot \alpha)^1$	$\cot \alpha \leq 2.6$	Svee, 1962

Note:

¹The constant in this equation varies with type of protection used.

TABLE X
MODEL RUNUP RESULTS

$\cot \alpha$	Runup, R (cm)	H_o^1 (cm)	R/H_o^2	H_o/L_o^3
2	3.5	3.80	0.92	0.14
	5.0	5.06	0.99	1.18
	7.0	6.30	1.11	1.13
	9.0	7.72	1.17	1.19
3	3.0	3.80	0.79	0.14
	4.0	5.06	0.79	0.18
	5.5	6.30	0.87	0.13
	7.5	7.72	0.97	0.19
4	2.5	3.80	0.66	0.14
	3.5	5.06	0.69	0.18
	5.0	6.30	0.79	0.13
	7.0	7.72	0.91	0.19
5	2.0	3.80	0.53	0.14
	3.0	5.06	0.59	0.18
	4.0	6.30	0.63	0.13
	6.5 ⁴	7.72	0.84	0.19

Notes:

¹ H_o = deepwater wave height

² R/H_o = relative runup

³ H_o/L_o = relative wave steepness

⁴1 in. = 2.54 cm

TABLE VIII
MINIMUM ZERO-DAMAGE STABILITY NUMBERS

Embankment Slope	$N_{ZD}^{\#}$
1 on 1 1/2	0.669 ¹
1 on 2	0.715
1 on 2 1/2	0.760 ¹
1 on 3	0.802
1 on 4	0.852
1 on 5	0.900
1 on 6	0.945 ¹

Note:

¹Obtained from Equation 18

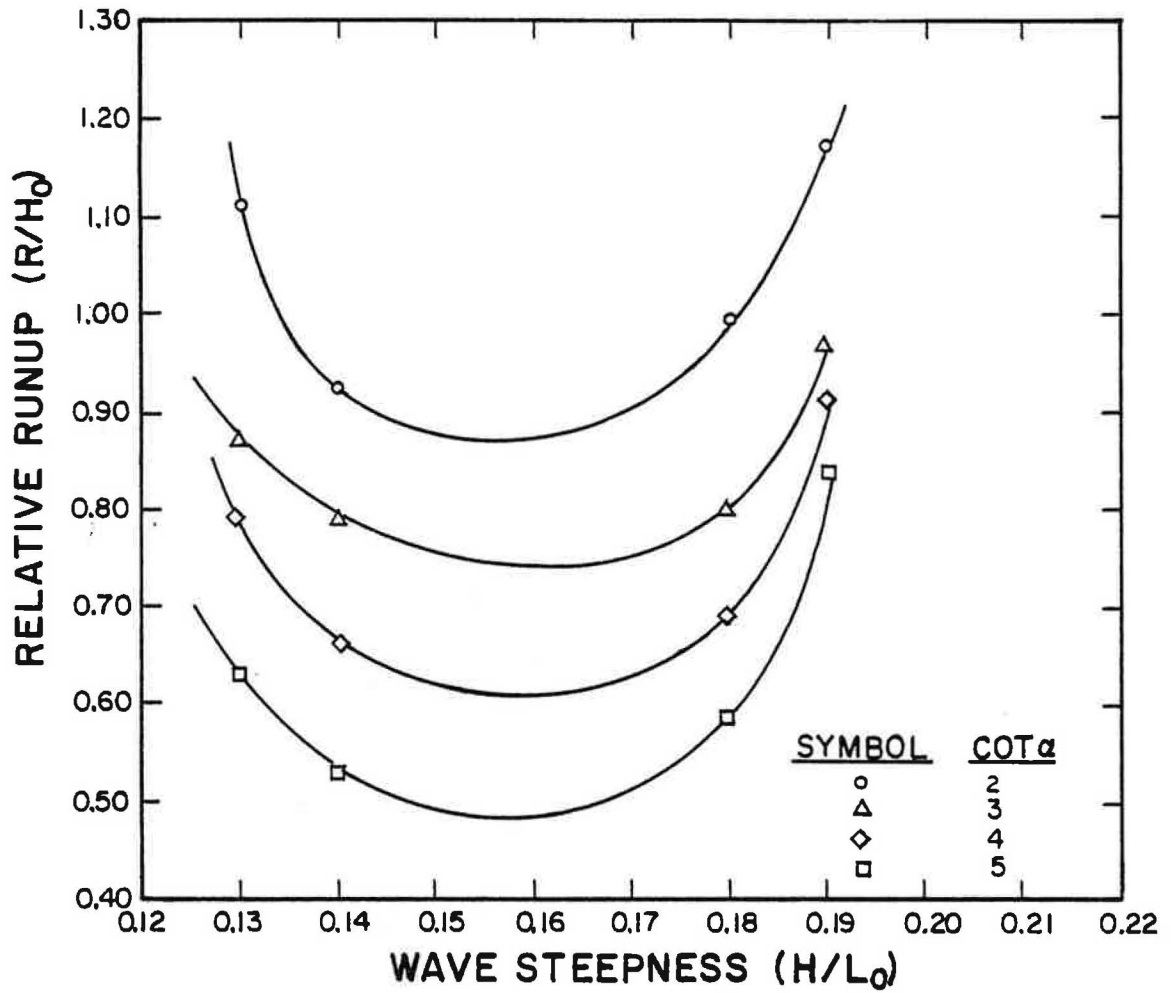


Figure 59. Relative Runup as a Function of Wave Steepness and Embankment Slope

5. Wave Runup Effects. The wave runup parameter was measured for various sets of conditions including measurements of runup on wood, soil, and sand bags.

The runup measurements for the plywood and soil slopes when plotted as relative runup (R/H_0) versus relative wave steepness (H_0/L_0) were such that relative runup decreased with decreasing slope angle and increasing wave steepness.

However, when relative runup on the sand pillows was plotted as a function of wave steepness, the relationship between runup and steepness was of an entirely different nature (Figure 59). It appears that there exists a minimum relative runup at a water wave steepness of approximately 0.155. At both larger and smaller values of wave steepness, relative runup is larger.

Due to the limited number of wave heights and lengths tested in this study, it is recommended that a more detailed examination be conducted on the sand pillows with a wider range of wave lengths and heights being used before any conclusion can be drawn from Figure 59. The values of runup that were measured and used in the analysis are listed in Table X with its corresponding wave weight that generated the runup.

6. Other Considerations. There are several factors that would appear to be a function of the stability of the sand bags that were not systematically investigated for this study, but some comment about them is deemed necessary.

Water depth would appear to have some influence on the stability of model sand bags. However, it has been shown that if the depth of water during testing was such that waves did not break, there was little variation of stability with variations of depth. The depth of water for this

back-calculate the zero-damage wave height, H'_{ZD} . This method of back-calculating is called hindcasting. The equation used to hindcast H'_{ZD} was developed from Appendix A, namely.

$$N = \frac{H_o}{(W/\gamma)^{1/3}(G_s-1)} \quad (19)$$

By substituting the zero-damage stability number and wave height and accounting for scale effect, Equation 19 can be reduced to

$$N'_{ZD} = \frac{F_R H_{ZD}}{(W_{50}/\gamma_{sat})^{1/3}(G_s-1)} \quad (20)$$

or

$$H'_{ZD} = (G_s - 1) \left(\frac{N'_{ZD}}{F_R} \right) \left(\frac{W_{50}}{\gamma_{sat}} \right)^{1/3} \quad (21)$$

where

$$G_s = 2.73$$

$$\gamma_{sat} = 1.79 \text{ g/cm}^3 \text{ (112 pcf).}$$

The hindcast zero-damage wave height was plotted against the observed or actual zero-damage wave height for all sixteen tests in Figure 60. The mean difference between actual and hindcast values was less than one percent and the standard deviation was 0.8 percent.

8. Stability Prediction and Design Equation. If Equation 21 is solved for the median weight of the sand pillows, W_{50} , an armor sizing equation for zero-damage stability against wave action on an embankment slope would be established, i.e.,

$$W_{50} = \frac{H_{ZD}^3 \gamma_{sat}}{(N'_{ZD}/F_R)^3 (G_s - 1)^3} \quad (22)$$

investigation was held constant for all tests and was such that there were no breaking waves.

Underlayers of the sand bags were not investigated since filter layers are not generally placed on local irrigation reservoirs. The sand bags are usually placed directly on the earth embankment. However, in previous work in which the filtering layer thickness for riprap was varied, it was concluded that the underlayering thickness had no affect on stability since very little erosion occurred between the individual stones.

Techniques of armor placement were also not investigated. It would appear that the most economical placement of the bags would be lengthwise across the slope as was done in all testing. By this placement, the largest area of the slope can be covered with the least amount of bags used for a given distance of protection up the slope. Furthermore, if the sand bags were placed lengthwise up the slope, the runup would possibly be greater and increase the possibility of downstream erosion during periods of high water level.

An attempt was made to measure the percent of soil lost from the sand bags that were in the direct path of the wave attack. After each of the initial tests, the numbered sand bags were completely emptied and washed and the soil remaining was oven-dried. From this weight and the initial oven-dried weight of soil, the percent soil lost was calculated.

However, due to the limited time the soil was subject to wave attack (maximum time was 5 1/2 hours), and due to the small size of the bags, the amount of soil lost varied considerably from bag to bag for each test and no conclusions could be reached.

7. Data Scatter. In order to test the consistency of the relationships developed in this investigation, Figures 56 and 57 were used to

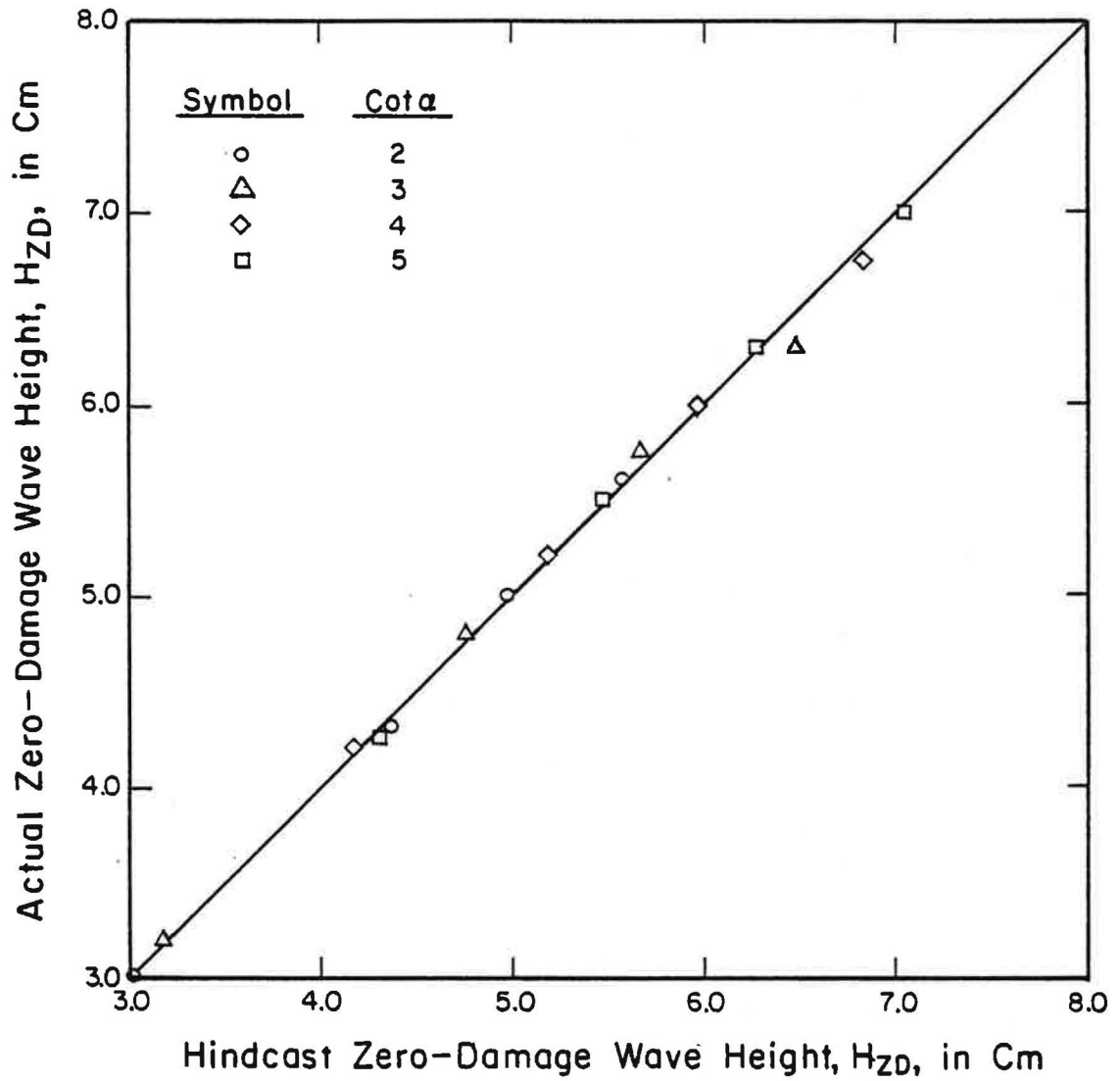


Figure 60. A Comparison of Hindcast Zero-Damage Wave Heights and Actual Zero-Damage Wave Heights for all Model Tests

This equation is very similar to the one developed by Thomsen, et al., (1972), except for the unit weights. Thomsen, et al, based their calculations on dry unit weights, whereas this study is based on saturated unit weights. Equation 22 is a general equation that can be adopted for any combination of wave period and geometric scale.

As seen in Figure 57, for wave steepness less 0.14, N_{ZD}^I approaches a constant minimum value that is independent of steepness or wave period. This minimum value, N_{ZD}^{II} , is a function only of embankment slope in this study. Also, from Figure 56 it can be seen that for large-scale or prototype design, the correction factor, F_R , approaches a constant value of 1.0. Therefore, by substituting into Equation 22 N_{ZD}^{II} for N_{ZD}^I and $F_R = 1.0$, the following equation results:

$$W_{50} = \frac{H_{ZD}^3 \gamma_{sat}}{(N_{ZD}^{II})^3 (G_s - 1)^3} . \quad (23)$$

By obtaining values of N_{ZD}^{II} for a given slope from Table IV or Equation 18, this equation could be adapted for prototype design. Note that Equation 23 will yield conservatively high values of W_{50} since N_{ZD}^{II} is based on minimum stability values with respect to wave period (Figure 57).

A design chart for various embankment slopes was developed based on Equation 23 (Figure 61). This chart facilitates the calculation of the median weight of the sand bags simply by knowing the zero-damage wave height and embankment slope. It should be noted, however, that Figure 61 is based on the Mexico clay soil with $G_s = 2.73$ and $\gamma_{sat} = 112$ pcf (1.79 g/cm³). Should this analysis be used for a different type soil, the design weight should be based on Equation 23 rather than the use of Figure 61.

To test the validity of Equation 23 and Figure 61, the required median weight of the sand pillows necessary to prevent slope instability was calculated for the field evaluation prototype embankment located near Mexico, Missouri. This embankment, owned by Mr. Jake Fryer, has been previously described.

The Corps of Engineers design method was used to calculate the zero-damage wave height (McCartney, 1976). By use of regional wind data charts, a design wind of 45 mph (72.4 kph) with a duration of seven minutes was calculated. The effective fetch length on the reservoir was determined to be 0.25 miles (0.4 km). This resulted in a forecast zero-damage wave height of 0.92 ft. (0.28 m) with a wave period of 1.75 sec, and a wave steepness of 0.06 which is less than the limiting value of 0.14.

From Table VIII, for a 1 on 3 slope, $N_{ZD}'' = 0.802$. With $\gamma_{sat} = 112$ pcf (1.79 g/cm^3) and $G_s = 2.73$, the required median weight necessary to protect the embankment slope should be 98.5 lb (44.7 kg) (Figure 61). The average weight of the sand pillows on Mr. Fryer's reservoir is approximately 85 - 90 lb (38.6 - 40.9 kg). The calculated weight resulted in approximately a ten percent conservatively high value, as anticipated. Since the sand pillow slope protection system appears to be adequate for Mr. Fryer's reservoir, with no removal of sand pillows due to wave action, this proposed design equation would appear to be a useful, although conservative, method of calculating the weight of the protection bags. However, Figure 61 was only tested on one prototype reservoir. Before any concrete statement can be made as to the reliability of Equation 23 or Figure 61, it should be tested against several other prototype reservoirs for different soil types and wind conditions.

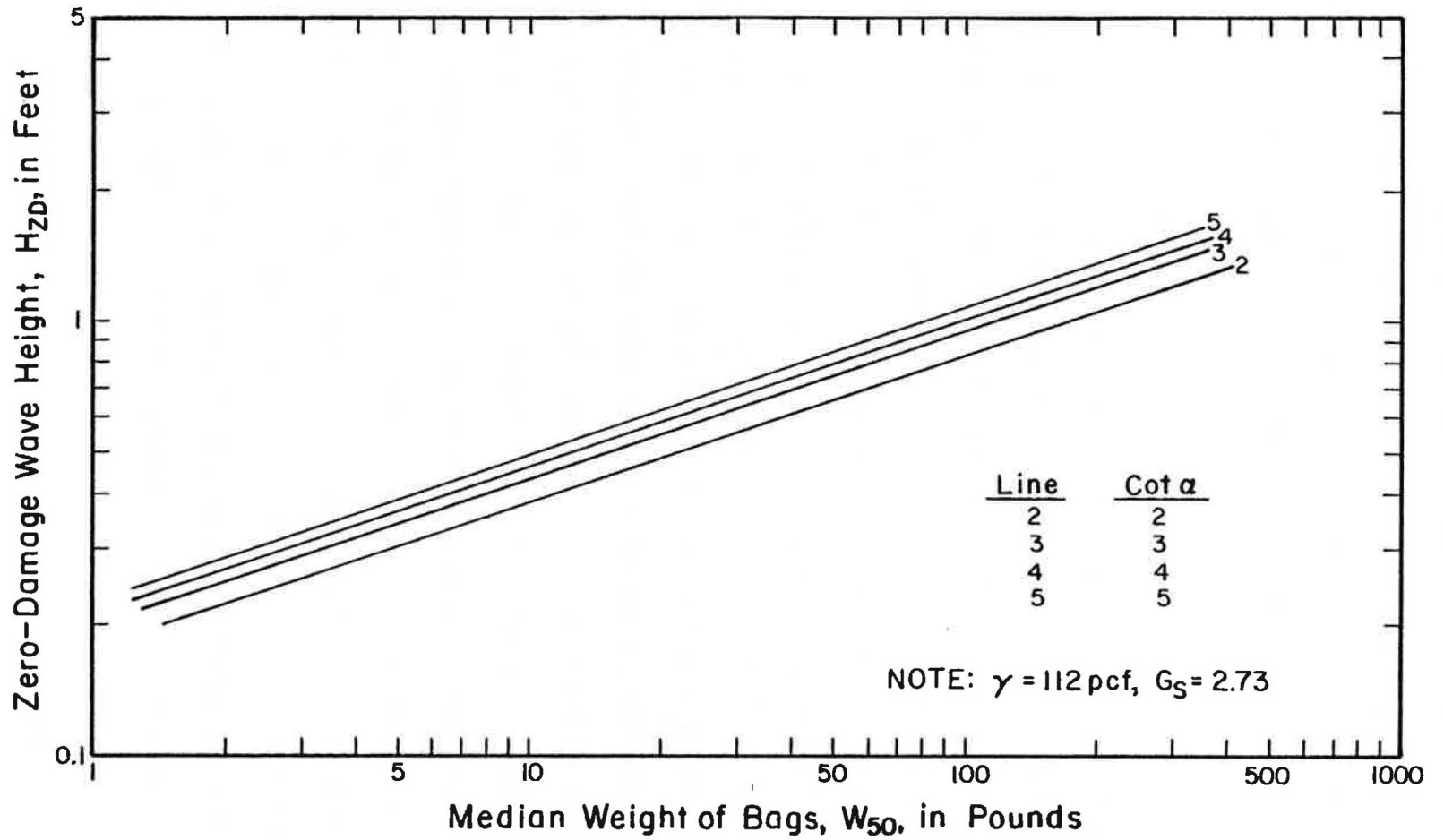


Figure 61. Zero-Damage Stability Curves for Acrilan Sand Pillows

3. The amount of wave erosion that occurs on an earth embankment varies with the time of the year. The greatest amount of erosion appears to take place between the months of April and May, when wind velocities and reservoir levels are generally highest.

4. The rate of erosion of silty clay embankments accelerates, to a certain degree, with time. Wave erosion tends to produce unstable vertical cuts on the embankment slope which slumps or slides easily when undercut by constant wave action. With time, the vertical cuts become larger, the instability increases, and the rate of failure increases with relatively small amounts of undercutting necessary to cause failure of the cut.

5. Although the cost of the fabric system is initially high, reduced maintenance costs and other factors may, in the future, make this technique attractive compared to other methods available to the farmer.

In addition, the following observations can be made:

1. Several irrigation dams near the project site were inspected. The performance of slope protection methods on these dams was evaluated. The natural rock materials utilized on these dams lacked adequate size material to resist normal wave action. The slope protection systems utilized also lacked the filter gradation necessary to retain the clay material used to construct the embankment.

2. The erosion observed on Missouri irrigation reservoirs indicates that wind generated waves from any direction will significantly deteriorate typical silty clay dams. The short fetch lengths associated with irrigation reservoirs restrict the size of wave generated, but require only short duration winds to produce the maximum possible wave height. The slopes of these irrigation dams are under maximum attack more frequently due to waves generated by winds from any direction.

VI. CONCLUSIONS AND APPLICATIONS

The objectives of this investigation were to evaluate the performances of a fabric slope protection system on an irrigation dam and to determine the effects of wave height, wave period, embankment slope angle and weight of the individual armor units have on the pillow. In addition, possible design criteria were to be developed for filling and placing the pillows on irrigation reservoirs. These objectives were accomplished by monitoring a full-scale installation of the slope protection system and by performing a model study of the system in a medium-scale laboratory wave tank. The soil retention characteristics of the fabric were determined by conducting laboratory immersion tests.

A. FIELD TESTING PROGRAM

The performance of the sand pillow slope protection system on a full-scale installation was monitored in northern Missouri. By comparison of results of unprotected sections of an irrigation embankment with sections protected by Acrilan sand pillows filled with on-site material, the effectiveness of the system was evaluated. The monitoring program resulted in the following conclusions:

1. The fabric pillow erosion control system was rapidly and easily placed on a Missouri irrigation dam using resources available to the farmer. Weather conditions during placement were not a factor and specialized personnel or training were not required.

2. The sand pillow protection system offered excellent protection after 18 months of wave and weather exposure particularly when compared to other erosion protection methods on other similar dams. Some of the constantly submerged pillows lost much of their fill material after a few months but when replaced with pillows filled with sand, the protection system performed quite adequately.

large-scale equivalence exists. A correction factor was developed based on the Reynolds number from each test.

3. Stability of the sand pillows is a direct function of wave period. Stability decreases as wave period increases and at a wave steepness (H_o/L_o) less than 0.14, a constant minimum value of stability is obtained that is relatively independent of wave period.

4. Stability increases as the embankment slope becomes flatter. The simple mathematical expression used to define this effect is:

$$N_{ZD}'' = 0.605(\cot \alpha)^{0.249}. \quad (18)$$

This equation is valid for sand pillows only and is limited to slopes in the range of $1.5 \leq \cot \alpha \leq 6.0$.

5. A design equation for calculating individual sand pillow weights was established based on data gathered from this study. The equation,

$$W_{50} = \frac{H_{ZD}^3 \gamma_{sat}}{(N_{ZD}'')^3 (G_s - 1)} \quad (23)$$

was based on a previously developed stability equation (Thomsen, et al., 1972). The stability constants, N_{ZD}'' , are unique to this study and sand pillows, and can be obtained for a given slope from Table VIII or Equation 18. The usefulness of this equation was shown by comparing the actual average weight of the sand pillows from a prototype field installation to the calculated weight using Equation 23 based on the prototype soil and wave characteristics. Equation 23 will give conservative values for prototype design because N_{ZD}'' is a limiting value with respect to wave period.

The capability of the sand pillow to retain its fill material when subject to repeated wave action was observed by performing immersion and

3. The acrylic fabric has not been adversely affected by exposure to the environment. After one year of exposure the tensile strength of samples taken from the field installation has remained equivalent to the values obtained for the original fabric.

B. MODEL TEST PROGRAM

Sixteen models were tested in the 32 foot (9.75 m) wave tank with the primary variables in each test being the weight of filled sand bags, the slope of the embankment, and the height of the generated waves. The wave heights were progressively increased during the test without rebuilding the model until extensive damage, in the form of sand pillow removal and displacement, had occurred. From each test a zero-damage wave height was established by graphical techniques. These wave heights were then used to calculate the sand pillow stability.

The various relationships that affect the weight of the individual sand pillows were experimentally determined. From this study the following conclusions were reached:

1. The amount of soil eroded from between the sand pillows was slight compared to the erosion that occurred on an unprotected slope. The erosion that did occur between the bags is a direct function of embankment slope and the weight of the pillow. The amount of erosion decreases as the slope flattens ($\cot \alpha$ increases) and the weight of the armor increases, to a limiting value of area damage. At area damage (D_A) equals 0.27, the amount of damage appears independent of slope or weight.

2. For medium-scale models with a Reynolds number greater than 3.3×10^4 , stability is independent of scale. However, from previous works it is shown that small- and medium-scale model tests are less stable than large-scale tests, therefore the need for correcting these tests to

1. Monitoring of the test sections to determine the extent and rate of wave erosion after additional exposure.
2. Alternate methods to close the bags in the field.
3. Determination of the erosion resistance and filter requirements of these silty clay soils when compacted to various densities.
4. Small- and large-scale models should be tested to determine exact effects of scaling on test results.
5. Increased weights of model sand pillows should be tested for small-, medium-, and large-scale models to determine if area damage becomes independent of weight as damage decreases and weight increases.
6. A wider range of wave periods should be developed and tested on the medium-scale model to further investigate the effect of wave period on sand pillow stability. A wider range of wave steepness should also be studied for the sand pillow protection system.
7. Flatter and steeper slopes for various size models should be tested to further investigate the effect of embankment slope angle on minimum zero-damage stability of the sand pillows.
8. Wave runup on the model sand pillows should be studied for longer and shorter wave lengths for each slope tested, such that the placement of actual sand pillows will be performed economically and effectively.
9. The design equation for calculating the individual weights of the sand pillows for use on irrigation reservoir embankments should be thoroughly tested for other wind and water conditions on other midwestern reservoirs.
10. Since the sand pillow weight calculation equation is based on one soil type, further investigation with other soils would be warranted such that design criteria could be developed for the use of sand pillow protection systems on various soil type embankments.

submergence tests on representative samples of soil-filled pieces of fabric. Twenty tests were conducted on the silty clay from the field evaluation embankment and thirty tests were conducted on loessial soil from Illinois. From the results of these tests, the following conclusions were reached:

1. The amount of soil lost through the fabric is directly proportional to the number of immersions. The longer the duration of wave pounding, the larger the percentage of soil that will be lost through the fabric. Both types of soil suffered excessive losses when subject to long term wave action.

2. The soil lost during immersion tests was through the fabric itself and not through the sand pillow seams.

3. The amount of vibration of the sand bag during testing greatly affected the results of the Quincy loess samples, with the greatest amount of vibration causing the soil lost to be in excess of 80%. Vibration appeared to have little effect on the Mexico clay samples.

4. The loess samples began losing fines through the fabric at particle sizes less than 0.06 mm, while the clay samples began losing fines at particle sizes less than 0.21 mm. This difference could possibly be attributed to aggregation of the clay particles when initially wet sieved through a No. 200 sieve and the subsequent separation of the particles during the immersion tests. Because of the different results, no conclusion could be made as to the maximum particle size that can be filtered through the fabric.

VII. RECOMMENDATIONS

From the results of this study it is recommended that the following topics be considered for further investigation:

modified and tested if such fine grained material is to be used as fill in bags subjected to these conditions.

2. These sand pillows or larger size bags might be used very effectively as protective units for shore structures. A field evaluation of the fabric system subjected to ocean waves would verify the effectiveness of the system under these conditions.

11. In order to establish minimum particle size criteria on soils to be used as sand pillow fill material, further immersion testing with various soil types should be performed and the grain size distribution of the "before and after" tested soils be plotted and compared.

12. Accelerated ultraviolet light exposure tests should be conducted on the acrylic fabric to measure the long term rate of deterioration of the material when exposed to sunlight. By performing these tests on both saturated and dry material samples, the expected life of the acrylic sand pillows when placed on earth embankments could be determined.

The following recommendations are made to the owners of irrigation reservoirs:

1. The upstream slopes of small irrigation reservoirs in northern Missouri are highly susceptible to wind generated wave erosion. Therefore, some slope protection method should be utilized. The results of this and previous studies show favorable performance of the Acrilan sand pillow slope protection system, and should be considered as a highly feasible method. Based on design criteria offered in this study, an effective design of the system can be obtained.

2. Before using any soil as sand pillow fill material, it should be thoroughly tested to determine if the amount of soil lost through the fabric will be excessive when subjected to constant wave action. This will eliminate much unnecessary maintenance and cost to the owner.

The following recommendations are made with regard to the fabric manufacturing:

1. The fabric did not retain silt and clay size soil particles when submerged or subjected to wave action. A proposed fill material should be thoroughly tested before utilized with this fabric. The fabric should be

- Bretschneider, C.L., 1952, "Revised Wave Forecasting Relationships," Proceedings, 2nd Conference on Coastal Engineering, Council on Wave Research, Engineering Foundation, Berkeley, California.
- Buzzell, D.A., Chairman of Subcommittee, 1948, "Review of Slope Protection Methods," Report of the Subcommittee on Slope Protection of the Committee on Earth Dams of the Soil Mechanics and Foundations Division, Proceedings, ASCE, pp. 845-866.
- Calhoun, C.C., 1972, "Development of Design Criteria and Acceptance Specifications for Plastic Filter Cloths," Technical Report S-72-7, U.S. Department of the Army, Corps of Engineers.
- Campbell, W.G. and S.V. Ballou, 1978, Form and Style, Boston, Houghton Mifflin Company Fifth Edition.
- Cassidy, J.J., 1976, "Riprap Design", Lecture Notes for Fundamental Hydraulics and Hydrology of Dam Design Short Course, presented at the University of Missouri-Rolla, May, pp. 2-6.
- Cassidy, J.J., 1977, "Reservoir Freeboard Design," Notes from Fundamental Hydraulics and Hydrology of Dam Design, A short course at the University of Missouri-Rolla, May.
- Clemence, S.P., 1977, "Wave Protection," Notes for 5th Annual Short Course on Embankment Dams with Special Workshop Including Mine Waste Dams, August.
- Cornish, V., 1910, Waves of the Sea and Other Water Waves, Chicago, The Open Court Publication Company, pp. 23-34.
- Corps of Engineers, U.S. Army, 1941, The Experiment Station Hydraulic Bulletin, U.S. Waterways Experiment Station, Vol. 4, No. 1, May, pp. 22-24.
- Corps of Engineers, U.S. Army, 1942, Model Study of Wave Forces Against Breakwaters, Interim Report, U.S. Waterways Experiment Station, Vicksburg, Miss., pp. 8-11.
- Corps of Engineers, U.S. Army, 1949, Slope Protection for Earth Dams, Preliminary Report, U.S. Waterways Experiment Station, Vicksburg, Miss., March, p. 37.
- Corps of Engineers, U.S. Army, 1952, Wind Setup and Waves in Shallow Water, TM-27, Beach Erosion Board, Washington, D.C., June, pp. 3-7, 19, 21, 35.
- Corps of Engineers, U.S. Army, 1957, Development of a Wave-Height Measuring Device, Misc. Paper No. 5-231, U.S. Waterways Experiment Station, Vicksburg, Miss., June, pp. 2-9.
- Corps of Engineers, U.S. Army, 1962, Waves in Inland Reservoirs, Summary Report on Civil Works Investigation Projects CW-164 and CW-165, TM-132, Beach Erosion Board, Washington, D.C., November.

BIBLIOGRAPHY

"Abrasive Rock, Asphalt Facing for Water Supply Dam," Engineering News-Record, November, 1956, p. 44.

Acrylic Sand Pillows: A New Approach to Erosion Control, Special Presentation to the Department of the Army, Shoreline Erosion Advisory Panel by the Monsanto Textiles Division, February, 1976.

"A First: Soil Cement for Dam Facing," Engineering News-Record, April, 1961, p. 24.

Ahrens, J.P., "Large Wave Tank Tests of Riprap Stability," Technical Memorandum No. 51, U.S. Department of the Army, Corps of Engineers, Coastal Engineering Research Center, Fort Belvoir, Virginia, 1975.

Airy, G.B., "On Tides and Waves," Encyclopedia Metropolitana, 1845.

Allen, W.B., et al., "Review of Slope Protection Methods," Report of the Subcommittee on Slope Protection on the Committee on Earth Dams of the Soil Mechanics and Foundation Division, Proceedings, American Society of Civil Engineers, 1948, Vol. 74, pp. 845-847, 853-855.

Arthur, R.S., "Variability in Direction of Wave Travel," Annals, N.Y. Acad. Sci., 1949, Vol. 51, Art. 3.

"Asphalt Deck is Dams Watertight Layer," Engineering News-Record, December, 1957, p. 36.

Asphalt on Earth- and Rock-Fill Dams, Norwegian Geotechnical Institute, Publication No. 48, Oslo, 1962.

Barrett, R.J., ("Use of Plastic Filters in Coastal Structures," Proceedings, Xth. International Conference on Coastal Engineering, 1966, Tokyo, Japan, pp. 1048-67.

Bartos, M.J., "\$70 Million for Dam Inspections," Civil Engineering, ASCE, 1978, Vol. 48, No. 3, pp. 64-68.

Bascom, W., 1964, Waves and Beaches; the Dynamics of the Ocean Surface, New York, Anchor Books, pp. 32-36.

Bertram, G.E., 1951, Slope Protection for Earth Dams, 4th Congress on Large Dams, New Delhi, India, Vol. 1, pp. 209-220.

Bores, P.S., 1970, Earth Dam Wave Protection, 10th Congress on Large Dams, Montreal, Canada, Vol. 1, pp. 869, 870, 885.

Brasfield, C.W., 1973, Wave Action and Breakwater Design, Hamlin Beach Harbor, New York, Hydraulic Model Investigation, U.S. Army, Corps of Engineers, Waterways, Experiment Station, Vicksburg, Miss., August.

Bretschneider, C.L., 1952, "The Generation and Decay of Wind Waves in Deep Water," Transactions, American Geophysical Union, Vol. 33, pp. 381-389.

- Giroud, J.P., J.P. Geuoc, and F. Bally, 1978, "Behavior of a Nonwoven Fabric in an Earth Dam," Report to the Monsanto Textiles Division, New York, New York.
- Godehn, D.J., 1977, "Nylon Matting: A Textile Structure Used for Soil and Civil Engineering Applications," Polym. Eng. and Science, Vol. 17, No. 5, pp. 317-319.
- Grantham, K.N., 1953, "A Model Study of Wave Runup on Sloping Structures," Transactions, American Geophysical Union, Vol. 34, No. 5, pp. 720-724.
- Gray, E.W., 1969, "At Glen Elder Dam Improved Soil-Cement Placement Procedure Used," Civil Engineering, ASCE, Vol. 39, No. 5, pp. 36-39.
- Groat, B.F., 1932, "Theory of Similarity and Models," Transactions, American Society of Civil Engineers, Vol. 96, p. 273.
- Grubbe, L.W., 1977, "Granular-Fill Dam Protected by PVC Membrane," Civil Engineering, ASCE, Vol. 47, No. 7, pp. 72-75.
- Harkauli, A.N. and P.N. Gupta, 1968, "Use of Wedge Shaped Cement Blocks for Slope Protection of Earthen Dams," Symposium on Earth and Rockfill Dams, Vol. I, Papers, pp. 279-286.
- Holtz, W.G. and F.C. Walker, 1962, "Soil-Cement as Slope Protection for Earth Dams," Journal of the Soil Mechanics and Foundation Division, ASCE, Vol. 88, No. SM6, pp. 107-134.
- Hovey, O.E., 1935, "Steel Dams," American Institute of Steel Construction, New York, New York, p. 79.
- Hudson, R.Y., 1961, "Laboratory Investigation of Rubble-Mound Breakwaters," Transactions, ASCE, Vol. 126, Part 4, pp. 492-518.
- Iribarren, R.C., 1949, "A Formula for the Calculation of Rock-Filled Dikes", Bulletin of the Beach Erosion Board, Washington, D.C., p. 1.
- Iribarren, R.R., 1950, "Generalizacion de la Formula Para el Calculo de los Diques de Escollera y Comprobacion de sus Coeficientes," Revista de Obras Publicas, Madrid, Spain, (Generalization of the Formula for Calculation of Rock-fill Dikes and Verification of its Coefficients) translated by A. Haritos, Waterways Experiment Station, Translation No. 51-4, U.S. Department of the Army, Corps of Engineers, Vicksburg, Mississippi.
- Iribarren, R.R. and C. Nogales, 1954, "Other Verivications of the Formula for the Calculation of Breakwater Embankments," Bulletin, Permanent Internatl. Assoc. of Navigation Congresses, No. 39, p. 119.
- Jewell, H.H., 1945, "Protecting Upstream Slope of Kingsley Dam," Civil Engineering, ASCE, Vol. 15, No. 11, pp. 493-496.
- Jewell, H.H., 1948, "Rock Riprap Replaces Porous Concrete Slope Protection at Santee-Cooper Project," Civil Engineering, ASCE, Vol. 18, No. 1, p. 14.

- Corps of Engineers, U.S. Army, 1966, "Computation of Freeboard Allowances for Waves in Reservoirs," ETL 1110-2-8, Office of the Chief of Engineers, Washington, D.C.
- Corps of Engineers, U.S. Army, 1970, Laboratory Soils Testing, Engineering Manual 1110-2-1906, Washington, D.C.
- Corps of Engineers, U.S. Army, 1971, Engineering and Design Manual, EM 1110-2-2300, Washington, D.C., March.
- Corps of Engineers, U.S. Army, 1973, Shore Protection Manual, Coastal Engineering Research Center, Ft. Belvoir, VA., Sec. 2,3,7.
- Creager, W.P., J.D. Justin and J. Hinds, 1945, Engineering for Dams, New York, Wiley and Sons, pp. 91-96.
- Callaire, G., 1976, "Filter Fabrics: Bright Future in Road and Highway Construction," Civil Engineering, ASCE, Vol. 46, No. 5, pp. 61-65
- Dallaire, G., 1977, "Filter Fabrics Can Cut Costs of River-bank and Shore-protection Structures," Civil Engineering, ASCE, Vol. 47, No. 3, pp. 74-79.
- Dennis, C.E. and L.G. Jackson, 1965, "Beaching Slope Protection for Soil Conservation Service Dams," U.S. Department of Agriculture, Soil Conservation Service.
- Dunham, J.W. and R.J. Barrett, 1974, "Woven Plastic Cloth Filters for Stone Seawalls," Journal of the Waterways, Harbors and Coastal Engineering Division, ASCE, Vol. 100, No. WW1, pp. 13-22.
- Dutton, D.C., 1979, "The Field Evaluation of a Synthetic Material for Use as a Slope Protection Method on Irrigation Dams", thesis presented to the University of Missouri-Rolla, in partial fulfillment of the requirements for the degree of Master of Science.
- Dwivedi, N.K. and P.N. Gupta, 1966, "An Approach Towards Economical Design of Handplaced Riprap for Earthen Dams," (Based on Prototype Behaviour) Central Design Directorate, Irrigation Department, U.P., Lucknow, India.
- Elges, H.F.W.K. and J.G. Du Plessis, 1973, "Some Aspects of the Methods of Slope Protection Used in the Construction of Earth Dams in the Department of Water Affairs, Rep. of South Africa," Transactions, 11th Congress on Large Dams, Madrid, Vol. III, Questions 42-43, pp. 173-190.
- Erosion Control, Inc., 1970, Erosion Control, Textile Products to Control the Movement of Sand and Soil, West Palm Beach, Florida, April, p. 3.
- Freuert, R.K., 1955, Soil and Water Conservation Engineering, New York, Wiley and Sons, pp. 218, 229, 235, 236.
- Gaillard, D.D., 1945, Wave Action in Relation to Engineering Structures, Professional Paper No. 31, Coastal Engineering Research Center, Ft. Belvoir, VA, pp. 218-223.

- Johnson, J.W., 1948, "The Characteristics of Wind Waves on Lakes and Protected Bays," Transactions, American Geophysical Union, Vol. 29, No. 5, October, pp. 671, 672, 679, 680.
- Johnson, J.W. and E.K. Rice, 1952, "A Laboratory Investigation of Wind-Generated Waves," Transactions, American Geophysical Union, Vol. 33, No. 6, December, pp. 845-849, 852, 853.
- "Laboratory Investigation of Asphaltic Concrete, Montgomery Dam, Colorado," 1958, Proceedings, Association of Asphalt Paving Technologists.
- Longuet-Higgins, M.S., 1952, "On the Statistical Distribution of the Heights of Sea Waves," Journal, Marine Res., Vol. 4, pp. 245-266.
- Mason, M.A., 1951, "The Problem of Wave Action on Earth Slopes," Transactions, American Society of Civil Engineers, Vol. 116, Paper No. 2472, October, pp. 1402-1406, 1409-1414.
- Mason, M.A., 1952, "Surface Water Wave Theories," Proceedings, American Society of Civil Engineers, Vol. 78, No. 120, March, pp. 11-12.
- McCallister, L.D., 1979, Personal communication regarding fabric tests.
- McCartney, B.L., 1976, "Wave Runup and Wind Setup on Reservoir Embankments," U.S. Department of the Army, Office of the Chief of Engineers, ETL 1110-2-221, Washington, D.C.
- Miano, R.R., 1977, "Porous Fabric Membranes for Soil Stabilization and Drainage," Polym. Eng. and Science, Vol. 16, No. 5, pp. 320-324.
- Miche, R., 1944, "Mouvements Ondulatoires de la Mer en Profondeur Constante ou Decroissante," Annales de Ponts et Chaussees, pp. 25, 270, 369.
- Monsanto Textiles Company, 1976, Acrylic Sand Pillows: A New Approach to Erosion Control, Special presentation to: The Department of the Army Shoreline Erosion Advisory Panel, St. Louis, Missouri, February.
- Morison, J.R., 1949, "Measurements of Heights, by Resistance Elements," Bulletin of the Beach Erosion Board, Vol. 3, No. 3, pp. 16-19.
- Murphy, G., 1950, Similitude in Engineering, New York, Wiley and Sons, pp. 5-7, 17, 32-47.
- Pierson, W.J., G. Neuman and R.W. James, 1947, "Practical Methods for Observing and Forecasting Ocean Waves by Means of Wave Spectra and Statistics," U.S. Navy Hydrographic Office, Publication No. 603.
- Powers, K.L., J.R. Benson and V.S. Meissner, 1952, "Asphaltic Concrete and Soil-Cement Test as Riprap Substitutes at Bonny Reservoir," Civil Engineering, ASCE, Vol. 22, No. 6, p. 34.
- Proudfit, D.P., 1968, "Asphaltic Concrete Facing for a Rock-fill Dam," Civil Engineering, ASCE, Vol. 38, No. 3, pp. 58-59.

- Putz, R.R., 1952, "Statistical Distribution for Ocean Waves," Transactions, American Geophysical Union, Vol. 33, No. 5, pp. 685-692.
- Redlinger, J.F., Chairman of Committee, 1975, Lessons from Dam Incidents, USA, By the Committee on Failures and Accidents to Large Dams of the United States Committee on Large Dams, American Society of Civil Engineers, New York, New York.
- Reid, H.I., 1932, "Steel Plates with Welded Joints Seal Rockfill Dam," Engineering News-Record, Vol. 108, p. 761.
- Savage, R.P., 1958, "Wave Runup on Roughened and Permeable Slopes," Journal of the Waterways and Harbors Division, ASCE, Vol. 84, No. WW3, p. 1640.
- Saville, T., Jr., 1952, "Wind Setup and Waves in Shallow Water," Technical Memorandum No. 27, U.S. Department of the Army, Corps of Engineers, Beach Erosion Board, Washington, D.C.
- Saville, T. and J.M. Caldwell, 1953, "Experimental Study of Wave Overtopping on Shore Structures," Procedure from Minnesota International Hydraulics Convention, September p. 261.
- Saville, T., 1954, The Effect of Fetch Width on Wave Generation, TM-70, Beach Erosion Board, U.S. Army, Corps of Engineers, December, pp. 2, 6, 7.
- Saville, T., 1958, "Wave Runup on Shore Structures," Transactions, ASCE, Vol. 123, pp. 138-150.
- Saville, T., 1960, "Scale Effects in Wave Runup," a paper presented at the 1960 ASCE Convention in Boston, Mass.
- Saville, T., E.W. McClendon, and A.L. Cochran, 1962, "Freeboard Allowances for Waves in Inland Reservoirs," Journal of the Waterways and Harbors Division, ASCE, Vol. 88, No. WW2, pp. 93-123.
- Schaefer, M.G., 1979, Personal Communications.
- Scheidenhelm, F.M., J.B. Sneath, and A.N. Vanderlip, 1960, "Montgomery Dam--Rockfill with Asphaltic Concrete Deck," Transactions, ASCE, Vol. 125, part 2, p. 431.
- Schuyler, J.D., 1905, Reservoirs for Irrigation, John Wiley & Sons, Inc., New York, New York.
- Seemel, R.N., 1976, "Plastic Filter Fabrics Challenging the Conventional Granular Filter," Civil Engineering, ASCE, Vol. 46, No. 3, pp. 57-59.
- Seeger, C.P., 1935, "Steel Used Extensively in Building El Vado Dam," Engineering News-Record, Vol. 115, p. 211.
- Sherard, J.L., 1959, "A Steel-Faced Rockfill Dam," Civil Engineering, ASCE, Vol. 29, No. 10, pp. 698-701.

- U.S. Department of the Army, 1955b, "Waves and Wind Tides in Shallow Lakes and Reservoirs, Summary Report, Project CW-167," Corps of Engineers, South Atlantic-Gulf Region, Engineer District, Jacksonville, FLA.
- U.S. Department of the Army, 1959, "Concepts for Surface Wind Analysis and Record Velocities," Technical Bulletin No. 1, Project CW-17, U.S. Army Engineer Division, Missouri River, Omaha, Nebraska.
- U.S. Department of the Army, 1960, "Severe Windstorms of Record," Technical Bulletin No. 2, Project CS-178, U.S. Army Engineer Division, Missouri River, Omaha, Nebraska.
- U.S. Department of the Army, 1971, Earth Embankment Manual, EM-1110-2-2300, Corps of Engineers, Washington, D.C.
- U.S. Department of the Army, 1978, "Slope Protection Design for Embankments in Reservoirs," ETL 1110-2-222, Office of the Chief of Engineers, Washington, D.C.
- U.S. Department of the Interior, 1965, "Mix Design Investigations of Asphaltic Concrete for Dam Facing-Glen Elder Dam", Chemical Engineering Laboratory Report No. CH E-42, Bureau of Reclamation.
- U.S. Department of the Interior, 1966, "Mix Design Investigation of Asphaltic Concrete for Facing Downs Protective Dike," Chemical Engineering Laboratory Report No. CH E-66, Bureau of Reclamation.
- U.S. Department of the Interior, 1974, Design of Small Dams, Revised Reprint, Bureau of Reclamation, Available from the Superintendent of Documents, U.S. Government Printing Office, Washington, D.C.
- Van Asbeck, W.F., H.A. Ferguson, and H.J. Schoemaker, 1953, "New Designs of Breakwaters and Seawalls with Special Reference to Slope Protection," Report, XVIIIth International Navigation Congress, Sect. 2, Question 1, Rome, Italy, p. 169.
- Woostenek, A.J., 1973, "Use of Asphalt for Slope Protection on Earth and Rockfill Dams," Transactions, 11th Congress on Large Dams, Madrid, Vol. III, Questions 42-43, pp. 769-788.

- Sherard, J.L., R.J. Woodward, S.F. Gizienski and W.A. Clavenger, 1963, Earth and Earth-Rock Dams, John Wiley & Sons, Inc., New York, New York.
- "Soil-Cement Slope Protection for Earth Dams," published by the Portland Cement Assn., Chicago, Ill., (undated).
- Stokes, G.C., 1880, "On the Theory of Oscillatory Waves," Mathematical and Physical Papers, Vol. 1, Cambridge.
- Svee, R., 1962, "Formulas for Design of Rubble-Mound Breakwaters", Journal of Waterways and Harbor Division, Proceedings, American Society of Civil Engineers, Vol. 88, No. WW2.
- Sverdrup, H.U. and W.H. Munk, 1946, "Empirical and Theoretical Relations Between Wind, Sea, and Swell," Transactions, American Geophysical Union, Vol. 27, No. 6, December, pp. 823-827.
- Sverdrup, H.U. and W.H. Munk, 1947, "Wind, Sea and Swell: Theory of Relations for Forecasting," U.S. Navy Hydrographic Office Publication, No. 601.
- Taylor, K.V., 1973, "Slope Protection on Earth and Rock-fill Dams," Transactions, 11th Congress on Large Dams, Madrid, Vol. III, questions 42-43, pp. 215-235.
- "Tetrapods Challenged by New Tribar Shape," Engineering News-Record, July, 1958, p. 36.
- Terra Aqua Conservation, Division of Bekaert Steel Wire Corporation, 1977, Bekaert Gabions, Reno, Nevada, January, pp. 6, 54.
- Terzaghi, K. and Peck, R.B., 1967, Soil Mechanics in Engineering Practice, Wiley and Sons, New York.
- Thom, H.C.S., 1969a, "Distributions of Extreme Winds in the United States," Journal of the Structural Division, ASCE, Vol. 86, No. ST4, pp. 11-24.
- Thom, H.C.S., 1969b, "New Distributions of Extreme Winds in the United States," Journal of the Structural Division, ASCE, Vol. 95, No. ST8, pp. 1769-1770.
- Thomsen, A.L., P.E. Wohlt, and S. Harrison, 1972, Riprap Stability on Earth Embankments Tested in Large- and Small-Scale Wave Tanks, TM-37, U.S. Army, Corps of Engineers, Coastal Engineering Research Center, Washington, D.C., June, pp. 3-12, 15, 22, 27-28, 33-34, 40, 42, 48-50, 69.
- United States Department of Agriculture, 1974, Analyzing Earth Dam Slope Protection Requirements from Wind Data, Soil Conservation Service, Advisory MO-ENG-6, Columbia, MO, April.
- U.S. Department of the Army, 1955a, "Laboratory Data on Wave Runup and Overtopping on Shore Structures, Technical Memorandum No. 64, Corps of Engineers, Beach Erosion Board, Washington, D.C.

THEORETICAL DEVELOPMENT OF THE STABILITY NUMBER, N*

Stability of riprap, tribars, sand bags or any other form of slope protection is a function of many variables with the most significant being listed in Table IX in terms of their dimensions where L, F and T represent length, force and time, respectively, and in terms of their developed dimensionless parameters. Since certain variables were not investigated, their interdependence can be eliminated, as noted in the table.

Dimensionless analysis using the Pi Theorem will reveal many combinations of dimensionless terms. However, since W, γ , and g, are the easiest to measure they are generally chosen as the repeating variables, whereas H_0 is generally chosen as the dependent variable. Therefore, H_0 cannot appear in more than one dimensionless parameter.

The term $(W/\gamma)^{1/3}$ is a representative width of an armor unit, in the case of the sand bags, and is therefore used as the normalizing term for obtaining geometric similarity between model and prototype. When different sized systems are to be compared, geometric similarity exists when the length $(W/\gamma)^{1/3}$ results in the same number in both systems. Dynamic similarity between model and prototype can be shown when the forces of fluid viscosity, inertia, and gravity are the same ratio in each test. By setting the Froude number,

$$N = \frac{\rho_f D^2 V^2}{(\gamma - \gamma_f) D^3}$$

and the Reynolds number,

* The development shown here is a summary of considerations developed by Thomsen, et al., (1972), Corps of Engineers (1942) and Ahren (1975) and are generally considered to be standard equations of model wave analysis. These equations were used for this report with some alterations made where noted to conform to sand pillow models developed by the author.

APPENDIX A

THEORETICAL DEVELOPMENT OF THE STABILITY NUMBER, N

$$R_N = \frac{\rho_f D^2 V^2}{\mu DV}$$

and substituting the following:

$$\rho_f = \gamma_f / g$$

$$D = (W/\gamma)^{1/3} = \text{a representative length}$$

$$V = (gH_o)^{1/2} = \text{a representative velocity}$$

$$G_s = \gamma/\gamma_f = \text{specific gravity of armor}$$

we have obtained for the Froude number,

$$N = \frac{H_o}{(W/\gamma)^{1/3} (G_s - 1)}$$

and the Reynolds number becomes,

$$R_N = \frac{\gamma_f}{\mu} \left(\frac{W}{\gamma}\right)^{1/3} \left(\frac{H_o}{g}\right)^{1/2}$$

Treating the stability number, N, as the dependent variable, it is known that

$$N = f\left[\frac{d}{(W/\gamma)^{1/3}}, R_N, \frac{gT^2}{(W/\gamma)^{1/3}}, \cot \alpha, \text{underlayering, armor placement, } J(W/\gamma)^{1/3}/b\right].$$

Since depth of water was not altered in each test, and neither underlayering or armor placement was studied, the stability,

$$N = f\left[R_N, \frac{gT^2}{(W/\gamma)^{1/3}}, \cot \alpha, J(W/\gamma)^{1/3}/b\right].$$

TABLE XI

VARIABLES AND CORRESPONDING DIMENSION AND DIMENSIONLESS PARAMETERS

<u>Variable</u>	<u>Dimension</u>	<u>Dimensionless Parameter</u>
Wave Height, H_o	L	$H_o/(W/\gamma)^{1/3}$
Wave Period, T	T	$gT^2/(W/\gamma)^{1/3}$
Wave Length, L_o	L	1
Wave Depth, d	L	$d/(W/\gamma)^{1/3}$
Wave Length Spectrum	-	2
Specific Wave Energy	$L \cdot F/L$	1
Angle of Wave Attack	-	2
Type of Breaking Wave	-	2
Duration of Attack	T	2
Weight of Armor, W	F	3
Unit Weight of Armor, γ	F/L^3	3
Porosity, n	-	1
Embankment Slope, α	-	$\cot \alpha$
Unit Weight of Fluid, γ_f	F/L^3	γ/γ_f
Absolute Viscosity, μ	$F \cdot T/L^2$	$\mu g^{1/2}/(W/\gamma)^{1/2}$
Gravitational Acceleration, g	L/T^2	3
Damage, J	-	$J(W/\gamma)^{1/3}/b$

Note:

¹These variables are implicit in the remaining variables

²Note studied in this report

³Repeating variables

APPENDIX B
DAMAGE CURVES

These four variables were used throughout this report to predict the stability of the model sand pillows.

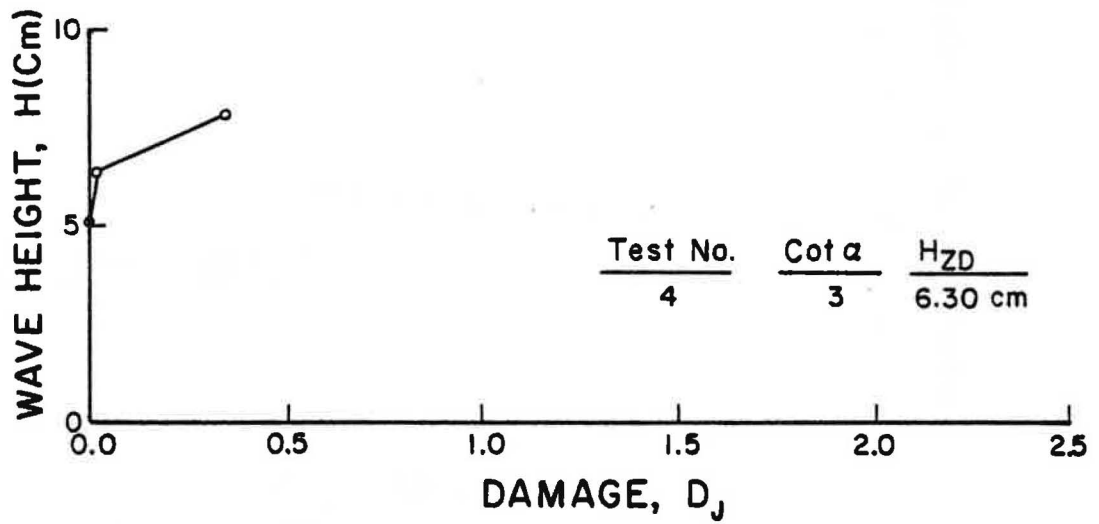
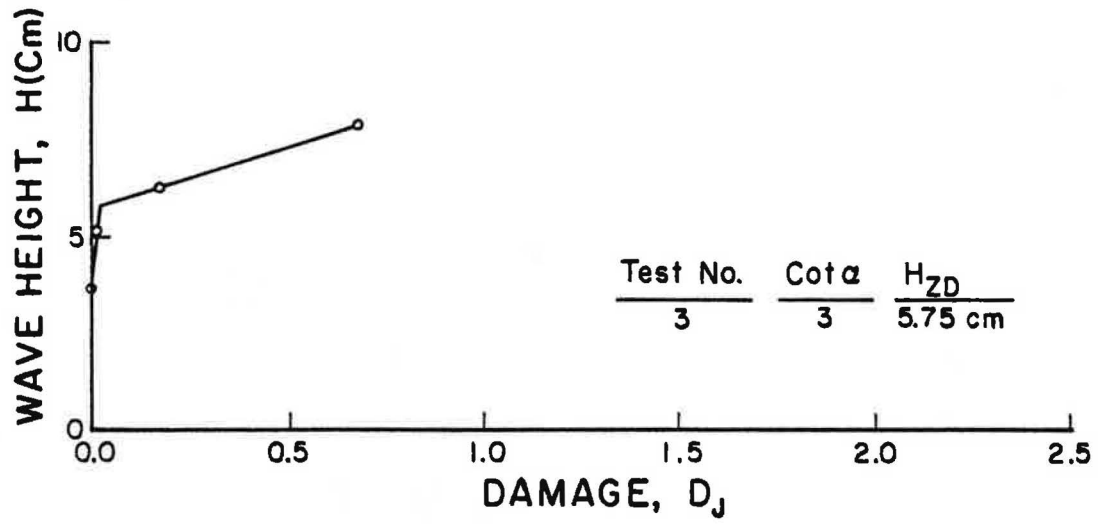


Figure 63. Damage Curves for Test Nos. 3 and 4

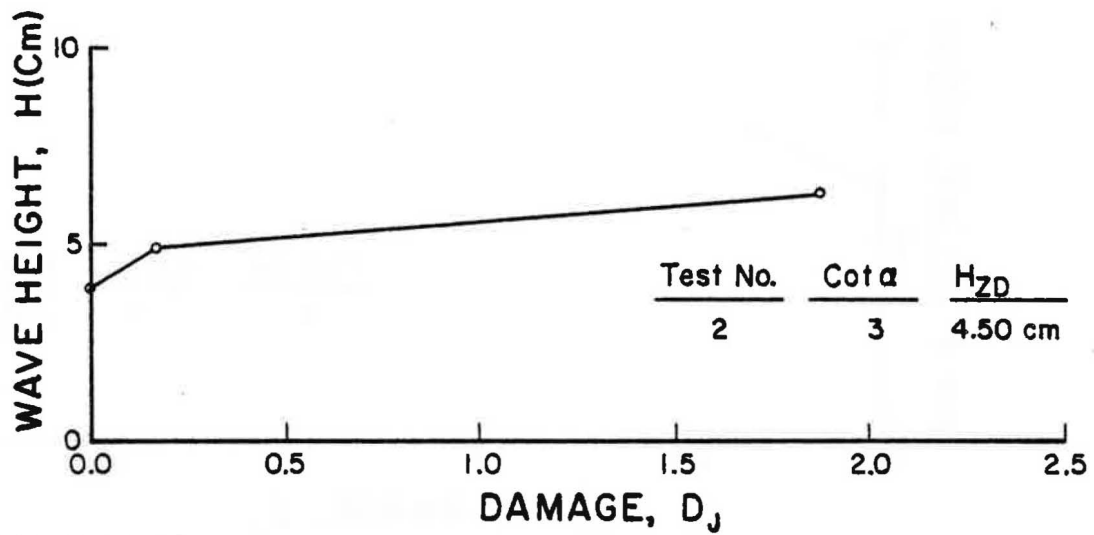
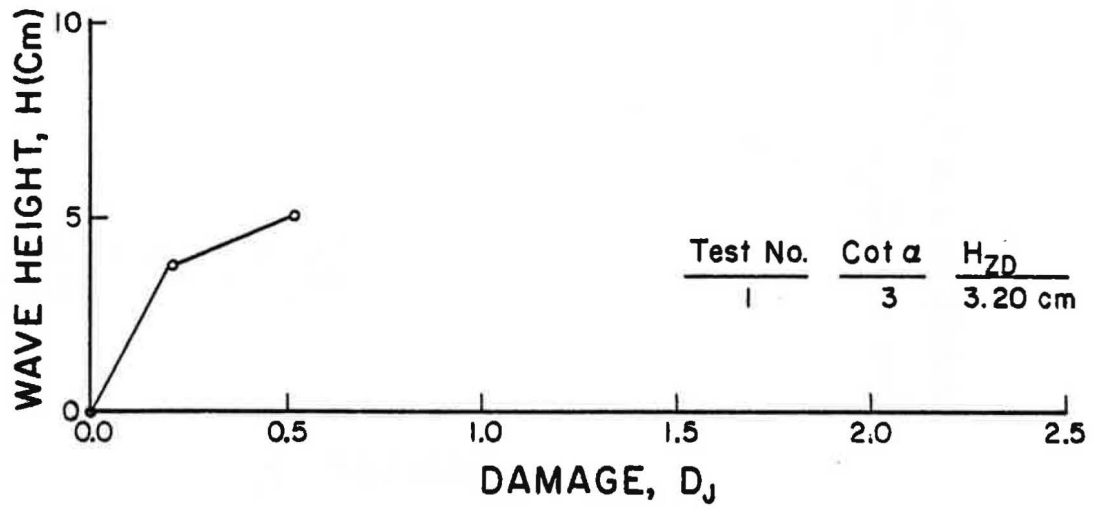


Figure 62. Damage Curves for Test Nos. 1 and 2

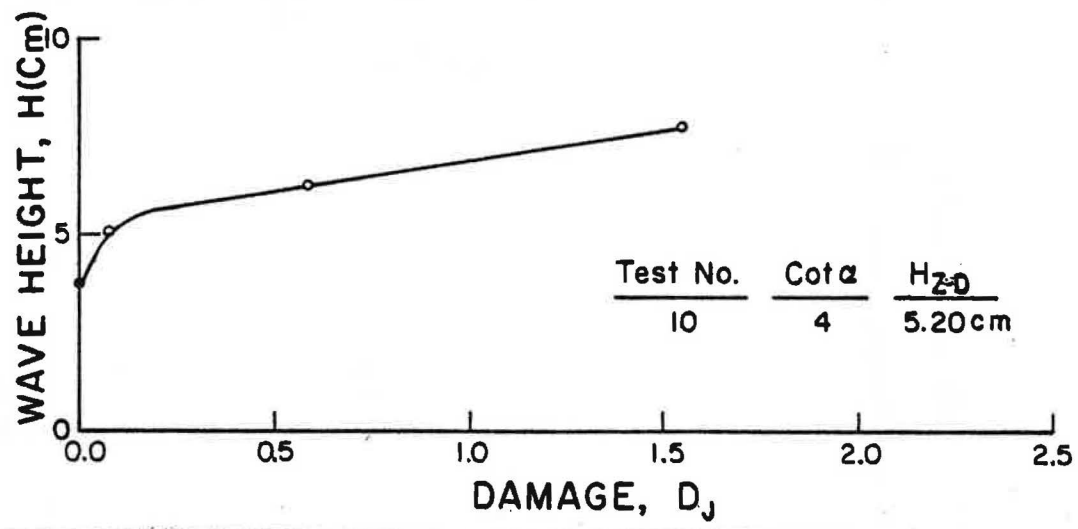
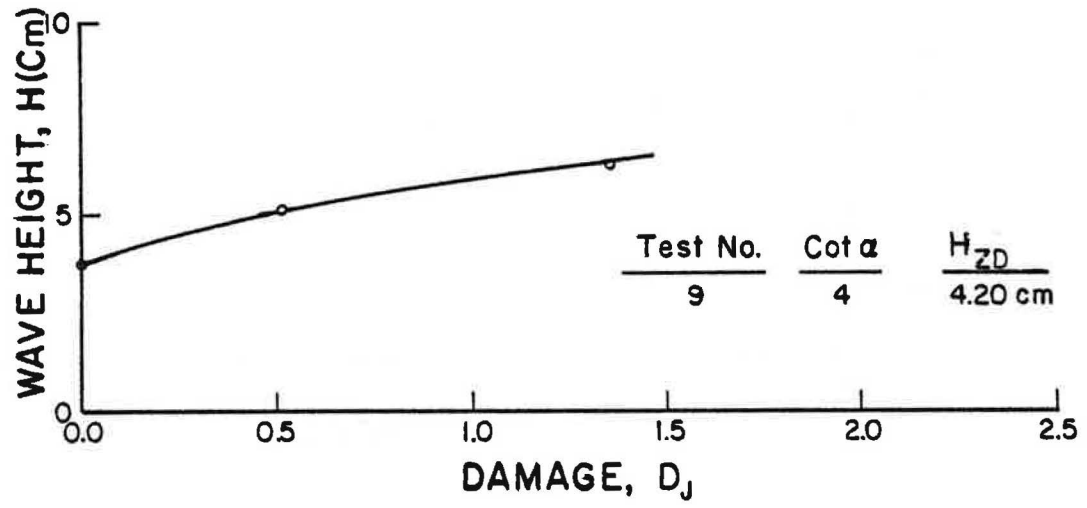


Figure 78. Damage Curves for Test Nos. 9 and 10

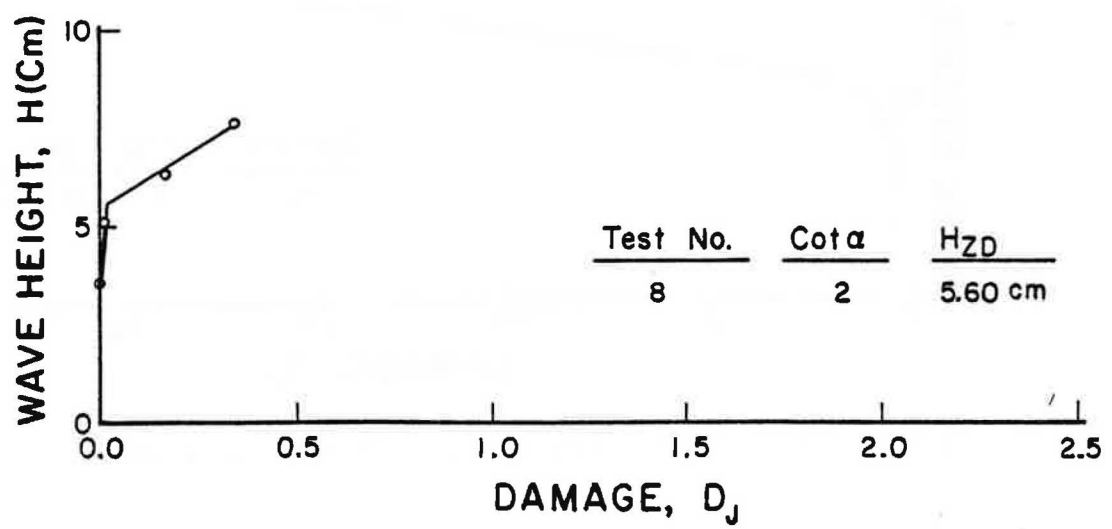
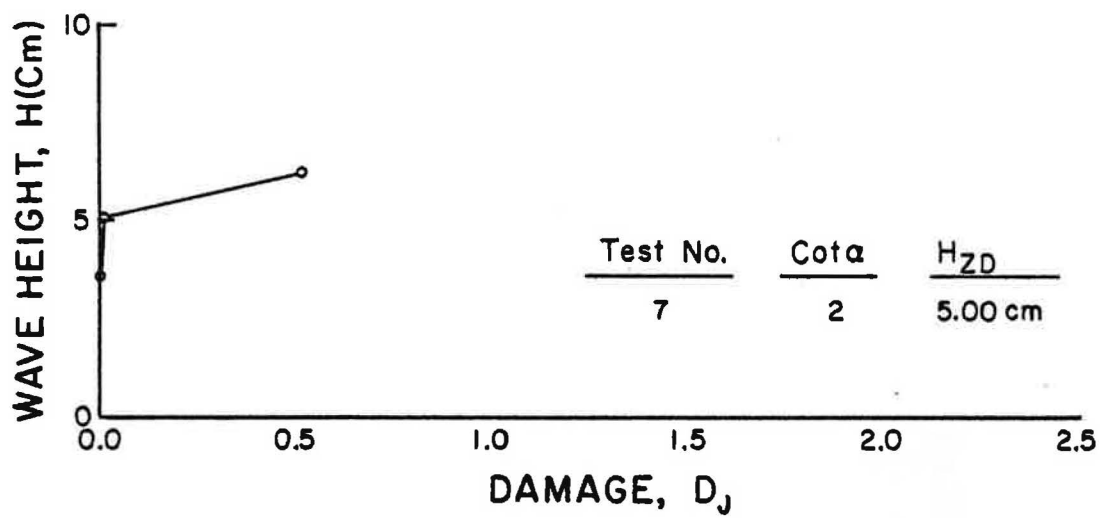
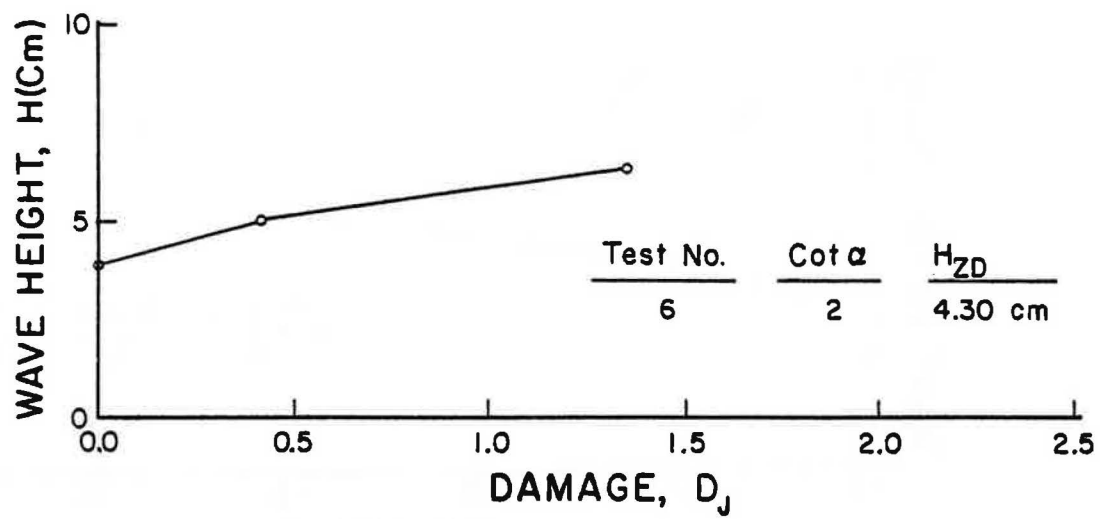


Figure 64. Damage Curves for Test Nos. 6, 7, and 8

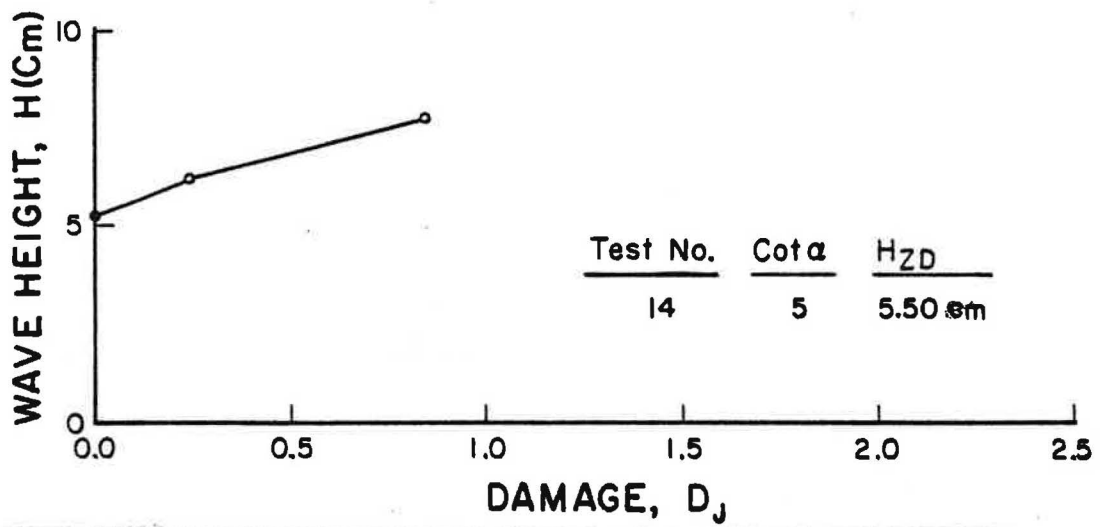
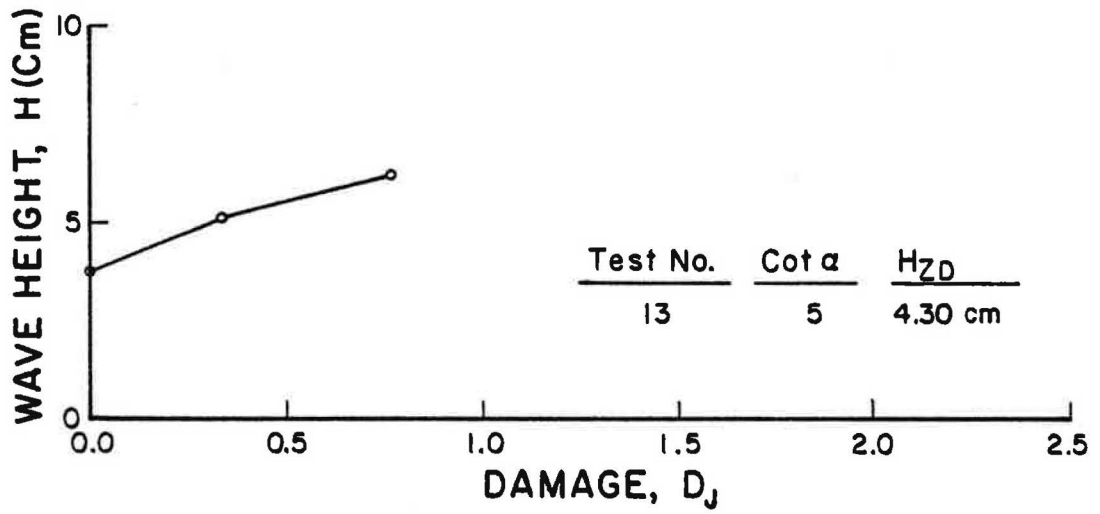


Figure 67. Damage Curves for Test Nos. 13 and 14

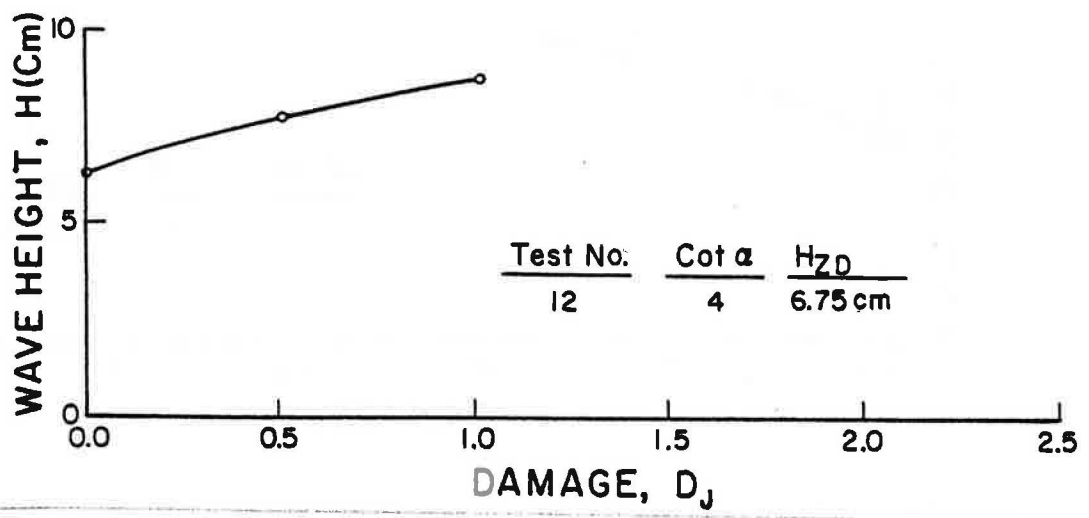
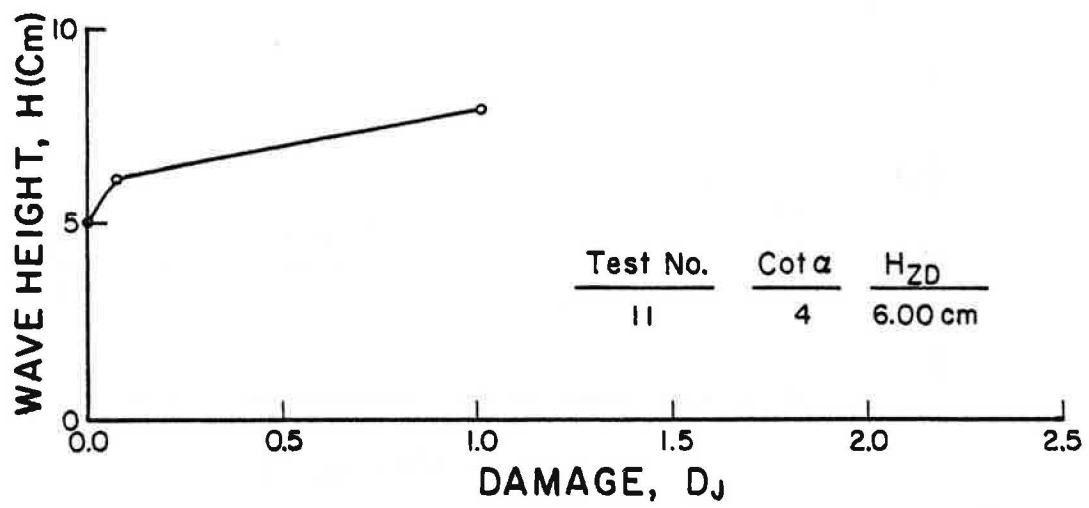


Figure 66. Damage Curves for Test Nos. 11 and 12

APPENDIX C
CROSS-SECTIONS OF THE UNPROTECTED SLOPE OF THE EMBANKMENT

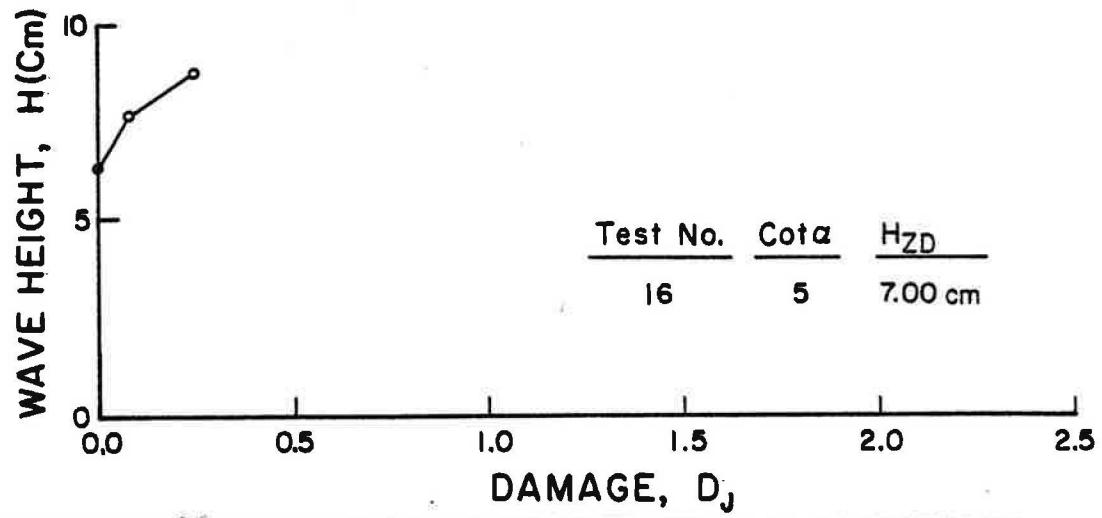
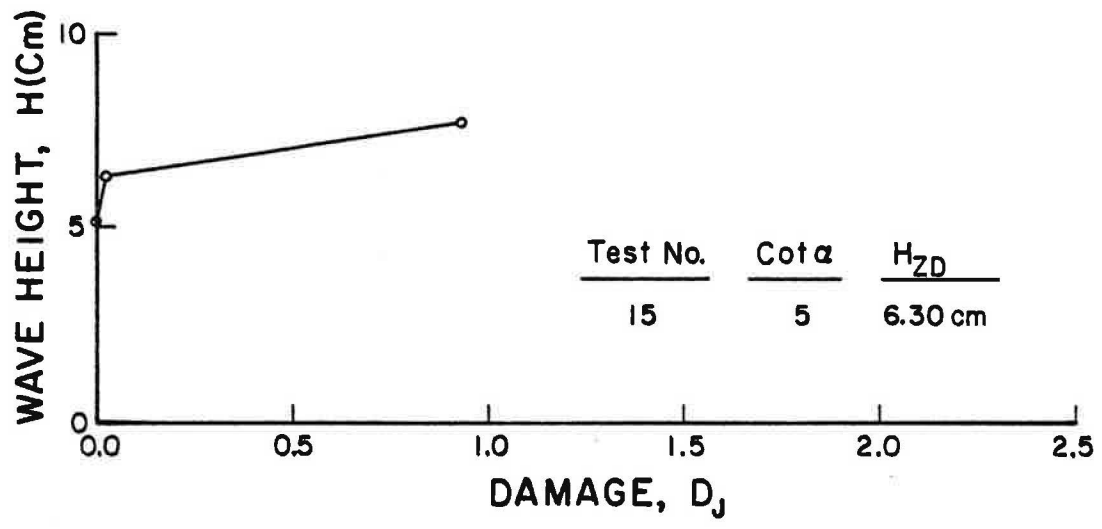


Figure 68. Damage Curves for Test Nos. 15 and 16

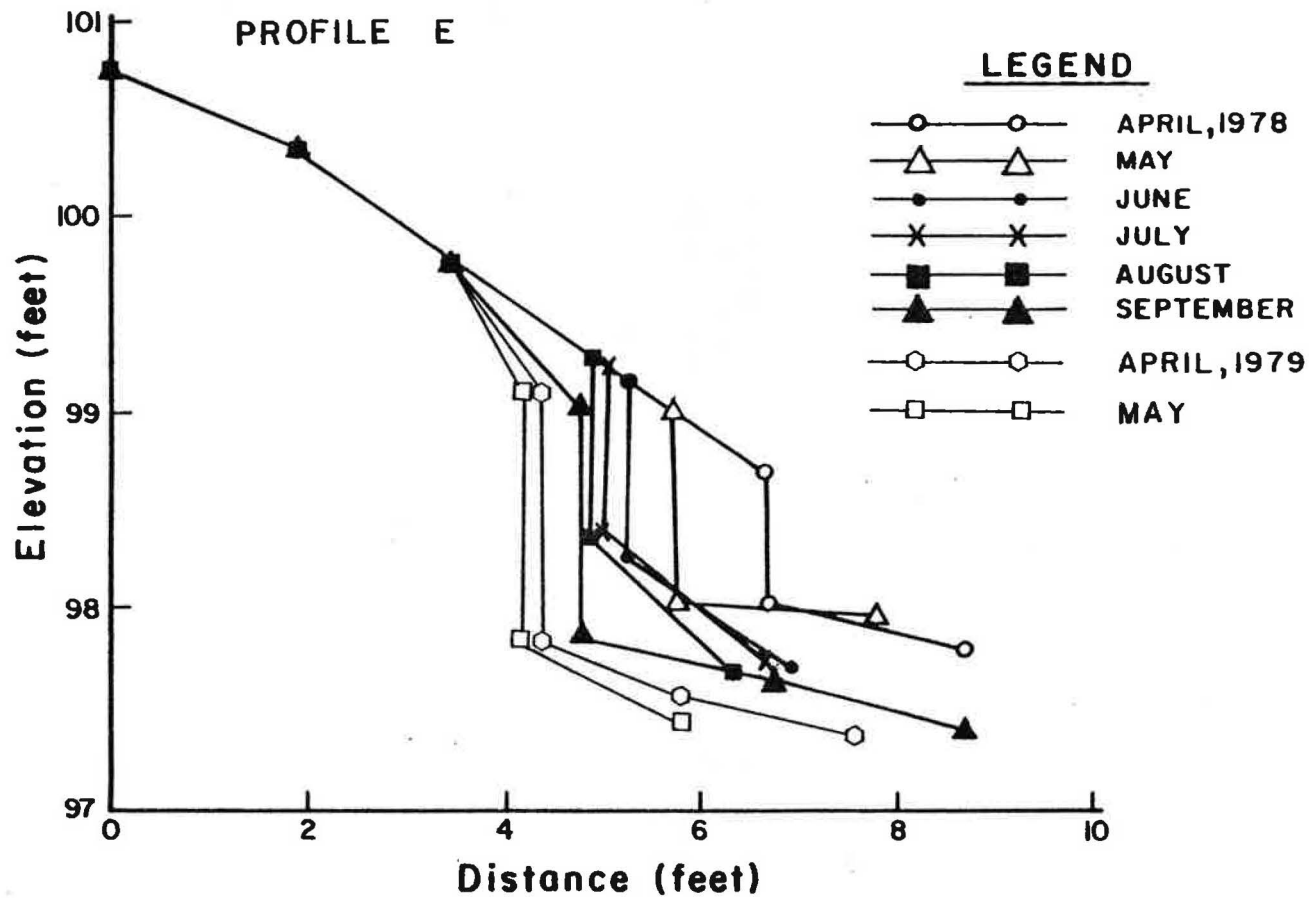


Figure 70. Cross-Section at Profile E

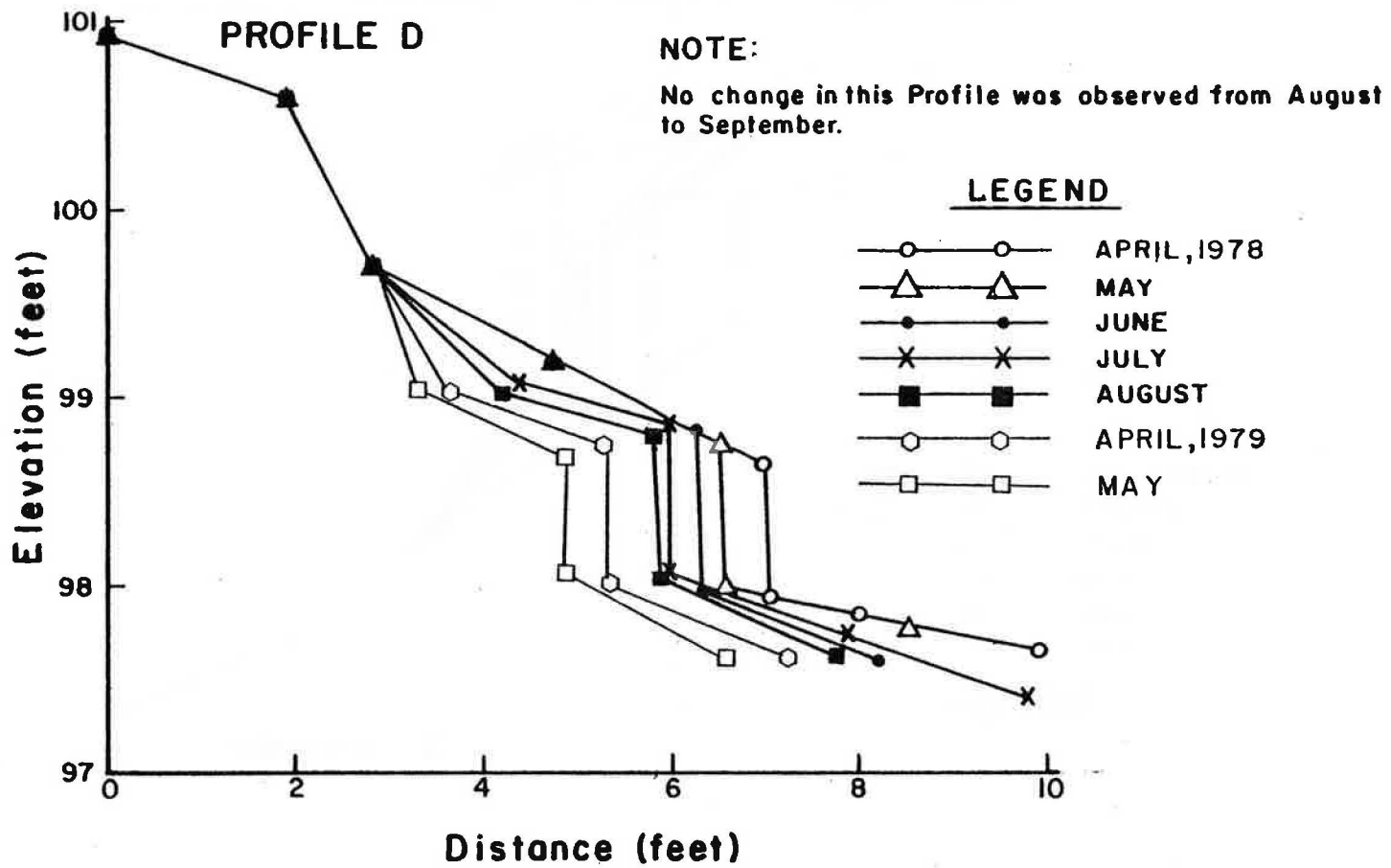


Figure 69. Cross-Section at Profile D

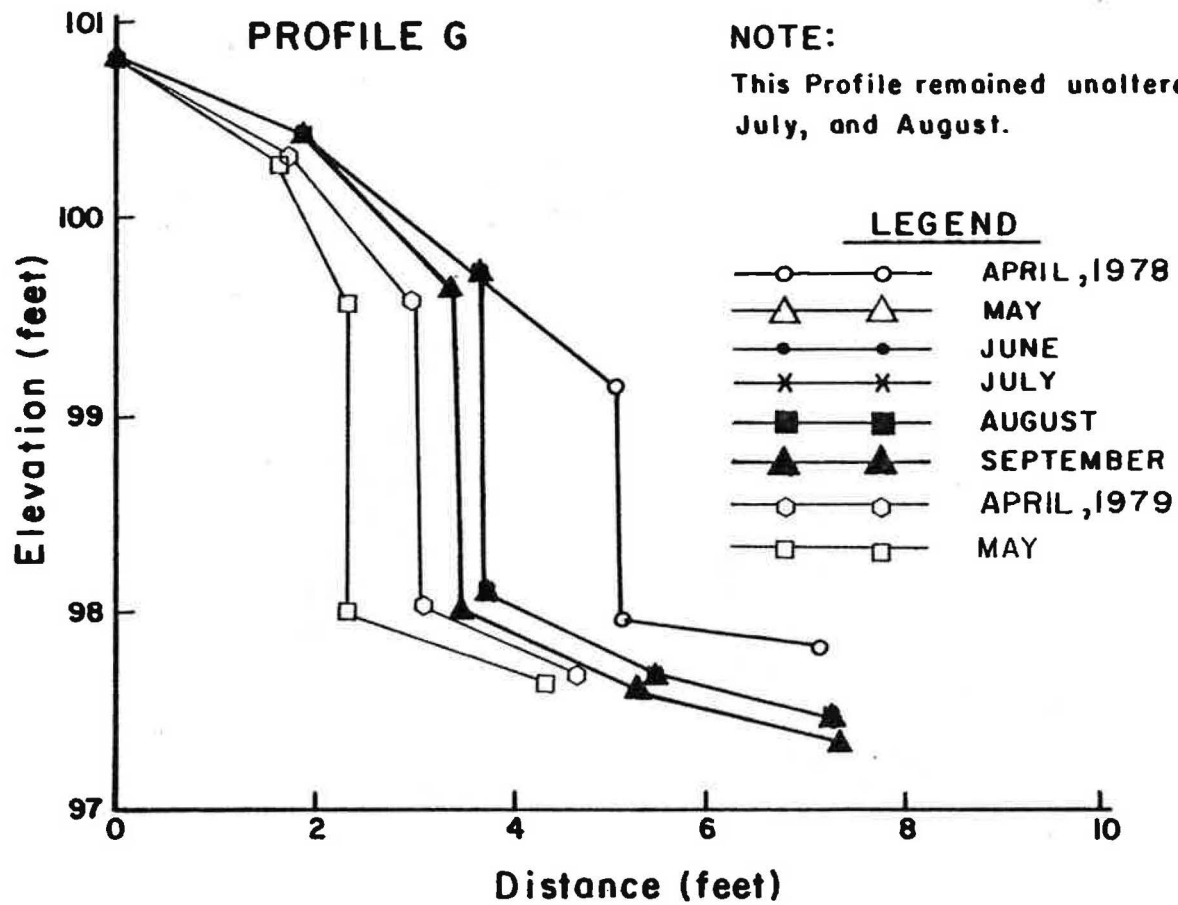


Figure 72. Cross-Section at Profile G

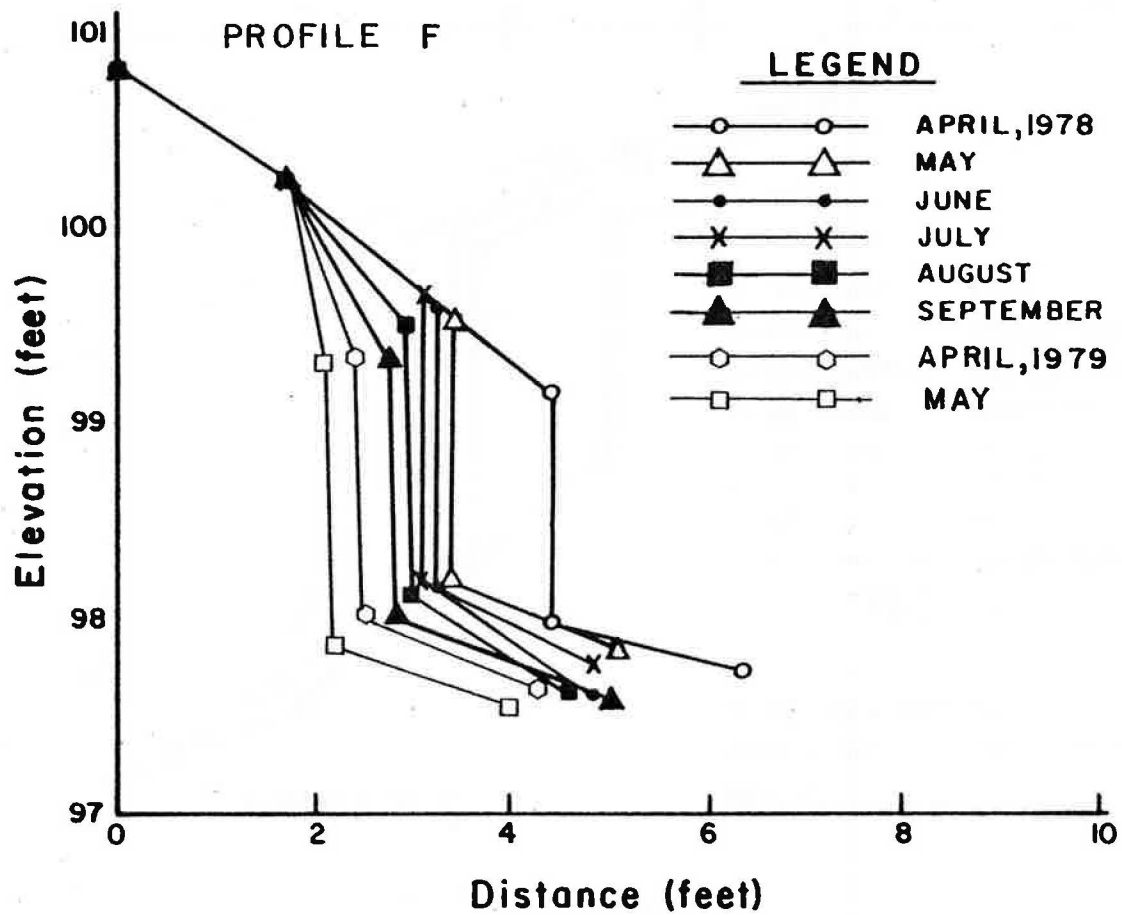


Figure 71. Cross-Section at Profile F

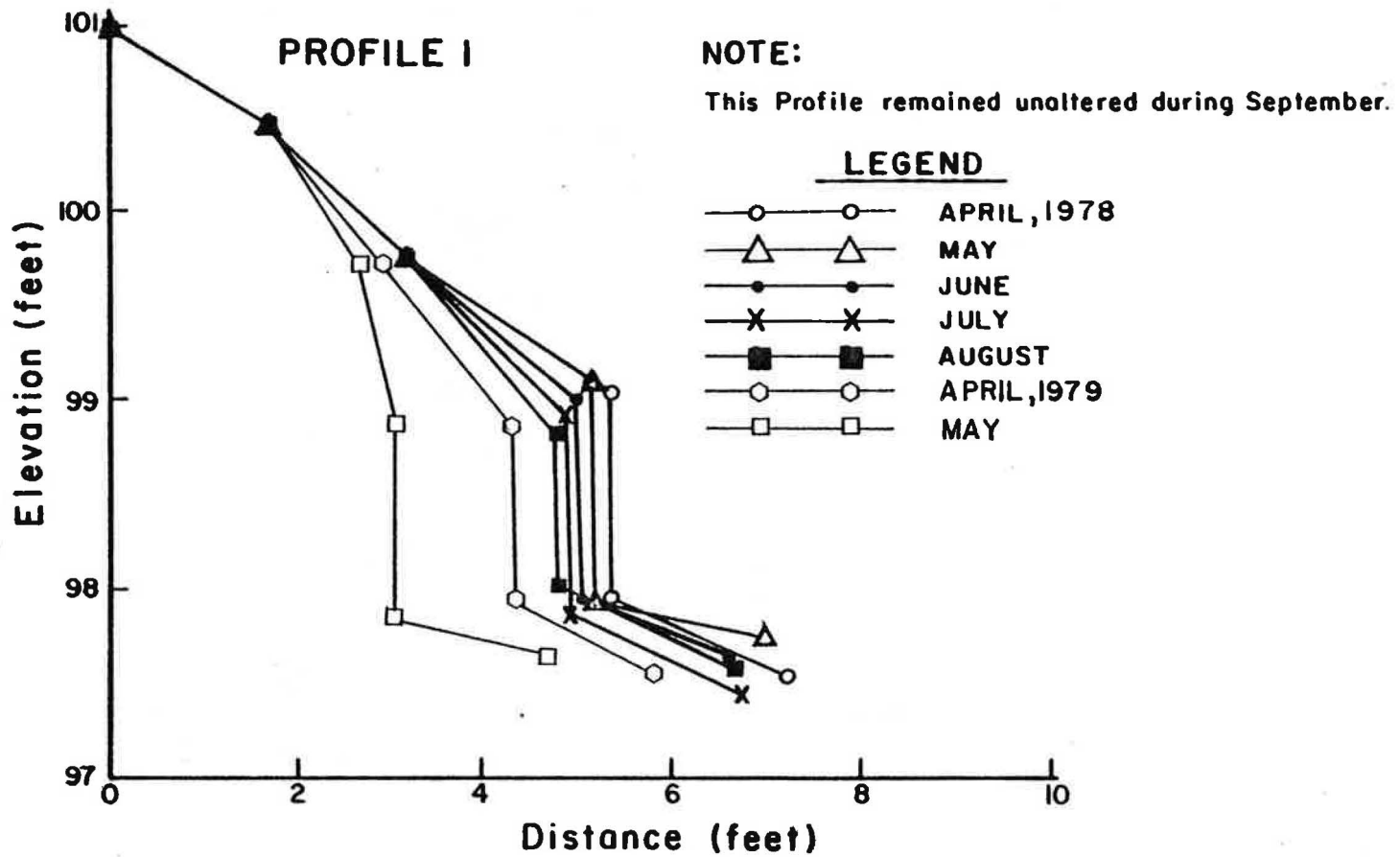


Figure 74. Cross-Section at Profile I

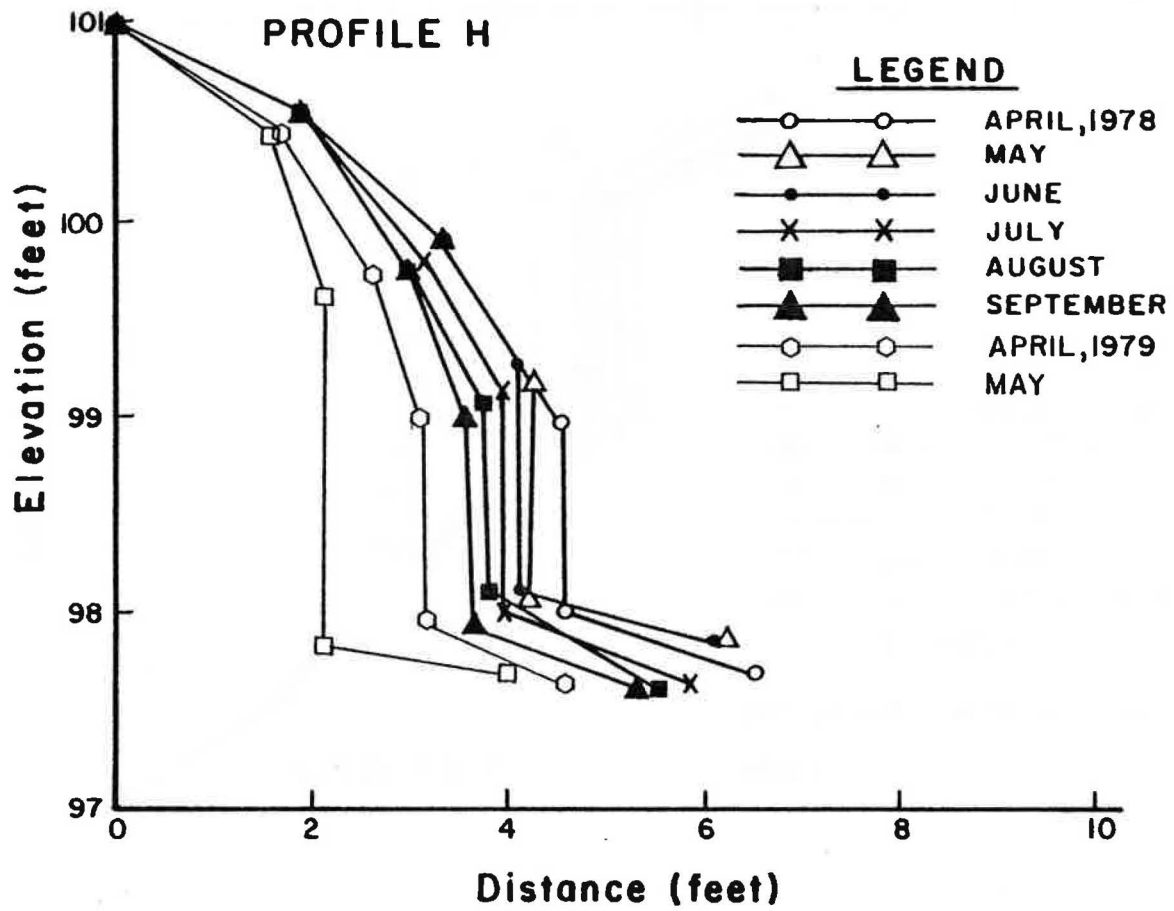


Figure 73. Cross-Section at Profile H

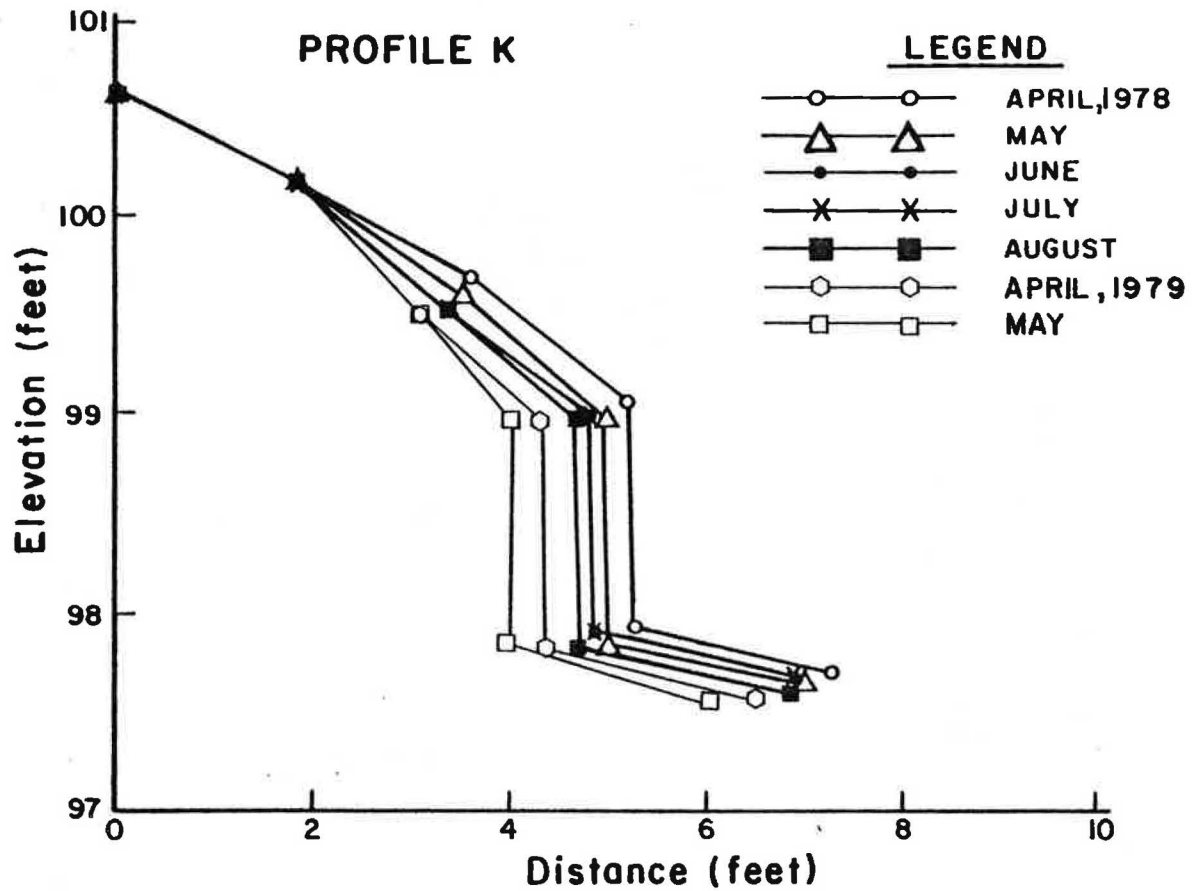


Figure 76. Cross-Section at Profile K

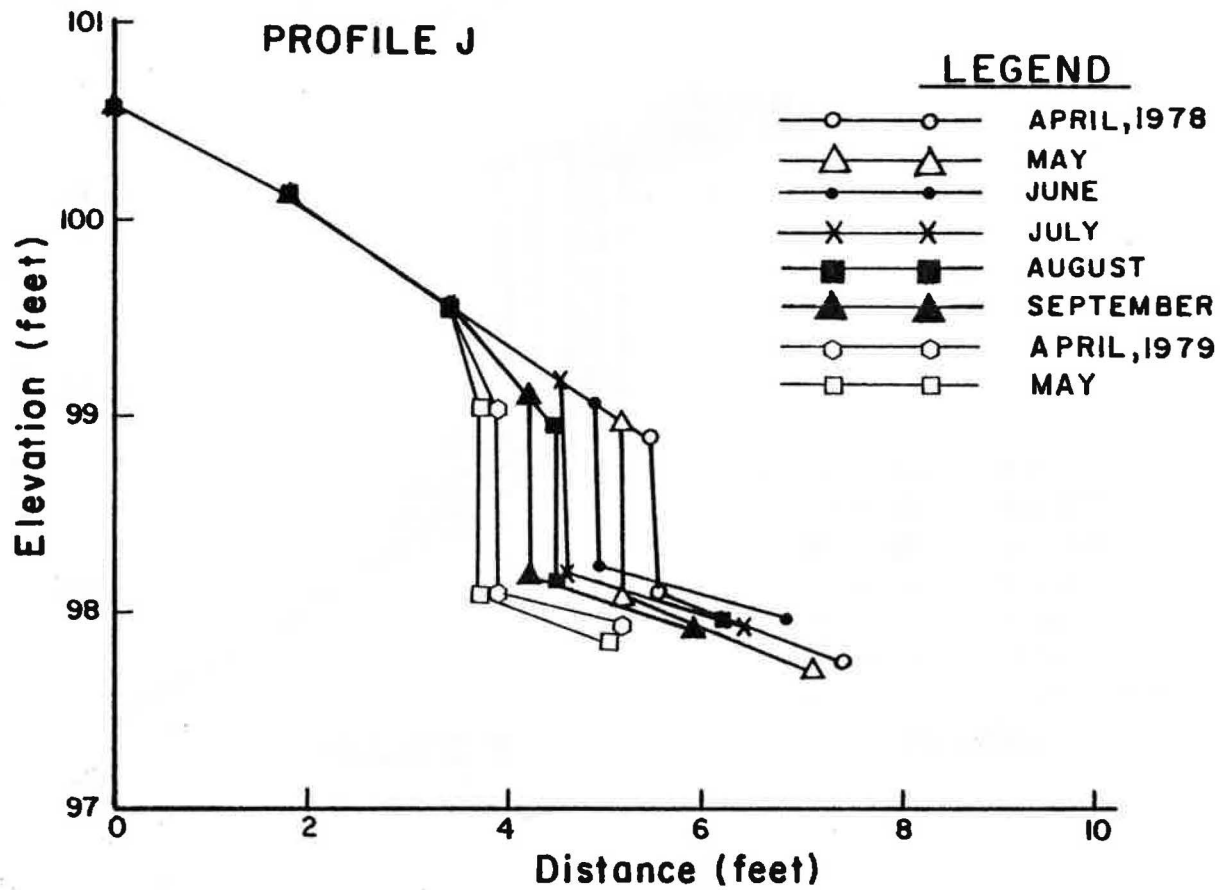


Figure 75. Cross-Section at Profile J

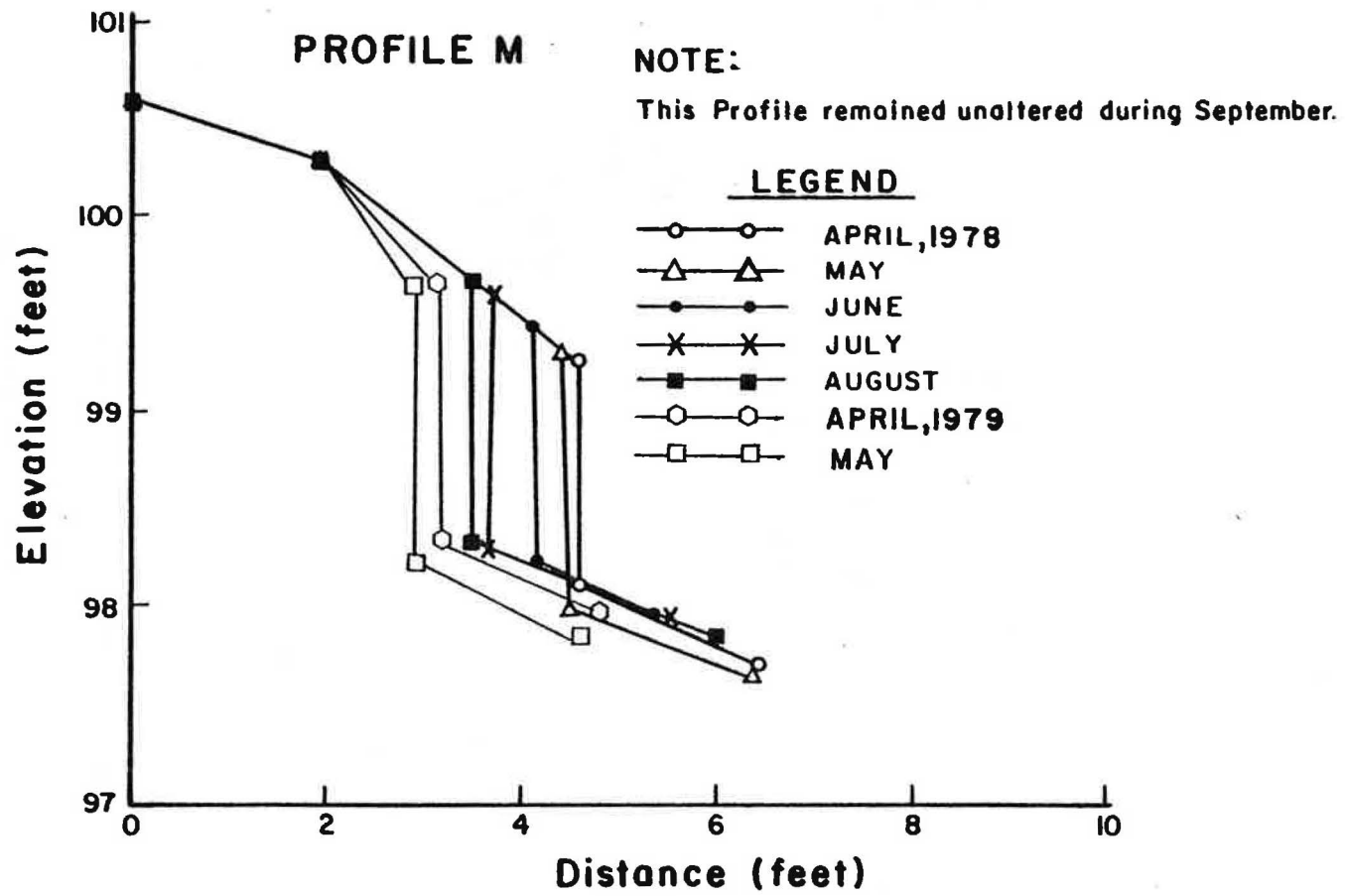


Figure 78. Cross-Section at Profile M

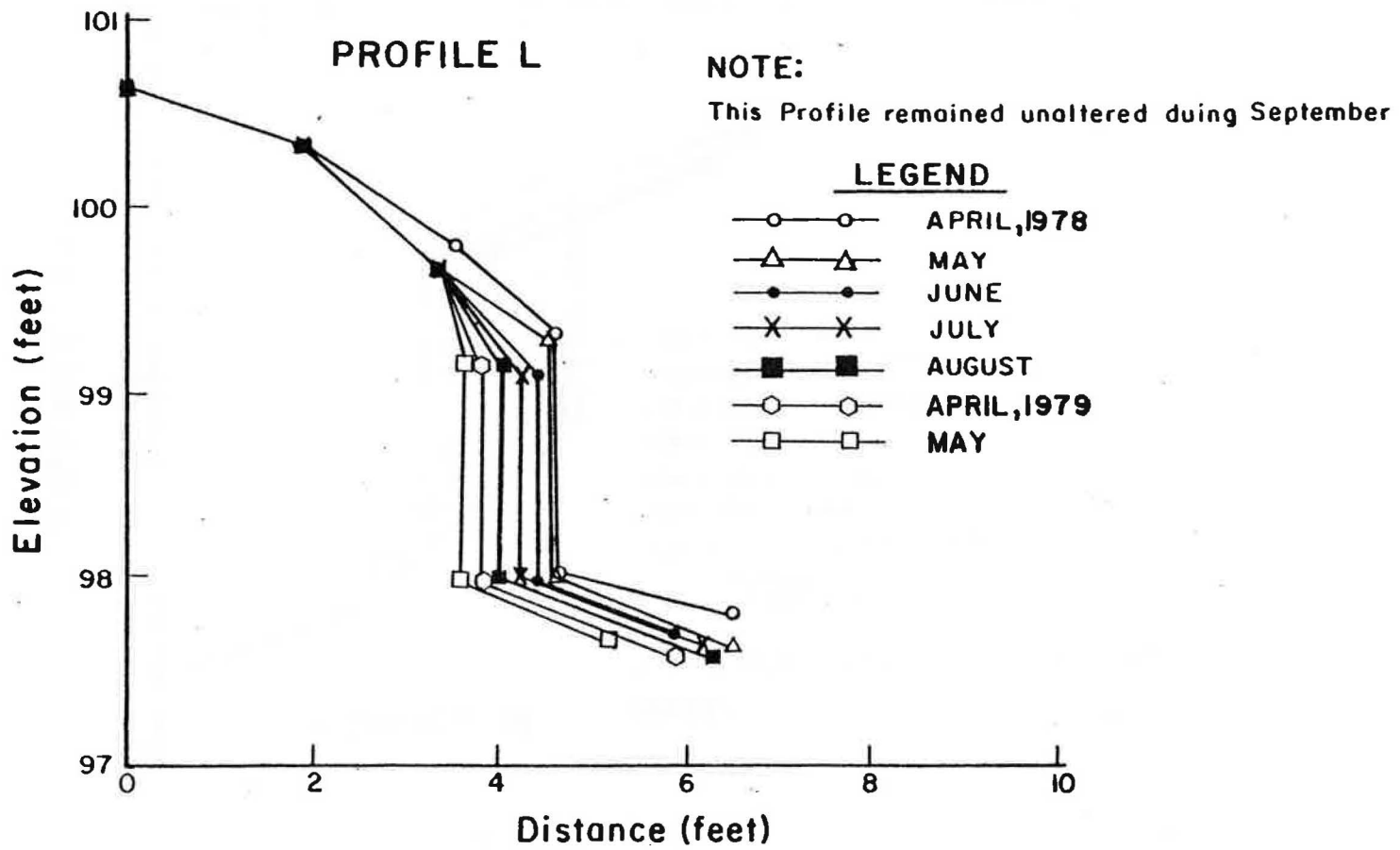


Figure 77. Cross-Section at Profile L

APPENDIX D
NOTATIONS

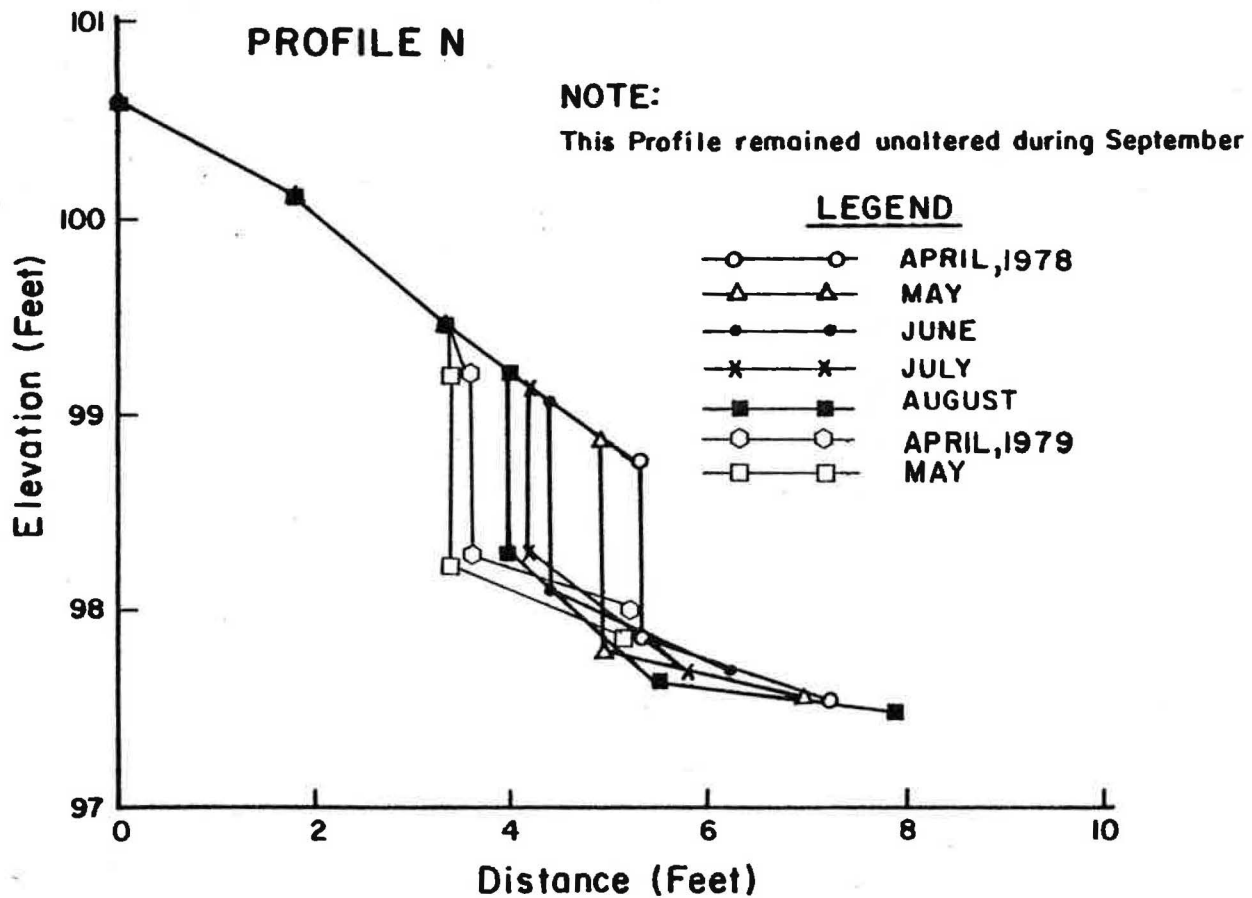


Figure 79. Cross-Section at Profile N

N_{ZD}^{min} = minimum zero-damage stability number after correcting for scale and used in conjunction with the most destructive wave periods

n = porosity of soil

R, R_s = wave runup

R_N = Reynolds number

S = wind setup or specific gravity of stone

T = wave period

U = wind velocity

V = volume

W = weight of armor units

W_{50} = weight of median size armor units

α, θ = angle of embankment slope from horizontal

$\cot \alpha$ = unit weight of armor or soil

γ_f = saturated unit weight of soil

γ_{sat} = saturated unit weight of soil

μ = absolute viscosity

ρ_f = density of fluid

The following symbols were used in this paper:

- A = cross sectional area of erosion of slope
 A' = cross sectional area of accretion of slope
 B = dimensionless damage
 b = test section width
 C_0 = deepwater wave velocity
 D = representative linear dimension of armor units
 D_A = area dimensionless damage
 D_J = dimensionless damage used with sand pillow removal
 d = water depth
 F = fetch length
 F_e = effective fetch length over water
 F_R = stability correction coefficient for scale effects
 G_S = specific gravity of soil
 g = acceleration of gravity
 H, h = any given wave height
 H_s = significant wave height
 H_{ZD} = zero-damage deepwater wave height
 H'_{ZD} = hindcast zero-damage deepwater wave height
 J = total number of armor units removed during a model test
 K = dimensionless coefficient used in Iribarren's formula
 K_{rr} = stability coefficient
 L_0 = deepwater wave length
 N, N_s = stability number
 N_{ZD} = zero-damage stability number
 N'_{ZD} = zero-damage stability number after correcting for scale effects
 N'_{ZD_0} = initial zero-damage stability number used when correcting for scale effects